# STOCHASTIC AND DETERMINISTIC ANALYSIS OF NONLINEAR MISSILE ENGAGEMENT SCENARIOS USING 5-DOF 6-DOF AND ADJOINT MODELS

A THESIS SUBMITTED
TO THE GRADUATE SCHOOL OF NATURAL AND APPLIED SCIENCES
OF
MIDDLE EAST TECHNICAL UNIVERSITY

BY

EMRAH SEZER

IN PARTIAL FULFILMENT OF THE REQUIREMENTS
FOR
THE DEGREE OF MASTER OF SCIENCES
IN
AEROSPACE ENGINEERING DEPARTMENT

DECEMBER 2015

Approval of the Thesis

**A STOCHASTIC AND DETERMINISTIC ANALYSIS OF NONLINEAR MISSILE ENGAGEMENT SCENARIOS USING 5-DOF 6-DOF AND ADJOINT MODELS**

submitted by **EMRAH SEZER** in partial fulfillment of the requirements for the degree of **Master of Science in Aerospace Engineering Department**, **Middle East Technical University** by,

Prof. Dr. Gülbin Dural Ünver _____
Dean, Graduate School of **Natural and Applied Sciences**

Prof. Dr. Ozan Tekinalp _____
Head of Department, **Aerospace Engineering**

Asst. Prof. Dr. Ali Türker Kutay _____
Supervisor, **Aerospace Engineering Dept., METU**

**Examining Committee Members**

Prof. Dr. Ozan Tekinalp _____
Aerospace Engineering Department, METU

Asst. Prof. Dr. Ali Türker Kutay _____
Aerospace Engineering Department, METU

Assoc. Prof. Dr. İlkay Yavrucuk _____
Aerospace Engineering Department, METU

Assoc. Prof. Dr. Funda Kurtuluş _____
Aerospace Engineering Department, METU

Asst. Prof. Dr. Yakup Özkazanç _____
Dept. of Electrical and Electronics Eng., Hacettepe Uni.

**Date:** 11.12.2015

**I hereby declare that all information in this document has been obtained and presented in accordance with academic rules and ethical conduct. I also declare that, as required by these rules and conduct, I have fully cited and referenced all material and results that are not original to this work.**

Name, Last name :

Signature :

# ABSTRACT

STOCHASTIC AND DETERMINISTIC ANALYSIS OF NONLINEAR MISSILE ENGAGEMENT SCENARIOS USING 5-DOF 6-DOF AND ADJOINT MODELS

Sezer, Emrah
M.S. Department of Aeropace Engineering
Supervisor : Asst. Prof. Dr. Ali Türker Kutay

December 2015, 80 pages

In this study, pseudo five degree of freedom and a linear time varying adjoint models are investigated in terms of their fidelity for conceptual design phase of a missile. The models are developed and compared for two analysis types such as, deterministic and stochastic. For the first analysis, pseudo five degree of freedom and adjoint models, which are developed, are compared with fully nonlinear six degree of freedom model for various performance analyses that are essential for conceptual design phases. Adjoint model includes time varying phenomena as an improvement over time invariant utilization, which exists in the literature. In the pseudo five degree of freedom model, roll dynamics are discarded and transfer function is implemented to represent missile acceleration response. The model includes improvements such as, more accurate drag coefficient estimation by using three dimensional incidence angle predictions, and better lateral angular dynamics estimation by using flight path kinematic equations. In addition, state space structured adjoint model is constructed and states are populated by obtaining a nonlinear model to capture the effects of engagement nonlinearity. Therefore, a proper linear time varying model is constructed and validated by comparing with nonlinear model. Finally, an approach is explained for stochastic disturbances for adjoint analysis.

Keywords: Adjoint Method, Nonlinear Simulation Model, Stochastic Disturbances

# ÖZ

DOĞRUSAL OLMAYAN FÜZE ANGAJMAN SENARYOLARININ BEŞ SERBESTLİK DERECELİ ALTI SERBESTLİK DERECELİ VE AKTIMLI MODELLER KULLANILARAK TEKLİ VE ÇOKLU ANALİZLERİ

Sezer, Emrah
Yüksek Lisans Havacılık ve Uzay Bölümü
Tez Yöneticisi : Yrd. Doç. Dr. Ali Türker Kutay

Aralık 2015, 80 sayfa

Bu çalışmada, füze konsept tasarım aşamasında kullanılan sözde 5 serbestlik dereceli ve zaman değişkenli katımlı modellerin sadakat seviyelerileri incelenmiştir. Tekil ve çoklu analizler karşılaştırıması yapılabilmesi için bu modeller geliştirilmiş ve kurulmuştur. Sözde 5 serbestlik dereceli ve katımlı modeller, 6 serbestlik dereceli modelin sonuçları esas alınarak konsept tasarımında önemli olan parameterelere göre değerlendirilmiştir. Literatürde teorik olarak var olan ama kullanılmayan zamana bağlı değişken parametreler katımlı modele entegre edilmiştir. Sözde 5 serbestlik dereceli modelde ise yuvarlanma dinamiği yok varsayılmış ve füze ivme cevabı transfer fonksiyon ile modellenmiştir. üç boyutlu hücum açı tahmini ile sürüklenme kuvveti daha doğru elde edilebilmektedir. Ayrıca füze açısal dinamikleri uçuş kinematik denklemlerinin kullanılması ile tahmin hesaplarında iyileştirme yapılmıştır. Ek olarak, katımlı analiz yöntemi ile füze ivme komutu limitlemesi çoklu analizler için çalışılmıştır. Son olarak, durum uzay yapısında katımlı analiz modeli oluşturularak doğrusal olmayan simülasyon modelleri ile karşılaştırması farklı girdi parametreleri için çoklu analiz yöntemi ile yapılmıştır.

Anahtar Kelimeler: Katımlı Analiz, Doğrusal Olmayan Simülasyon Modelleri, Çoklu Analiz

## ACKNOWLEDGEMENTS

I would like to express my gratitude to my supervisor, Asst. Prof. Dr. Ali Türker Kutay, and my co-advisor and also colleague, Mehmet Ozan Nalcı, for their unlimited hours of expertise and guidance throughout my study. It would have been impossible for me to find my way through the complicated work, without their mentoring.

I am also thankful to my colleagues and my chief Ercan Örücü in ROKETSAN Missile Industries Inc. for their understanding and support.

I would like to express my gratitude for my family, Ahmet, Fethiye and Halil Sezer for their life-long support and effort to stand by me.

I wish to express my sincere thanks to my friend Özge Doğan for the patience she has shown throughout my lengthy graduate program experience. I've always felt as a part of a much bigger family than my own.

For her kind and loving embracement, for her understanding, and for the inspiration in any circumstances she granted, I am grateful to my dear, Beren Üstünkaya. If I hadn't her understanding, I wouldn't have completed this study.

## TABLE OF CONTENTS

## LIST OF TABLES

TABLES

## LIST OF FIGURES

FIGURES

## LIST OF SYMBOLS/ABBREVIATIONS

$p$ : Body roll angular velocity

$q$ : Body pitch angular velocity

$r$ : Body yaw angular velocity

$\dot{p}$ : Body roll angular acceleration

$\dot{q}$ : Body pitch angular acceleration

$\dot{r}$ : Body yaw angular acceleration

$u$ : Body axial velocity

$v$ : Body lateral velocity

$w$ : Body vertical velocity

$\dot{u}$ : Body axial acceleration

$\dot{v}$ : Body lateral acceleration

$\dot{w}$ : Body vertical acceleration

$\alpha$ : Angle of attack

$\beta$ : Side slip angle

$M$ : Mach number

$a$ : Speed of sound

$\rho$ : Air density

$S_{ref}$ : Reference area of the missile

$l_{ref}$ : Reference length of the missile

$V$ : Total velocity

$V_{air}$ : Air speed

$x_{CG}$ : Center of gravity

$x_{ref}$ : Reference point

$g$ : Gravitational acceleration

$m$ : Mass of the missile

$\omega^{(B)}_{O_B/O_I}$ : Body angular velocity in body coordinate system with respect to inertial frame

$\omega^{(B)}_{O_B/O_I,0}$ : Body initial angular velocity in body coordinate system with respect to inertial frame

$\dot{\omega}^{(B)}_{O_B/O_I}$ : Body angular acceleration in body coordinate system with respect to inertial frame

$\omega^{(I)}_{O_B/O_I}$ : Body angular velocity in inertial coordinate system with respect to inertial coordinate frame

$\omega_0$ : Flight path coordinate system yaw angular velocity

$\omega_N$ : Flight path coordinate system pitch angular velocity

$\omega_T$ : Flight path coordinate system roll angular velocity

$V^{(B)}_{O_B/O_I}$ : Body translational velocity in body coordinate system with respect to inertial frame

$V^{(B)}_{O_B/O_I,0}$ : Body initial translational velocity in body coordinate system with respect to inertial frame

$\dot{V}^{(B)}_{O_B/O_I}$ : Body translational acceleration in body coordinate system with respect to inertial frame

$V^{(I)}_{O_B/O_I}$ : Body translational velocity in inertial coordinate system with respect to inertial frame

$P^{(I)}_{O_B/O_I}$ : Missile position in inertial coordinate system with respect to inertial frame

$P^{(I)}_{O_B/O_I,0}$ : Missile initial position in inertial coordinate system with respect to inertial frame

$\phi$ : Missile body Euler roll angle with respect to inertial coordinate system

$\theta$ : Missile body Euler pitch angle with respect to inertial coordinate system

$\psi$ : Missile body Euler yaw angle with respect to inertial coordinate system

$\phi_0$ : Missile body initial Euler roll angle with respect to inertial coordinate system

$\theta_0$ : Missile body initial Euler pitch angle with respect to inertial coordinate system

$\psi_0$ : Missile body initial Euler yaw angle with respect to inertial coordinate system

$\dot{\phi}$ : Missile body Euler roll angle velocity with respect to inertial coordinate system

$\dot{\theta}$ : Missile body Euler pitch angle velocity with respect to inertial coordinate system

$\dot{\psi}$ : Missile body Euler yaw angle velocity with respect to inertial coordinate system

$C^{(I,B)}$ : Transformation matrix from inertial to body coordinate system

$F_T^{(B)}$ : Total force in body coordinate system

$F_A^{(B)}$ : Aerodynamic force in body coordinate system

$F_P^{(B)}$ : Propulsive force in body coordinate system

$F_G^{(B)}$ : Gravitational force in body coordinate system

$M_T^{(B)}$ : Total moment in body coordinate system

$I^{(B)}$ : Inertia matrix in body coordinate system

$\vec{M}_T$ : Total moment vector

$\breve{I}$ : Inertia dyadic

$\vec{\omega}_{O_B/O_I}$ : Body angular velocity vector with respect to inertial coordinate system

$T$ : Thrust magnitude

$C_X$ : Aerodynamic axial static coefficient

$C_Y$ : Aerodynamic lateral static coefficient

$C_Z$ : Aerodynamic vertical static coefficient

$C_L$ : Aerodynamic roll moment static coefficient

$C_M$ : Aerodynamic pitch moment static coefficient

$C_N$ : Aerodynamic yaw moment static coefficient

$C_{Yr}$ : Aerodynamic lateral dynamic coefficient depends on body yaw rate

$C_{Y\dot{\beta}}$ : Aerodynamic lateral dynamic coefficient depends on side slip angle rate

$C_{Lp}$ : Aerodynamic roll dynamic coefficient depends on body roll rate

$C_{Zq}$ : Aerodynamic vertical dynamic coefficient depends on body pitch rate

$C_{Z\dot{\alpha}}$ : Aerodynamic vertical dynamic coefficient depends on angle-of-attack rate

$C_{Mq}$ : Aerodynamic pitch moment dynamic coefficient depends on body yaw rate

$C_{M\dot{\alpha}}$ : Aerodynamic pitch moment dynamic coefficient depends on angle-of-attack rate

$C_{Nr}$ : Aerodynamic yaw moment dynamic coefficient depends on body yaw rate

$C_{N\dot{\beta}}$ : Aerodynamic yaw moment dynamic coefficient depends on side slip angle rate

$\delta_e$ : Virtual elevation deflection angle

$\delta_r$ : Virtual rudder deflection angle

$\delta_a$ : Virtual aileron deflection angle

$\delta_1$ : Deflection angle of fin 1

$\delta_2$ : Deflection angle of fin 2

$\delta_3$ : Deflection angle of fin 3

$\delta_4$ : Deflection angle of fin 4

$\vec{a}_n$ : Normal acceleration vector of flight path coordinate system

$\vec{a}_0$ : Lateral acceleration vector of flight path coordinate system

$\vec{a}_t$ : Tangential acceleration vector of flight path coordinate system

$\vec{x}_B$ : Body coordinate frame axial direction

$\vec{y}_B$ : Body coordinate frame lateral direction

$\vec{z}_B$ : Body coordinate frame vertical direction

$\vec{x}_I$ : Inertial coordinate frame axial direction

$\vec{y}_I$ : Inertial coordinate frame lateral direction

$\vec{z}_I$ : Inertial coordinate frame vertical direction

$\vec{a}_{O_B/O_I}$ : Body total acceleration vector with respect to inertial frame

$a_t$ : Body tangential acceleration in flight path coordinate system

$a_n$ : Body normal acceleration in flight path coordinate system

$\vec{u}_{T,O_F/O_I}$ : Flight path coordinate system tangential unit vector

$\vec{u}_{N,O_F/O_I}$ : Flight path coordinate system normal unit vector

$\vec{u}_{0,O_F/O_I}$ : Flight path coordinate system lateral unit vector

$\vec{\omega}_{O_F/O_I}$ : Flight path coordinate system angular velocity vector with respect to inertial coordinate system

$\vec{\omega}_{O_F/O_B}$ : Flight path coordinate system angular velocity vector with respect to body coordinate system

$\vec{\omega}_{O_B/O_I}$ : Body coordinate system angular velocity vector with respect to inertial coordinate system

$\vec{u}_{Y,O_B/O_I}$ : Body coordinate system lateral unit vector

$P_T^{(B)}$ : Target position in missile body coordinate system

$P_M^{(B)}$ : Missile position in missile body coordinate system

$R^{(B)}$ : Line-of-Sight vector from missile to target

$V_T$ : Target total velocity

$V_M$ : Missile total velocity

$V_C$ : Closing velocity

$L$ : Lead angle, which is the necessary angle to intercept with the target without generating acceleration command

$\Phi$ : Power spectral density

$K$ : Describing function value

$a_{Lim}$ : Missile acceleration limit value

$\sigma_X$ : Standard deviation value of the acceleration command

$\mu$ : Mean value

$\sigma$ : Standard deviation value

$p(x)$ : Probability density function of variable $x$

$A(x,t)$ : System matrix of the two dimensional nonlinear model

$B(x,t)$ : Input matrix of the two dimensional nonlinear model

$C(x,t)$ : Output matrix of the two dimensional nonlinear model

$A(t)$ : Linear time varying model system matrix

$B(t)$ : Linear time varying model input matrix

$C(t)$ : Linear time varying model output matrix

DOF : Degree of Freedom

SAM : Surface to Air Missile

TPNG : True Proportional Navigation Guidance

LTV : Linear Time Varying

RMS : Root Mean Square

LOS : Line-of-Sight

FOR : Field-of-Regard

MD : Miss Distance, which is the minimum distance between the missile and the target

| | |
|---|---|
| STD | : Standard Deviation |
| TOF | : Time of Flight |
| CAS | : Control Actuation System |
| INS | : Inertial Navigation System |

# CHAPTER 1

# INTRODUCTION

Surface-to-air missile (SAM) systems are basically designed to prevent air vehicles activity. The way of preventing missions shows difference such as, destroying, frightening and even the existence of armed missile on the surface. The most effective and guaranteed way is to destroy and this is not an easy task. Fighter aircrafts, helicopters, cruise missiles, air-to-surface missiles, unmanned aircrafts etc. are the main targets for SAM systems and each of them have different specifications and so SAM systems also have variants for different targets. Requirements for SAM systems are assigned by military, which is the actual user. From specifying the requirements to producing the system, system design procedure is divided into different stages and in the literature names of the stages vary. In this study, missile design phases are divided into three stages namely, conceptual design, preliminary design and final design phases. Stages represent different level of system design maturity however; they should be linked to each other in order to develop a proper system.

Each stage has particular tasks and they get more detailed as systems design progresses. In the conceptual design phase, although only the general system requirements are known, number of system design solutions must be decreased to a few proper alternatives. Therefore, time and generating reasonable results are crucial to guide design and specify the detailed requirements. Due to this fact, conceptual design phase is the main focus in this thesis study.

Tasks to be done in this stage can be divided into five such as 1) mission/scenario definition, 2) weapon requirements, sensitivity analysis and trade studies, 3) physical integration of the platform, 4) concept design synthesis and 5) technology assessment. In the first task, customer needs are the main system design inputs to

evaluate the feasibility against general requirements. Then, more detailed specifications are derived such as, time-of-flight, missile engagement speed which is related to aerodynamic capability, seeker lock-on-range etc. Physical integration of missile with the platform is important due to missile sizing constraints. Based on these three tasks, system design matures and existing alternatives can be eliminated to reduce the number of system solutions. At last, best candidate technology is selected and further subsystems are specified but not in detail(Fleeman, 2001).

While obtaining different design alternatives, various fidelity levels of simulation models are developed and utilized according to needs. Since at the beginning of the system design, lots of design parameters are unknown, building high fidelity simulation model is not an easy task and is not applicable. Also, complex models are not convenient for parametric analysis and even unreasonable results may be generated since they need more detailed parameters. Therefore, deciding on the right fidelity level is crucial and is not an easy task to understand and systematic design progress is necessary. At the beginning, simple models are convenient tools to understand system sensitivities and to derive specifications. Then, simulation models evolve with the system maturity.

6-DOF has the highest fidelity level compared to other simulations and all systems/subsystems such as; fully nonlinear kinematic equations of motion, aerodynamics, autopilot, seeker, propulsion, control actuation system, guidance algorithms etc. can be implemented. Therefore, before constructing the 6-DOF simulation model, system and subsystem level requirements must be well defined to study on detailed system analysis. Links between design phases and relevant simulation models must be well established due to reasons mentioned above.

There are many lower fidelity level simulation models such as; 1-DOF, 2-DOF, 3-DOF, Pseudo 5-DOF, Pseudo 6-DOF etc. In addition to these classical forward time models; adjoint method is utilized for initial system design works. In this dissertation, the adjoint technique and Pseudo 5-DOF simulation model are studied and compared to 6-DOF to understand their convenience.

Utilizing a linear model is important to figure out system sensitivities in a short time. In the literature, various adjoint method applications exist for homing guidance loop studies. At the beginning of the conceptual design phase, the technique is convenient since it can generate many linear forward simulation results in a single adjoint run. On the other hand, system sensitivities against different deterministic and stochastic disturbances can be obtained in a single run thanks to linearity assumption. Although adjoint is very powerful method for sensitivity analyses, limitations should be well understood in order to begin the system design properly.

Adjoint method was studied over hundreds years ago by mathematicians but first practical use was at 1918 (Domenic Bucco, 2010). Since then, the method was studied for various purposes such as; effects of perturbations on a system and hit dispersion of theoretical artillery(Laning & Battin, 1956). Adjoint applications to homing missile systems became more popular with publication of Zarchan's book of "Tactical and Strategic Missile Guidance" (Zarchan, 2012). In this book, deterministic and stochastic theory of the adjoint method, construction rules, homing guidance loop linearization and more advanced adjoint applications are explained in detail. On the other hand, Martin Weiss published a paper about state space structured adjoint technique against deterministic and stochastic disturbances(Martin Weiss, 2005). In this paper, classical homing guidance loop is derived and related equations are implemented in state space form of the adjoint method. In addition, different form is explained in detail against conventional and unconventional stochastic target maneuvers by deriving related shaping filters. Also, since the technique is valid for time varying phenomena, rolling missile concept is taken into account to figure out the rolling airframe effects on the system performance by defining transformation matrix between missile body coordinate system to inertial coordinate system. While building an adjoint model, classical system input transfer function is implemented as adjoint output and Zarchan and Bucco have a paper about implementing unconventional inputs to adjoint model (D Bucco, 2012).

Since the homing guidance engagement must be linearized, adjoint method performance becomes questionable for some analysis types and this is among the main limitations of the technique. Weiss and Bucco studied this constraint by

utilizing state space structure on adjoint for stochastic analysis(M Weiss & Bucco, 2005).In addition, effects of nonlinear parameters on the adjoint performance are discussed and some nonlinear system states can be neglected since they do not affect the result critically(Moorman, Warkomski, Lam, & Elkanick, 2005).

Apart from the limitation caused by geometric nonlinearity, missile acceleration capability has a crucial effect on system performance and it brings saturation nonlinearity. In addition to adjoint technique, covariance method also exists and it is used to simulate system performance against stochastic disturbances as a variance matrix that shows coupled and uncoupled relations of the states(Gelb, Joseph, Nash, Price, & Sutherland, 2001). Similar with the adjoint applications, homing loop guidance engagement scenario must be linearized and nonlinear geometric affects still exist.

In addition to covariance, describing function method is utilized to linearize system nonlinearities such as; saturation, relay etc. The method is based on the assumption of sinusoidal input and nonlinearities are linearized according to related input. The technique is important to understand the effects of the nonlinearity on the crossover frequency. Besides, describing function can be obtained against random input, which is taken as white noise(Gelb & Velde, 1968). By implementing both covariance and describing function technique, Zarchan published a paper about missile acceleration limit and accuracy of the method (Zarchan, 2012).

Note that even though the adjoint method is improved by implementing different techniques; it is not enough for more detailed analyses since results are generated only at a single time snapshot, which is at the end of the forward simulation model, and limitations caused by linearity assumption. At the beginning of the system design, general performance parameters are more important and adjoint method is a suitable tool but as the design matures, states histories and their interaction to each other become more important for detailed design applications.

At the conceptual design phase, requirements such as; range-to-go, time-of-flight, seeker field-of-regard angle should be specified so simulation models with higher fidelity compared to adjoint are needed. The word of “fidelity” means basically

degree-of-freedom (DOF) and generally, higher the fidelity higher the degree-of-freedom. Also, fidelity does not depend only on the DOF but also it relies on level of detail of the system and subsystem models.

In the literature, various fidelity level of simulation model studies for different degree-of-freedom levels exist namely, 3-DOF, Pseudo 5-DOF, and 6-DOF. From second task to last one at the conceptual design phase, these models are developed according to system maturity. When the adjoint technique fidelity is not enough for design, 3-DOF simulation models are good choices to continue. Note that number of the degree-of-freedom represents the system motion in terms of translational and angular dynamics. In the literature, different types of 3-DOF simulation models are developed for example; two translational one angular or three translational. In this model, system/subsystem models are not modeled in detail and based on the requirements; simple aerodynamic models and thrust tabular data can be implemented. As the system design evolves, mode detailed system/subsystem model, higher degree-of-freedom are essential so more complex simulation models should be developed. Pseudo 5-DOF is a good candidate to proceed since it does not require all detailed information of the system and it still allows parametric study to guidance & control applications. Generally, SAM systems are stabilized around zero roll rates; roll dynamics of the missile is discarded to simplify the simulation model. In addition, although 5-DOF seems like the angular dynamics are solved by the model, pitch and yaw dynamics are estimated that makes the model Pseudo. This enables to designer develop a model, which represents the system angular dynamics without implementing the moment equations and aerodynamic angular coefficients in tabular form. Also, missile acceleration response to an acceleration command can be represented as a transfer function that can be based on the states. Utilizing transfer function enables parametric study for integrated guidance & control performance evaluation which has a crucial effect on the 6-DOF development. Otherwise, proper guidance algorithm must be implemented and an appropriate autopilot must be designed which generally takes huge time for iteration. Compared to 3-DOF, better aerodynamic drag force calculation can be done by estimating incidence angles and

more accurate trajectory can be estimated due to estimation of pitch and yaw dynamics.

As the design process continues, a more detailed simulation model, which is 6-DOF, is required to analyze more detailed analyses. All nonlinear elements can be implemented and detail levels of the system/subsystem models continue to improve. Whole aerodynamic data, thrust data and full state system equations of motions are implemented. On the other hand, an autopilot must be designed to figure out system performance and possible critical flight envelopes.

In this thesis study, capabilities of the adjoint method and Pseudo 5-DOF model are investigated by comparing them with 6-DOF model, which is assumed to generate true data. Note that exact match of the generated results is not expected for this comparison especially for the adjoint method. The point is to understand the accuracy of the models and reasonable analysis types before developing the 6-DOF model and it is expected to get a sense about where to increase fidelity level while design process is continuing.

Adjoint method is a powerful method in terms of parametric study capability and time; however, it not suitable for whole requirement analyses therefore, validity of the technique has a limit in the design process. On the other hand, Pseudo 5-DOF model has a huge fidelity compared to adjoint but it not advised to use at the beginning of the design since it requires information about the system.

In addition, Pseudo 5-DOF model shortens time and reduces burden from specifying aerodynamic requirements to performance analysis. In Figure 1, the procedure is depicted for 6-DOF simulation model. Aerodynamic design is done according to specified requirements, which are derived by the system engineer. Then aerodynamic database is created and is checked whether it satisfies the requirements or not. On the other hand, autopilot design is done according to missile aerodynamic capability and autopilot requirements that are specified by the system engineer also. Before studying on performance analyses, autopilot must be implemented to 6-DOF and autopilot performance tests must be done. Finally, 6-DOF model can be utilized for detailed performance analyses and this is the perfect scenario (shown by green lines).

In real world, generally this is not the actual case since proper solution cannot be obtained at first time so some of the tasks may have to be repeated. For example; if unexpected performance analysis results are obtained, aerodynamic design, autopilot requirements and autopilot design must be checked and should be repeated if necessary. Also, same examination must be done if unforeseen outcomes are generated at autopilot tests.

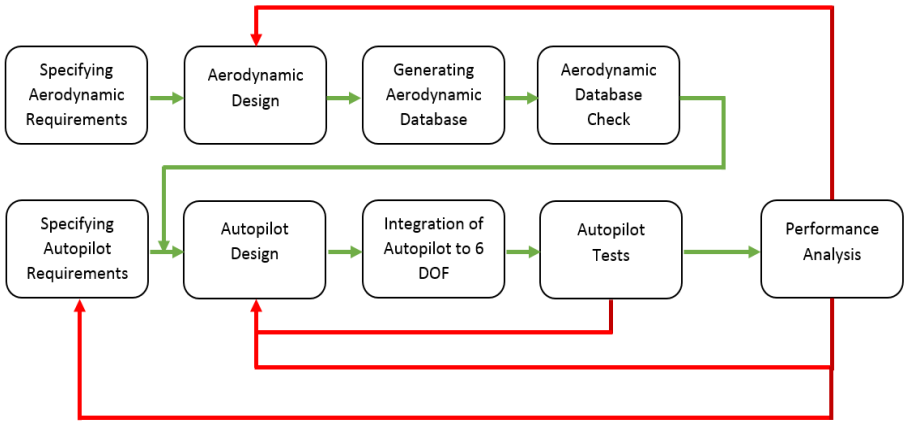


**Figure 1 Iterative Process for 6-DOF Simulation Model**

The procedure is different for Pseudo 5-DOF simulation model since it requires less information to build and develop. In Figure 2, the process is shown for Pseudo 5-DOF simulation model. Since both models require aerodynamic database, aerodynamic requirement, design, generating database and check tasks still remain; however, Pseudo 5-DOF simulation model does not need aerodynamic database for rotation dynamics, which accelerates the process. On the other hand, missile acceleration response to acceleration command is represented by a transfer function; order of the function depends on the designer choice, without designing autopilot. Therefore, autopilot design, integration and test tasks are cancelled. Even this figure explains that less complex models should be used before developing 6-DOF model in order to generate requirements in a short time. Otherwise, both specifying requirements and performance analysis are placed in the same procedure.

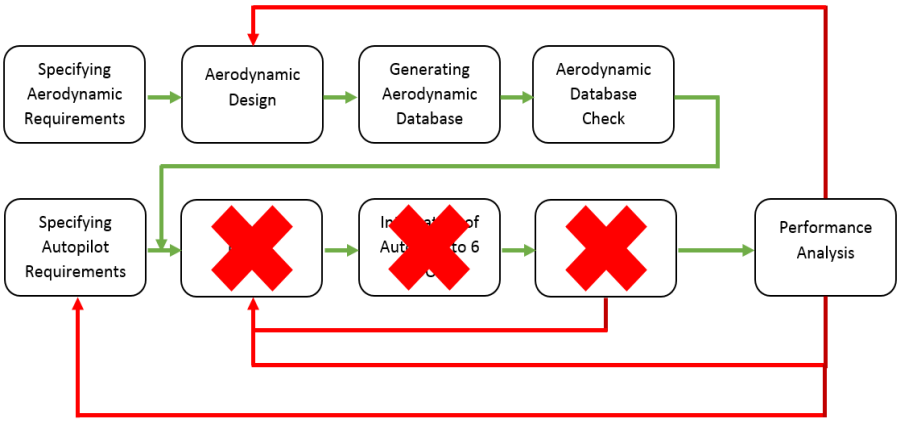


**Figure 2 Iterative Process for Pseudo 5-DOF Simulation Model**

In this thesis study, expected benefits are, 1) understanding the adjoint technique power and limitations, time varying phenomena effect on the results that does not exist in the literature explicitly, 2) developing Pseudo 5-DOF simulation model by implementing flight path kinematic equations instead of using transfer function to represent pitch and yaw angular dynamics, 3) building state-space structured stochastic adjoint model and to investigate the accuracy for a nonlinear missile-target engagement scenario and 4) comparing accuracy of the adjoint and linear forward models are monitored with respect to nonlinear simulation model against stochastic target maneuver disturbances by utilizing the describing function technique.

# CHAPTER 2

# MODELING

## 2.1 6-DOF Model

6-DOF simulation model has the highest fidelity and has a crucial role for system design. Properly validated and verified 6-DOF model is an invaluable tool to minimize the flight tests that cause too much cost and to figure out system performance(Sezer, Nalcı, & Kutay, 2015). The model is convenient for all flying vehicles but in different forms. Also, these models can have various fidelity levels depending on the system/subsystem detail. For SAM applications, 6-DOF model is developed and constructed to predict miss distance, to generate fire envelope, to study integrated guidance, control & navigation, to test seeker performance, to understand integrated missile, fuze and warhead performance, to analyze flight test security, to use in hardware-in-the-loop tests, to examine flight test telemeter data etc. In addition, the model is suitable for stochastic analysis to figure out the effects of uncertainties.

The developed and constructed 6-DOF model in this study is divided into ten subsystems namely; missile kinematics, missile dynamics, aerodynamics, environment, propulsion, inertia & mass, control actuation system, autopilot, guidance algorithm, and seeker. Note that it is assumed there is no inertial navigation system (INS) dynamics so INS model is not implemented.

### 2.1.1 Missile Kinematics

In this section, missile translational and rotational velocity vectors, position vectors, Euler and flight path angles and direction cosine matrix calculations are presented. In Eq.(1), body angular velocity vector is shown and it can be seen that the angular velocities are the direct integration of the angular accelerations with initial condition by defining in the body coordinate system.

$$\begin{bmatrix} \dot{p} \\ \dot{q} \\ \dot{r} \end{bmatrix}^{(B)} = \dot{\omega}^{(B)}_{O_B/O_I} \quad \text{then} \quad \omega^{(B)}_{O_B/O_I} = \int \dot{\omega}^{(B)}_{O_B/O_I} dt + \omega^{(B)}_{O_B/O_I,0} \tag{1}$$

In Eq.(2), the missile body translational velocity vector exists and similar with the angular velocity, it is a direct integration of the body translational acceleration with initial condition by defining in the body coordinate system.

$$\begin{bmatrix} \dot{u} \\ \dot{v} \\ \dot{w} \end{bmatrix}^{(B)} = \dot{V}^{(B)}_{O_B/O_I} \quad \text{then} \quad V^{(B)}_{O_B/O_I} = \int \dot{V}^{(B)}_{O_B/O_I} dt + V^{(B)}_{O_B/O_I,0} \tag{2}$$

In Eq.(3), the missile inertial translational velocity and inertial position vectors are depicted and note that the inertial velocity is the transformation from body coordinate system to inertial coordinate system and the inertial position is the direct integration of the inertial velocity with proper initial condition.

$$\begin{bmatrix} V_X \\ V_Y \\ V_Z \end{bmatrix}^{(I)} = V^{(I)}_{O_B/O_I} = C^{(I,B)} V^{(B)}_{O_B/O_I} \quad \text{then} \quad P^{(I)}_{O_B/O_I} = \int V^{(I)}_{O_B/O_I} dt + P^{(I)}_{O_B/O_I,0} \tag{3}$$

In Eq.(4), the transformation matrix from missile body to inertial coordinates system and Euler Angle calculation are considered. Once the Euler Angles of the missile are obtained, forming the transformation matrix is easy and is used in Eq.(3).

$$\begin{bmatrix} \phi \\ \theta \\ \psi \end{bmatrix} = \int \omega^{(I)}_{O_B/O_I} dt + \begin{bmatrix} \phi_0 \\ \theta_0 \\ \psi_0 \end{bmatrix}$$
$$C^{(I,B)} = \begin{bmatrix} \mathrm{c}\phi\,\mathrm{c}\theta & \mathrm{s}\psi\,\mathrm{c}\theta & -\mathrm{s}\theta \\ \mathrm{c}\psi\sin\theta\,\mathrm{s}\phi - \mathrm{s}\psi\,\mathrm{c}\phi & \mathrm{s}\psi\,\mathrm{s}\theta\,\mathrm{s}\phi + \mathrm{c}\psi\,\mathrm{c}\phi & \mathrm{c}\theta\,\mathrm{s}\phi \\ \mathrm{c}\psi\sin\theta\,\mathrm{c}\phi + \mathrm{s}\psi\,\mathrm{s}\phi & \mathrm{s}\psi\,\mathrm{s}\theta\,\mathrm{c}\phi - \mathrm{c}\psi\,\mathrm{s}\phi & \mathrm{c}\theta\,\mathrm{c}\phi \end{bmatrix} \tag{4}$$

However, in Eq.(4), $\omega^{(I)}_{O_B/O_I}$ is essential so that Euler Angle calculation can be done therefore, the missile body angular velocity is required to transform in to the inertial coordinate system and the transformation matrix is depicted in Eq.(5).

$$\begin{bmatrix}\dot{\phi}\\ \dot{\theta}\\ \dot{\psi}\end{bmatrix}=\omega_{O_B/O_I}^{(I)} \quad \text{then} \quad \omega_{O_B/O_I}^{(I)}=\begin{bmatrix}1 & \mathrm{s}\phi\tan\theta & \mathrm{c}\phi\,\mathrm{t}\theta\\ 0 & \mathrm{c}\phi & -\mathrm{s}\phi\\ 0 & \mathrm{s}\phi/\mathrm{c}\theta & \mathrm{c}\phi/\mathrm{c}\theta\end{bmatrix}\omega_{O_B/O_I}^{(B)} \tag{5}$$

### 2.1.2 Missile Dynamics

In this section, total force and moment acting on the missile, total accelerations and flight parameters are calculated. Total force formulations are showed in Eq.(6) and Eq.(7) (Zipfel, 2007).

$$F_T^{(B)}=F_A^{(B)}+F_P^{(B)}+C^{(B,\mathrm{I})}F_G^{(I)} \tag{6}$$

$$\begin{bmatrix}F_X\\ F_Y\\ F_Z\end{bmatrix}_T^{(B)}=0.5\rho V^2 S_{ref}\begin{bmatrix}C_{X,total}\\ C_{Y,total}\\ C_{Z,total}\end{bmatrix}+\begin{bmatrix}T\\ 0\\ 0\end{bmatrix}+C^{(B,\mathrm{I})}\begin{bmatrix}0\\ 0\\ mg\end{bmatrix} \tag{7}$$

Total force calculation is done for missile body coordinate system and it is represented by $F_T$, which is the summation of $F_A$, $F_P$ and $F_G$ that are aerodynamic, propulsive and gravitational forces respectively. It is assumed that thrust force is perfectly aligned with missile body, which means there is no misalignment so the motor does not generate moment on the body. Gravitational acceleration is modeled on earth coordinate system so it is transformed in to missile body coordinate system for consistency.

Similar with the forces, moment equations are written in missile body coordinate system and the formulation is depicted in Eq.(8) (Zipfel, 2007).

$$\begin{aligned}\vec{M}_T&=\frac{d\left(\breve{I}\cdot\vec{\omega}_{O_B/O_I}\right)}{dt}+\vec{\omega}_{O_B/O_I}\times\breve{I}\cdot\vec{\omega}_{O_B/O_I}\\ M_T^{(B)}&=I^{(B)}\dot{\omega}_{O_B/O_I}^{(B)}+\tilde{\omega}_{O_B/O_I}^{(B)}I^{(B)}\omega_{O_B/O_I}^{(B)}\end{aligned} \tag{8}$$

$$\begin{bmatrix} M_X \\ M_Y \\ M_Z \end{bmatrix}_T^{(B)} = \begin{bmatrix} I_{XX} & I_{XY} & I_{XZ} \\ I_{XY} & I_{YY} & I_{YZ} \\ I_{XZ} & I_{YZ} & I_{ZZ} \end{bmatrix} \begin{bmatrix} \dot{p} \\ \dot{q} \\ \dot{r} \end{bmatrix} + \begin{bmatrix} 0 & -r & q \\ r & 0 & -p \\ -q & p & 0 \end{bmatrix} \begin{bmatrix} I_{XX} & I_{XY} & I_{XZ} \\ I_{XY} & I_{YY} & I_{YZ} \\ I_{XZ} & I_{YZ} & I_{ZZ} \end{bmatrix} \begin{bmatrix} p \\ q \\ r \end{bmatrix}$$
$$\begin{bmatrix} M_X \\ M_Y \\ M_Z \end{bmatrix}_T^{(B)} = 0.5\rho V^2 S_{ref} l_{ref} \begin{bmatrix} C_{L,total} \\ C_{M,total} \\ C_{N,total} \end{bmatrix} \tag{9}$$

Total aerodynamic moment coefficients and therefore, total moment action on the body is known. On the other hand, total moment is a function of missile moment of inertia, body angular velocity and body angular acceleration. Note that, in the first line of the Eq.(8), dot product of moment of inertia and body angular velocity vector exist but derivative of the moment of inertia is assumed negligible depending on time.

Finally, missile flight parameter equations are presented in Eq.(10).

$$\begin{aligned} \alpha &= \arctan\left(\frac{w}{u}\right) \\ \beta &= \arcsin\left(\frac{v}{V}\right) \\ V &= \sqrt{u^2 + v^2 + w^2} \\ M &= \frac{V}{a} \end{aligned} \tag{10}$$

$$\begin{bmatrix} \delta_e \\ \delta_r \\ \delta_a \end{bmatrix} = \begin{bmatrix} 0.25 & 0.25 & -0.25 & -0.25 \\ 0.25 & -0.25 & -0.25 & 0.25 \\ 0.25 & 0.25 & 0.25 & 0.25 \end{bmatrix} \begin{bmatrix} \delta_1 \\ \delta_2 \\ \delta_3 \\ \delta_4 \end{bmatrix}$$

Missile angle-of-attack, side-slip angle, total velocity, Mach number and virtual aerodynamic control surface deflection angles, which are used to obtain aerodynamic coefficients, are generated.

### 2.1.3 Aerodynamics

Missile aerodynamic properties are implemented in tabular form to read in terms of states. Database is basically divided in to two sections such as; static and dynamic coefficients. Static coefficients are presented in Eq.(11).

$$
\begin{aligned}
&C_X\left(M,\alpha,\beta,\delta_e,\delta_r\right)\\
&C_Y\left(M,\alpha,\beta,\delta_e,\delta_r\right)\\
&C_Z\left(M,\alpha,\beta,\delta_e,\delta_r\right)\\
&C_L\left(M,\alpha,\beta,\delta_a\right)\\
&C_M\left(M,\alpha,\beta,\delta_e,\delta_r\right)\\
&C_N\left(M,\alpha,\beta,\delta_e,\delta_r\right)
\end{aligned}
\tag{11}
$$

Note that four control surfaces are popular for missile systems; control surface angles depicted in Eq.(11), are virtual control surface angles and are obtained by utilizing pseudo inverse transformation matrix.

In Eq.(12), dynamic coefficients are depicted and these parameters depend on Mach number and center of gravity of the missile. Since the center of mass decreases during the boost phase (motor is burning, propellant is consuming), control effectiveness changes also.

$$
\begin{aligned}
&C_{Yr}\left(M,x_{cg}\right) \qquad C_{Mq}\left(M,x_{cg}\right)\\
&C_{Y\dot{\beta}}\left(M,x_{cg}\right) \qquad C_{M\dot{\alpha}}\left(M,x_{cg}\right)\\
&C_{Lp}\left(M,x_{cg}\right) \qquad C_{Nr}\left(M,x_{cg}\right)\\
&C_{Zq}\left(M,x_{cg}\right) \qquad C_{N\dot{\beta}}\left(M,x_{cg}\right)\\
&C_{Z\dot{\alpha}}\left(M,x_{cg}\right)
\end{aligned}
\tag{12}
$$

In Eq.(13), total aerodynamic translational and rotational coefficient formulations are depicted.

$$
\begin{aligned}
Cx_{total} &= Cx \\
Cy_{total} &= Cy + \left(\frac{l_{ref}}{2V_{air}}\right)\left(Cy_r r + Cy_{\dot{\beta}}\dot{\beta}\right) \\
Cz_{total} &= Cz + \left(\frac{l_{ref}}{2V_{air}}\right)\left(Cz_q q + Cz_{\dot{\alpha}}\dot{\alpha}\right) \\
Cl_{total} &= Cl + \left(\frac{l_{ref}}{2V_{air}}\right)Cl_p p \\
Cm_{total} &= \left(Cm - l_{ref}\left(x_{cg} - x_{ref}\right)Cz\right) + \left(\frac{l_{ref}}{2V_{air}}\right)\left(Cm_q q + Cm_{\dot{\alpha}}\dot{\alpha}\right) \\
Cn_{total} &= \left(Cn + l_{ref}\left(x_{cg} - x_{ref}\right)Cy\right) + \left(\frac{l_{ref}}{2V_{air}}\right)\left(Cn_r r + Cn_{\dot{\beta}}\dot{\beta}\right)
\end{aligned}
\tag{13}
$$

### 2.1.4 Environment

Proper environment model is crucial since it affects the missile performance directly. In this 6-DOF simulation model, gravity and atmosphere models are utilized based on the missile altitude. Although gravity does not change too much since the 6-DOF model flight altitude is between from 0 to 6000m, gravitational effects are not neglected. On the other hand, atmosphere model is more dominant compared to gravity especially variation in air density and speed of sound, which are considered to missile acceleration capability.

### 2.1.5 Propulsion

Generic boost motor is implemented in tabular form for a fixed time interval to get the thrust and exit mass values. and shown in Figure 3.

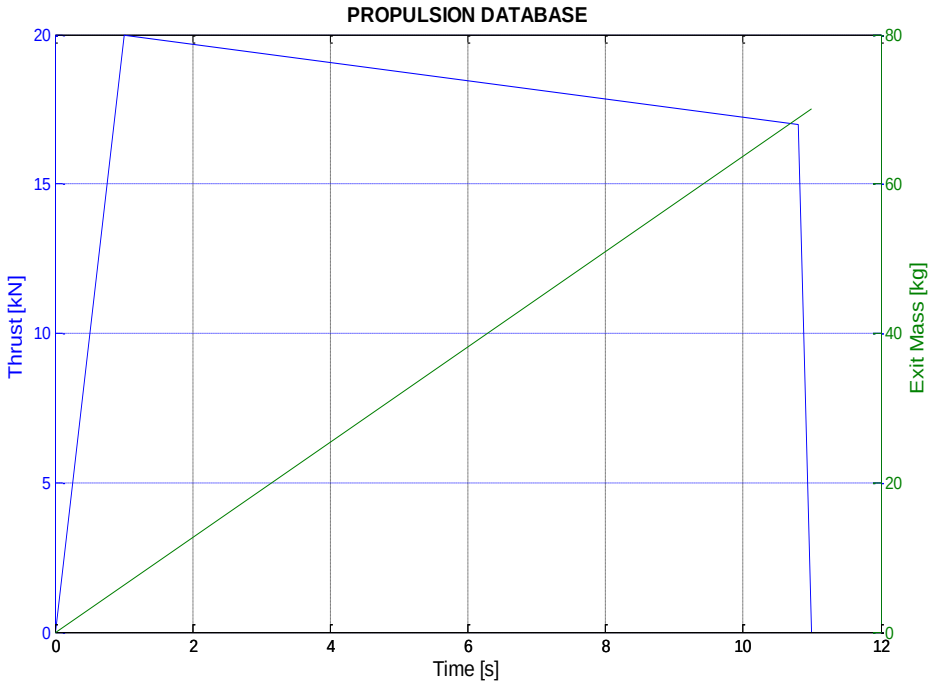


**Figure 3 Generic Boost Motor Thrust**

### 2.1.6 Inertia & Mass

Missile mass and moment of inertia values are implemented to the model according to propulsion database since exit mass is taken from propulsion database. Therefore, change in the mass, moment of inertia and missile center of gravity can be generated.

### 2.1.7 Control Actuation System (CAS)

Generic second order transfer function is used to represent the control actuation system dynamics with control surface deflection and deflection rate limits.

### 2.1.8 Autopilot

Autopilot is responsible for tracing commands coming from guidance by generating control surface deflection commands to steer the missile. Generic 3-Loop acceleration autopilot is utilized in the 6-DOF model and the structure is depicted in Figure 4.

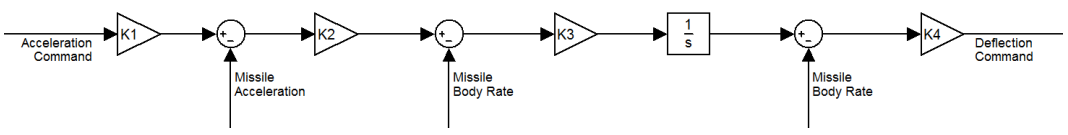


**Figure 4 Generic 3-Loop Acceleration Autopilot Structure**

### 2.1.9 Guidance Algorithm

Missile flight is divided in to three phases namely; launch phase, midcourse and terminal phases. In the launch phase, the missile is fired directly to the target and body pursuit guidance law is used to turn the body to the target for a fixed time interval. Target velocity and position information are assumed to be known perfectly. In the midcourse phase, True Proportional Navigation Guidance (TPGN) law is utilized to generate proper acceleration commands and same guidance law is used for terminal phase, too. However; line-of sight rate, which is one of the variables of the guidance law, is generated by the seeker and more aggressive acceleration commands are demanded by the algorithm since higher guidance gain value is applied. Note that terminal phase is started with the seeker lock-on to the target for a fixed range-to-go value.

### 2.1.10 Seeker

Generic second order transfer function is used to represent the seeker gimbal dynamics with field-of-regard angles limits. Therefore, generated line-of-sight rate by the seeker has a direct effect on the acceleration commands.

## 2.2 Pseudo 5 DOF Model

Various fidelity level of Pseudo 5-DOF simulation model studies exist in the literature for different purposes such as flight simulator, aircraft and missile performance analysis (Sezer et al., 2015). As explained in the introduction chapter, roll dynamic is discarded since most of the SAM systems are stabilized around zero roll rate. In addition, although the pitch and the yaw motions are not removed, they are not calculated in the model directly since these lateral angular dynamics are estimated to simplify the model. Accuracy of the approximation of these motions is crucial for missile Euler Angle prediction, which directly affects the missile trajectory estimation. Various techniques are utilized to represent behavior of the angular motions such as, implementing transfer functions (Hildreth, Linse, Ph, & Park, 2008). Transfer function approach is an easy way to understand the system behavior; however, it cannot capture the nonlinear behavior of the angular dynamics. On the other hand, Zipfel has derived the equations of motions of the Pseudo 5-DOF simulation for velocity coordinate system since the system is assumed as if point

mass with pseudo angular dynamics and all external forces, which are aerodynamic, propulsive and gravitational, acting on the missile are expressed to get the angular velocity of the velocity coordinate system with respect to the inertial coordinate system. In addition, pitch and yaw rates of the missile body with respect to inertial coordinate system are still required to calculate the missile Euler Angles and the incidence angles. Therefore, a simple autopilot is designed to simulate the missile lateral acceleration response to guidance acceleration command and related angular dynamics such as incidence angles and body rates (Zipfel, 2007).

Studies existing in the literature about the Pseudo 5-DOF simulation models show that it's fidelity is close to the 6-DOF and can be used for various purposes instead of the 6-DOF.

In this thesis study, the capability of the Pseudo 5-DOF simulation model is examined and it has two improvements compared to the studies found in the literature and these are 1) more accurate drag prediction by the integration of three dimensional incidence angle estimation, 2) better lateral angular dynamics calculation by implementing flight path kinematic equation, which is explained following sections. Note that, since the capability of the model is considered, similar guidance algorithm, aerodynamic and propulsive databases, autopilot gains, seeker dynamics are utilized with the 6-DOF model. It basically has nine subsystems namely; missile kinematics, missile dynamics, aerodynamics, environment, propulsion, mass, autopilot - control actuation - airframe, guidance algorithm and seeker.

### 2.2.1 Missile Kinematics

In this section, the Pseudo 5-DOF simulation model kinematic equations are explained and Eq.(1), Eq.(2), Eq.(3), Eq.(4) and Eq.(5) are utilized for the calculations.

In addition to above equations, missile body angular velocity vector, which is represented as $\vec{\omega}^{(B)}_{O_B/O_I}$, is crucial for kinematic calculations and it is estimated by

implementing the flight path kinematic equations mentioned as improvement on the body angular velocity prediction.

It is better to mention the coordinate systems, which is depicted in Figure 5, before deriving the flight path equations.

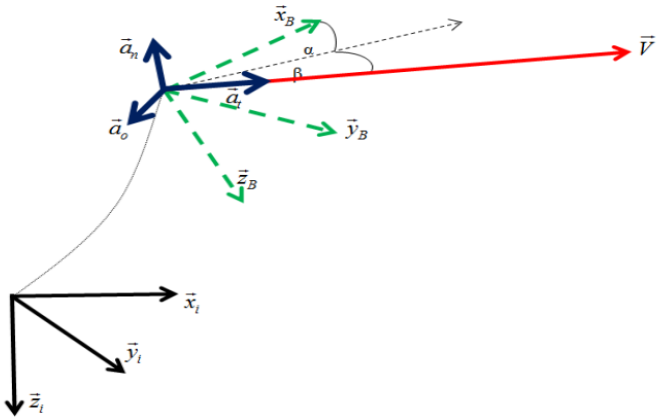


**Figure 5 Coordinate Systems (Sezer et al., 2015)**

Inertial coordinate, body coordinates and flight path coordinate systems are shown in $(\vec{x}_I, \vec{y}_I, \vec{z}_I)$, $(\vec{x}_B, \vec{y}_B, \vec{z}_B)$ and $(\vec{a}_T, \vec{a}_0, \vec{a}_N)$ respectively and note that flight path coordinate system is also used to represent the missile translational accelerations. Tangential and normal accelerations defined on the flight coordinate system are implemented as $\vec{a}_T$ and $\vec{a}_N$ respectively. Therefore, the total translational acceleration of the missile in the related coordinate is shown in Eq.(14).

$$\vec{a}_{O_B/O_I} = a_T \vec{u}_{T,O_F/O_I} + a_N \vec{u}_{N,O_F/O_I} \tag{14}$$

In addition, total translational acceleration of the missile can be formulated according to the Coriolis theorem and depicted in Eq.(15).

$$\begin{aligned}
\vec{a}_{O_B/O_I} &= \frac{d\vec{V}_{O_F/O_I}}{dt} + \vec{\omega}_{O_F/O_I} \times \vec{V}_{O_F/O_I} \\
\vec{a}_{O_B/O_I} &= \dot{V}\vec{u}_{T,O_F/O_I} + \left[\vec{\omega}_{0,O_F/O_I} + \vec{\omega}_{T,O_F/O_I} + \vec{\omega}_{N,O_F/O_I}\right] \times \left[V\vec{u}_{T,O_F/O_I}\right] \\
\vec{a}_{O_B/O_I} &= \dot{V}\vec{u}_{T,O_F/O_I} + \omega_0 V\vec{u}_{N,O_F/O_I} - \omega_N V\vec{u}_{0,O_F/O_I}
\end{aligned} \tag{15}$$

By the definition of the oscillation plane, $\vec{a}_0$ is taken as zero and by equating the Eq.(14) with the Eq.(15), following relation is obtained.

$$\begin{aligned} \omega_0 V &= a_N \\ \omega_0 &= \frac{a_N}{V} \end{aligned} \tag{16}$$

In addition, it is known that $\vec{u}_0 = \vec{u}_T \times \vec{u}_N$, which is the binormal unit vector, the angular velocity of the binormal axis is obtained in Eq.(17).

$$\begin{aligned} \vec{u}_{0,O_F/O_I} &= \frac{\vec{V}_{O_F/O_I} \times \vec{a}_{O_F/O_I}}{\left|\vec{V}_{O_F/O_I} \times \vec{a}_{O_F/O_I}\right|} \\ \vec{\omega}_{0,O_F/O_I} &= \frac{a_N}{V} \frac{\vec{V}_{O_F/O_I} \times \vec{a}_{O_F/O_I}}{\left|\vec{V}_{O_F/O_I} \times \vec{a}_{O_F/O_I}\right|} \end{aligned} \tag{17}$$

Since vectors are additive by definition, the body angular velocity vector is obtained and shown in Eq.(18).

$$\vec{\omega}_{O_F/O_I} = \vec{\omega}_{O_F/O_B} + \vec{\omega}_{O_B/O_I} \tag{18}$$

Then, the angular velocity of the missile can be expressed as in Eq.(19).

$$\begin{aligned} \vec{\omega}_{O_B/O_F} &= -\dot{\beta}\vec{u}_{N,O_F/O_I} + \dot{\alpha}\vec{u}_{Y,O_B/O_I} \\ \vec{\omega}_{O_F/O_B} &= \dot{\beta}\vec{u}_{N,O_F/O_I} - \dot{\alpha}\vec{u}_{Y,O_B/O_I} \\ \omega^{(B)}_{O_F/O_B} &= \begin{bmatrix} -\dot{\beta}\sin\alpha \\ -\dot{\alpha} \\ \dot{\beta}\cos\alpha \end{bmatrix} \\ \omega^{(B)}_{O_F/O_I} &= \begin{bmatrix} p \\ q \\ r \end{bmatrix} + \begin{bmatrix} -\dot{\beta}\sin\alpha \\ -\dot{\alpha} \\ \dot{\beta}\cos\alpha \end{bmatrix} = \begin{bmatrix} p - \dot{\beta}\sin\alpha \\ q - \dot{\alpha} \\ r + \dot{\beta}\cos\alpha \end{bmatrix} \end{aligned} \tag{19}$$

Angular velocity vector of the flight path with respect to inertial, flight path with respect to body and body to inertial coordinates are represented as $\vec{\omega}_{O_B/O_F}$, $\vec{\omega}_{O_F/O_B}$ and $\vec{\omega}_{O_B/O_I}$ respectively. Flight path coordinate to body coordinate transformation sequence is $]^B \xleftarrow{\alpha}] \xleftarrow{-\beta}]^F$ (Zipfel, 2007)

and the related transformation matrix is shown in Eq.(20).

$$C^{(B,F)} = \begin{bmatrix} \mathrm{c}\alpha\,\mathrm{c}\beta & -\mathrm{c}\alpha\,\mathrm{s}\beta & -\mathrm{s}\alpha \\ \mathrm{s}\beta & \mathrm{c}\beta & 0 \\ \mathrm{s}\alpha\,\mathrm{c}\beta & -\mathrm{s}\alpha\,\mathrm{s}\beta & \mathrm{c}\alpha \end{bmatrix} \tag{20}$$

Note that by definition $\omega_N$ is zero so the body angular velocity can be defined as;

$$\begin{aligned} \vec{\omega}_{O_F/O_I} &= \omega_0 \vec{u}_{0,O_F/O_I} + \omega_N \vec{u}_{N,O_F/O_I} + \omega_T \vec{u}_{T,O_F/O_I} \\ \vec{\omega}_{O_F/O_I} &= \omega_0 \vec{u}_{0,O_F/O_I} + \omega_T \vec{u}_{T,O_F/O_I} \\ \omega^{(B)}_{O_F/O_I} &= \begin{bmatrix} \omega_T \cos\alpha\cos\beta \\ \omega_T \sin\beta \\ \omega_T \sin\alpha\cos\beta \end{bmatrix} + \begin{bmatrix} \omega_0^{B1} \\ \omega_0^{B2} \\ \omega_0^{B3} \end{bmatrix} \end{aligned} \tag{21}$$

Since the $\vec{\omega}_0^B$ is obtained in Eq.(17), components are utilized as $\omega_0^{B_1}$, $\omega_0^{B_2}$ and $\omega_0^{B_3}$ then the Eq.(19) and Eq.(21) are implemented together so that the angular velocity of the missile is obtained in Eq.(22). Finally, roll dynamics is discarded based on the assumption of the zero roll rate, equation is solved for pitch and yaw rates that are depicted as $q$ and $r$ respectively.

$$\begin{aligned} \begin{bmatrix} p \\ q \\ r \end{bmatrix} + \begin{bmatrix} -\dot{\beta}\sin\alpha \\ -\dot{\alpha} \\ \dot{\beta}\cos\alpha \end{bmatrix} &= \begin{bmatrix} \omega_T \cos\alpha\cos\beta \\ \omega_T \sin\beta \\ \omega_T \sin\alpha\cos\beta \end{bmatrix} + \begin{bmatrix} \omega_0^{B1} \\ \omega_0^{B2} \\ \omega_0^{B3} \end{bmatrix} \\ \begin{bmatrix} p \\ q \\ r \end{bmatrix} &= \begin{bmatrix} \omega_T \cos\alpha\cos\beta + \omega_0^{B1} + \dot{\beta}\sin\alpha \\ \omega_T \sin\beta + \dot{\alpha} + \omega_0^{B2} \\ \omega_T \sin\alpha\cos\beta - \dot{\beta}\cos\alpha + \omega_0^{B3} \end{bmatrix} \end{aligned} \tag{22}$$

### 2.2.2 Missile Dynamics

In this section, total forces that are aerodynamic, propulsion and gravity, acting on the missile are considered. Propulsive and gravitational forces are obtained similar to the 6-DOF model but there is a difference in the calculation of the aerodynamic forces. Also, note that the moment acting on the missile is not implemented according to the assumption of the model. Aerodynamic forces acting on the missile are divided in to two parts such as, translational and lateral forces.

Translational force is generated by utilizing the drag coefficient acting on the missile, which is obtained from drag coefficient database. Lateral forces are based on the missile lateral accelerations that are generated by the autopilot – control actuation system – airframe subsystem. Once the total acceleration is calculated, the missile translational acceleration on the body coordinate is obtained and is used in kinematic equations and flight parameters shown in Eq.(23).

$$\begin{aligned} \alpha &= \arctan\left(\frac{w}{u}\right) \\ \beta &= \arcsin\left(\frac{v}{V}\right) \\ V &= \sqrt{u^2 + v^2 + w^2} \\ M &= \frac{V}{a} \quad \text{where} \quad a\text{: speed of sound} \end{aligned} \tag{23}$$

### 2.2.3 Aerodynamics

Missile aerodynamic coefficients are used in tabular form in terms of the flight states similar with the 6-DOF model. However, since the classical autopilot structure is not used in this model, control surface effects must be discarded; therefore, five dimensional aerodynamic databases are reformed for trim regions and static coefficients are shown in Eq.(24).

$$\begin{aligned} &Cx(M, \alpha, \beta) \\ &Cy(M, \beta) \\ &Cz(M, \alpha) \end{aligned} \tag{24}$$

Note that, lateral coefficients are decoupled so that it is assumed that the lateral force depends on the Mach number and dominant angular motion. Although these lateral forces exist in tabular form, they are not utilized to direct calculation of the missile aerodynamic forces since they are used for incidence angle estimation to predict better drag coefficient due to missile lateral acceleration.

### 2.2.4 Environment

The importance of the environment model is explained in the previous sections and same environment of the 6-DOF model is implemented so that the Pseudo 5-DOF model make as similar as possible to the 6-DOF.

### 2.2.5 Propulsion

Same propulsion database of the 6-DOF is implemented and used for this model.

### 2.2.6 Mass

Same mass properties of the 6-DOF is implemented and utilized. Note that, since the missile angular dynamics are not solved but estimated, inertia properties are discarded also.

### 2.2.7 Autopilot – Control Actuation System (CAS) – Airframe

As mentioned in the previous sections, missile acceleration response is represented by utilizing transfer function and the structure of this subsystem is shown in Figure 6.

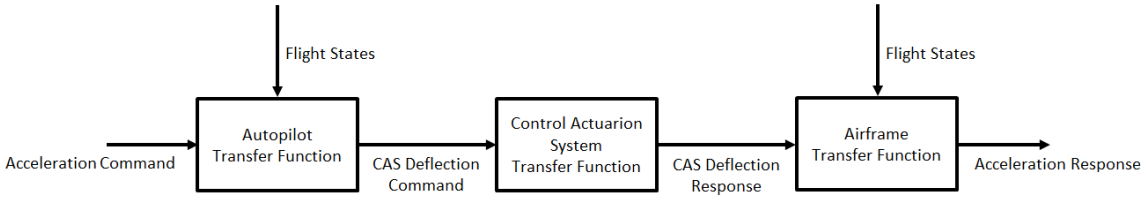


**Figure 6 Autopilot-Control Actuation System-Airframe Structure**

In order to figure out the capability of the Pseudo 5-DOF model, acceleration response is tried to make as similar as possible; therefore, 6-DOF autopilot gains are utilized and generated transfer functions depending on the Mach number. In addition, same control actuation system dynamics of the 6-DOF is taken and 6-DOF airframe is modeled as transfer function.

On the other hand, since same parameters of the 6-DOF are implemented, the structure of the Pseudo 5-DOF model enables the designer to perform parametric study especially for the integrated guidance and control study.

### 2.2.8 Guidance Algorithm

Same guidance algorithm of the 6-DOF is implemented and used for this model.

### 2.2.9 Seeker

Same seeker model of the 6-DOF is implemented and used.

## 2.3 Adjoint Model

In this study, different Adjoint models are developed and constructed to figure out the technique's capability and to improve the method. Three types of the Adjoint models are constructed such as, classical adjoint approach with time varying parameters, adjoint with describing function to monitor the performance of the method for missile acceleration saturation nonlinearity and state space structured adjoint whose states are populated by the nonlinear simulation model to handle the engagement nonlinearities.

### 2.3.1 Classical Adjoint Model

It is better to mention about the mathematics of the technique before explaining the model.

There is an adjoint impulse response for every linear original system impulse response and relation is expressed in Eq.(25) (Zarchan, 2012).

$$h^{*}\left(t_F - t_I, t_F - t_O\right) = h\left(t_O, t_I\right) \tag{25}$$

$t_F$, $t_O$ and $t_I$ are final time, observation time and impulse application time respectively, which means that the impulse applied at $t_I$ and the response observed at $t_O$ is equal to the adjoint of the impulse at $t_F - t_O$ and observed at $t_F - t_I$. Note that, classical linear analysis is essential for whole simulation time however, a single solution in the adjoint outcome is enough to get the same results meaning that a single adjoint run for whole simulation time is sufficient for to generate many classical simulation responses for different impulse application times and a single observation time. In Figure 7, various impulse times and the same observation time is depicted clearly.

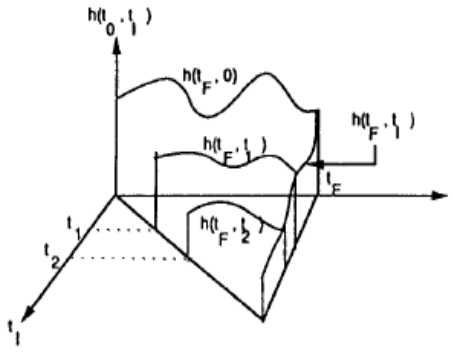


**Figure 7 Impulse Response of the Classical Model** (Zarchan, 2012)

The observation time and simulation final time are taken as equal to each other for adjoint applications in general therefore, the Eq.(25) is modified like in Eq.(26).

$$h^*\left(t_F - t_I, 0\right) = h\left(t_F, t_I\right) \tag{26}$$

Convolution integral is utilized to obtain the response of the linear system to an input and is depicted in Eq.(27) where $\tau$ and $t$ represent the impulse application time and observation time (final time) respectively.

$$\begin{aligned} y(t) &= \int_{-\infty}^{t} x(\tau) h\left(t, \tau\right) d\tau \\ y(t) &= \int_{0}^{t} x(\tau) h\left(t, \tau\right) d\tau \end{aligned} \tag{27}$$

It is assumed that a step input $a$ is applied to the system and the Eq.(27) becomes;

$$y(t) = a\int_{0}^{t} h\left(t, \tau\right) d\tau \tag{28}$$

If the adjoint impulse response is implemented to the Eq.(28), following formulations are obtained.

$$\begin{aligned} y(t) &= a\int_{0}^{t} h^*\left(t_F - \tau, t_F - t\right) d\tau \\ x &= t_F - \tau \\ dx &= -d\tau \\ y(t) &= a\int_{t_F - t}^{t_F} h^*\left(x, t_F - t\right) dx \\ &\text{if } t = t_F \\ y(t) &= a\int_{0}^{t_F} h^*\left(x, 0\right) dx \end{aligned} \tag{29}$$

Since the original system inputs become the adjoint output and the technique is linear, it allows to superpose the adjoint results then, system response to different inputs can be obtained and the formulation is shown in Eq.(30) (Zarchan, 2012).

$$y(t_F) = \frac{y(t_F)}{\sqrt{x_1}} + \frac{y(t_F)}{\sqrt{x_2}} + \ldots \tag{30}$$

According to adjoint method derivation and equations, it seems very powerful technique to figure out the system response especially for the conceptual design phase of the missile. However, the issue is to find the adjoint impulse response and in the book of (Laning & Battin, 1956), construction rules are derived to simulate the adjoint method, which is easy to construct and compatible with today's simulation programs. In order to construct Adjoint model, following rules must be applied (Domenic Bucco, 2010).

1) Convert all system inputs to the equivalent impulses,
2) All signal directions must be reversed,
3) All system inputs and outputs are switched in to adjoint outputs and inputs respectively,
4) Change all summing and branch points in to branch and summing points respectively,
5) All time varying elements must be changed in to the adjoint time,
6) Adjoint input, which is impulse, is applied at the selected output of the original system,

In this thesis study, classical adjoint technique performance is compared with nonlinear models as mentioned although the concept of the method is different from 6-DOF and Pseudo 5-DOF simulation models. It is expected that the results of the models matches at some point that the nonlinearities are not dominant. It is important to understand under what conditions the adjoint method loses its power due to nonlinearity. On the other hand, the model is constructed to include the nonlinearities to observe if any reasonable requirement can be derived for the conceptual design phase without depending on the nonlinear models.

In order to utilize adjoint method, engagement geometry must be linearized (Zarchan, 2012) and linearization will be expressed for better understanding of the structure. In the Zarchan's book, the procedure is explained clearly but it is required to detail the engagement for the comparison analyses.

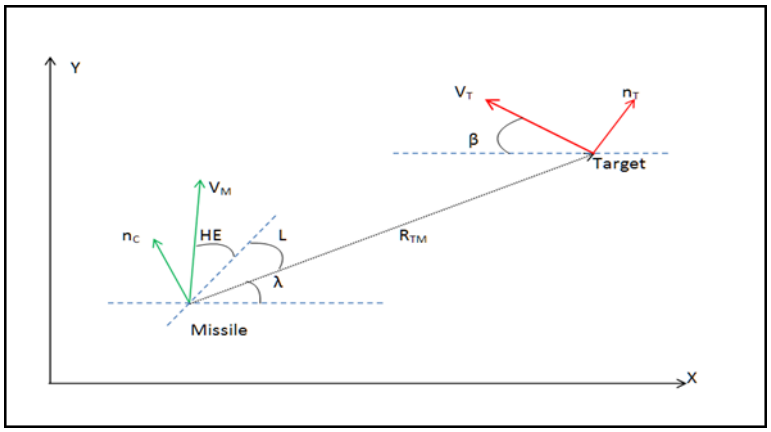


**Figure 8 Engagement Geometry** (Sezer et al., 2015)

In Figure 8, head-on missile-target engagement scenario is depicted and small angle assumption is considered for the compatibility. Note that the angles, which are shown, are not small enough to make this assumption, fidelity of the adjoint technique would be questionable.

The difference between the positions of the missile and the target is defined as miss distance and expressed in $y$ and the relation is formulated in Eq.(31).

$$\begin{aligned} \ddot{y} &= n_T \cos(\beta) - n_C \cos(\lambda) \\ \ddot{y} &= n_T - n_C \end{aligned} \tag{31}$$

$n_T$, $n_C$, $\beta$ and $\lambda$ are the target acceleration, missile acceleration, target heading and line-of-sight angles respectively and angles are takes as zero due to small angle assumption. In this model, TPNG is implemented and the guidance law generates acceleration commands to keep the line-of-sight (LOS) angle around zero but LOS angle rate is essential to generate acceleration command so the LOS angle is expressed analytically in Eq.(32).

$$\lambda(t) = \frac{y(t)}{R(t)} \tag{32}$$

Closing velocity of the scenario is the summation of the missile and target velocities since they are almost head-on.

$$V_C(t) = V_M(t) + V_T(t) \tag{33}$$

$R(t)$, which represents the range-to-go value of the missile to the target, can be obtained by direct integration of the closing velocity in reverse direction in time due to time-to calculation.

$$R(t) = (t_F - t)V_C(t) \tag{34}$$

The acceleration command is shown in Eq.(35).

$$n_C = NV_C(t)\dot{\lambda} \tag{35}$$

$N$ is the effective guidance navigation constant and $\dot{\lambda}$ represents the LOS rate, which is expressed in Eq.(36).

$$\begin{aligned} \dot{\lambda} &= \frac{\dot{y}(t)R(t) - y(t)\dot{R}(t)}{R(t)^2} = \frac{\dot{y}(t)V_C(t)(t_F - t) - y(t)V_C(t)}{V_C^2(t)(t_F - t)^2} \\ \dot{\lambda} &= \frac{\dot{y}(t)}{V_C(t)(t_F - t)} - \frac{y(t)}{V_C(t)(t_f - t)^2} \end{aligned} \tag{36}$$

In Figure 8, $HE$ and $L$ exist to represent heading error and lead angles respectively. The meaning of the lead angle is the necessary angle to hit the target without generating acceleration command, zero effort. Heading error is utilized for the deviation angle with respect to the lead angle. For example, if the target maneuvers, missile velocity vector should not be aligned with the LOS that is defined in Figure 8. On the other hand, adjoint analyses are held generally for the terminal phases of the missile fly-out where the seeker is locked-on the target. However, when the seeker is locked on the target, missile velocity vector is not aligned with the required direction due to uncertainties and the error on the system in real world so that $HE$ is implemented to model this uncertainty as initial condition.

In addition, target and the missile are not at the same line and it is considered as target initial cross range position initial condition. In order to represent these initial conditions, engagement geometry, which is shown in Figure 8, should be decomposed to linearized homing geometry.

At first, target initial cross range position condition can be implemented as initial LOS angle and depicted in Eq.(37).

$$y(0) = R(0)\sin\left(\lambda(0)\right) \tag{37}$$

Then, $HE$ and $L$ are used to represent the heading error and lead angle and these angles are implemented as missile initial lateral velocity that is expressed in Eq.(38).

$$\dot{y}(0) = V_T(0)\sin\left[\beta(0)\right] - V_M(0)\sin\left[\lambda(0) + L + HE\right] \tag{38}$$

In addition, the Adjoint model includes missile acceleration response dynamics to acceleration command generated by the guidance and seeker gimbal dynamics. Response of the missile is implemented as transfer function that depends on the missile speed, which is implemented as time varying parameters. Similar gains are used for autopilot-control actuation system-airframe as implemented in the Pseudo 5-DOF model. Also, seeker gimbal dynamics is modeled as a first order transfer function with the same time constant value of the 6-DOF and the Pseudo 5-DOF. Original linear system is depicted in Figure 9. Note that initial conditions defined in Eq.(37) and Eq.(38) are implemented as impulse function for the legacy of the adjoint construction rules since they are the outcomes of the adjoint but they can also be implemented in integrator blocks.

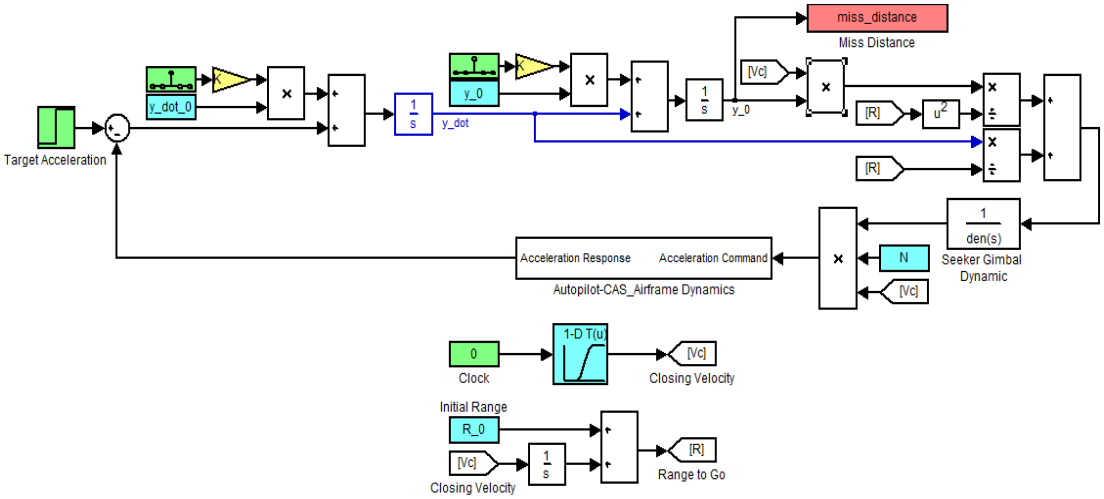


**Figure 9 Original Linear Simulation Model**

The adjoint model is constructed by applying the construction rules, which are explained, and is presented in Figure 10.

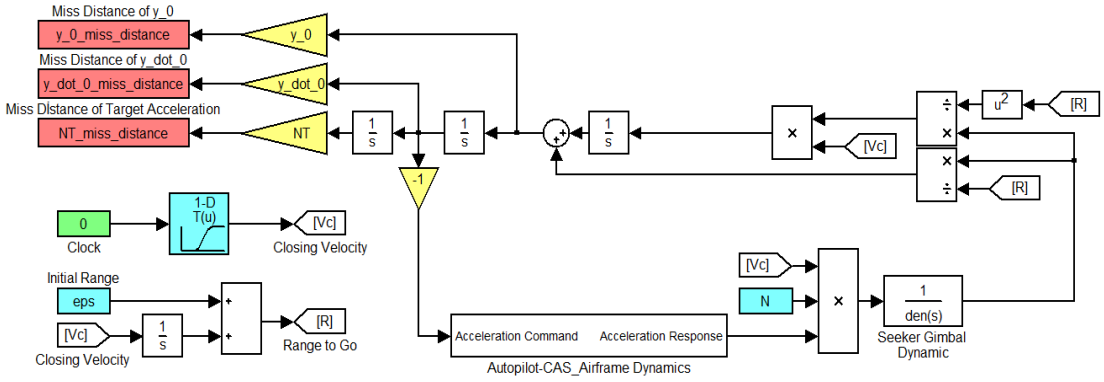


**Figure 10 Adjoint Model**

### 2.3.2 Adjoint Model with Describing Function Technique

Stochastic property of the adjoint method is the main power of the technique since a single adjoint run is enough to get data equivalent to hundreds of monte carlo runs for each impulse time for the original model. On the other hand, higher the monte carlo run number better the convergence therefore, stochastic adjoint analysis can simply be considered as infinite monte carlo runs. However, note that approximately 200 monte carlo runs are generally enough to converge but the method is still very powerful in terms of time and ability of the obtaining the sensitivity for different inputs.

The response of a linear system to a white noise can be expressed as in Eq.(39).

$$\begin{aligned} \mathrm{E}\left[y^2(t)\right] &= \Phi\int_{-\infty}^{t} h^2(t,\tau)\,d\tau \\ \mathrm{E}\left[y^2(t)\right] &= \Phi\int_{0}^{t} h^2(t,\tau)\,d\tau \end{aligned} \tag{39}$$

Then, adjoint impulse response function of Eq.(26) is implemented in Eq.(39) and the following formulation is obtained (Zarchan, 1997).

$$\begin{aligned} \mathrm{E}\left[y^2(t)\right] &= \Phi\int_{0}^{t}\left[h^*\left(t_F-\tau,t_F-t\right)\right]^2 d\tau \\ x &= t_F - t \\ dx &= -d\tau \\ &\text{if } t = t_F \text{ then} \\ \mathrm{E}\left[y^2(t)\right] &= \Phi\int_{0}^{t_F}\left[h^*(x,0)\right]^2 dx \end{aligned} \tag{40}$$

From Eq.(40), the mean square response of the original system to a white noise can be determined and the block diagram form is presented in Figure 11.

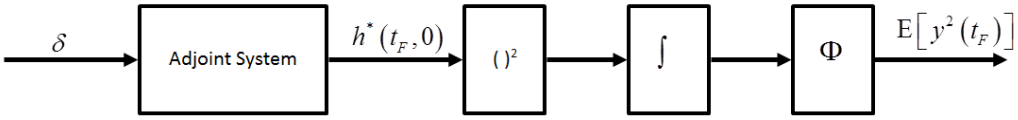


**Figure 11 Stochastic Adjoint Block Diagram Form**

$\Phi$ is the power spectral density of the stochastic disturbance parameter and if there are more than one stochastic disturbances, total mean square response is the summation of the all mean square response, which is expressed in Eq.(41).

$$\mathrm{E}\left[y^2(t)\right] = \mathrm{E}\left[y_1^2(t)\right] + \mathrm{E}\left[y_2^2(t)\right] + \ldots \tag{41}$$

At this point, the adjoint technique is explained for both deterministic and stochastic input parameters and it can be understood that it is powerful method in term of time, parametric study ability and disturbance sensitivity. However, the method is based on the linearity assumption so nonlinear effects that are missile lateral acceleration capability, engagement geometry, changing in the missile speed that is not implemented as time varying parameter, are not considered and the designer must be careful while using the adjoint technique. On the other hand, various methods have

been studied on this technique to handle the nonlinearity for example, acceleration capability depending on the missile Mach number that brings saturation.

Apart from the adjoint method, covariance analysis technique exists and it is used to figure out the system response to stochastic disturbances in a single run however, it is not completely similar with the adjoint. In this covariance technique, stochastic analysis can be done instead of hundreds of Monte Carlo analyses for a single impulse time. It seems like no advantage exists compared to adjoint but covariance generates mean square response time history of the system states and is shown in Eq.

$$\begin{aligned} \dot{X}(t) &= F(t)X(t) + \left[F(t)X(t)\right]^T + Q(t) \\ X(t) &= \mathrm{E}\left[x(t)x^T(t)\right] \end{aligned} \tag{42}$$

where $F(t)$ and $Q(t)$ are the system and power spectral density matrices and $Q(t)$ is formed by the white noise vector of $u(t)$ (Zarchan, 2012).

$$Q(t) = \mathrm{E}\left[u(t)u^T(t)\right] \tag{43}$$

In addition, describing function technique is used for various purposes especially for the controller design to find the limit cycle. The method is based on the assuming the input signal form to the nonlinear element and it is linearized according to the form of the input and the nonlinear element type such as, saturation, hysteresis (Gelb & Velde, 1968). Also, describing function method can be applied to random input such as zero mean Gaussian disturbances. Therefore describing function technique can be utilized with covariance method to handle the acceleration saturation for stochastic disturbances since the covariance generates the states time histories, which is essential for the describing function.

Describing function for the zero mean Gaussian input form is derived and the following equation is obtained (Zarchan, 1979).

$$K = 1 - \left( \frac{2}{\sqrt{2\pi}} \right) e^{\left( \frac{-a_{Lim}^2}{2\sigma_X^2} \right)} \left[ 0.4361836\omega - 0.1201676\omega^2 + 0.937298\omega^3 \right]$$

where (44)

$$\omega = \frac{1}{1 + \frac{0.33267 a_{Lim}}{\sigma_X}}$$

$a_{Lim}$ and $\sigma_X$ are the acceleration limit and the standard deviation of the missile acceleration time history obtained from covariance analysis. Note that this technique is valid for stochastic adjoint analyses since covariance enables to estimate the form of the input signal to the nonlinear element.

### 2.3.3 State Space Structured Adjoint Model

In order to construct adjoint in a state space form, dual of the system, which is shown in the Eq.(45) , is defined according to control system terminology (Martin Weiss, 2005).

$$\begin{aligned} \dot{x}^{\circ} &= A^T \left( t_F - t_D \right) x^{\circ} + C^T \left( t_F - t_D \right) u^{\circ} \\ y^{\circ} \left( t_D \right) &= B^T \left( t_F - t_D \right) x^{\circ} \left( t_D \right) \\ x^{\circ} (0) &= C^T \left( t_F \right) \end{aligned} \tag{45}$$

$t_D$ denotes the dual system time and it is assumed that the system has a single output to obtain the adjoint response that is depicted in Eq.(46).

$$\begin{aligned} \dot{x}^{adj} &= A^T \left( t_F - t_D \right) x^{adj} \\ y^{adj} \left( t_D \right) &= B^T \left( t_F - t_D \right) x^{adj} \left( t_D \right) \\ x^{adj} (0) &= C^T \left( t_F \right) \end{aligned} \tag{46}$$

According to adjoint construction rules, signal flow must be reversed and the original system's input and output become the adjoint system's output and input respectively. Therefore, it can be observed that the original system input matrix is converted to the adjoint output while the output becomes input. However, note that it is assumed that the original system has a single output and original system output matrix can be used as an impulse for the adjoint.

In addition, stochastic analysis can be done with this state space form of the adjoint method by only applying the same technique to the adjoint output, which means that power spectral density of the disturbance is still needed.

In this thesis, state space form of the adjoint is utilized to capture the engagement nonlinearities. In the literature, studies exist about this topic. For example, states of the nonlinear system are investigated to understand whether it is possible to simplify the system by populating the non-dominant states before to increase the fidelity(Moorman et al., 2005). This method is valid for both deterministic and stochastic disturbances however, although some system parameters do not have dominant effect on the system response, interactions of the states are not considered completely since the non-dominant states are populated before.

In addition, a handover analysis is available in the literature to obtain seeker pointing error before passing the terminal phase (M Weiss & Bucco, 2005). In this paper, state space form of the adjoint technique is utilized so that missile fly-out is investigated before terminal engagement against stochastic disturbances.

In this thesis, a two dimensional nonlinear simulation model is developed and constructed to analyze nonlinear missile-target engagement scenarios in order to obtain the system matrix. Then, a proper linear time varying (LTV) model is built and validated by comparing the nonlinear simulation model. In order to form a LTV model, fully nonlinear two dimensional engagement equations are derived by considering the disturbances namely, deterministic target maneuver, range dependent seeker line-of-sight rate noise and stochastic initial heading error. The idea behind the selecting these disturbance parameters is to represent the missile-target terminal scenarios when the seeker is locked-on with the initial heading error against target that maneuvers different range-to-go values.

Once the time histories of the states are obtained from nonlinear model, system matrix can be generated which means that the principal trajectory is available for the LTV model. Note that the LTV model is validated in terms of the selecting a proper system matrix but it must be keep in mind that if the system response dispersion differs from principal trajectory significantly due to disturbances, linearity

assumption of the method is violated and the accuracy of the method becomes questionable.

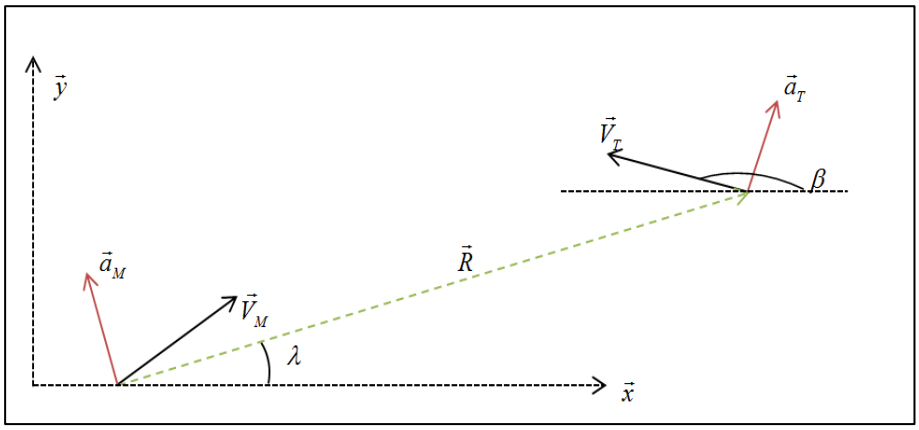


**Figure 12 Two Dimensional Engagement Geometry**

In Figure 12, missile target engagement geometry is presented and nonlinear homing equations are derived based on it.

The target kinematic equations are derived and shown in Eq.(47).

$$\begin{aligned} a_{TX} &= a_T \cos\left(\beta - \frac{\pi}{2}\right) \\ a_{TY} &= a_T \sin\left(\beta - \frac{\pi}{2}\right) \\ \beta &= \arctan\left(\frac{V_{TY}}{V_{TX}}\right) \end{aligned} \tag{47}$$

The missile kinematic equations are derived and shown in Eq.(48).

$$\begin{aligned} a_{MX} &= a_M \cos\left(\lambda_{SN} + \frac{\pi}{2}\right) \\ a_{MY} &= a_M \sin\left(\lambda_{SN} + \frac{\pi}{2}\right) \end{aligned} \tag{48}$$

In order to define the missile kinematic equations, $\lambda_{SN}$ and $a_M$ must be obtained. Note that in this homing guidance loop, seeker gimbal dynamic and missile acceleration responses are implemented as first order transfer functions. In Figure 13, generic first order block diagram is presented and response equations are derived according to this structure.

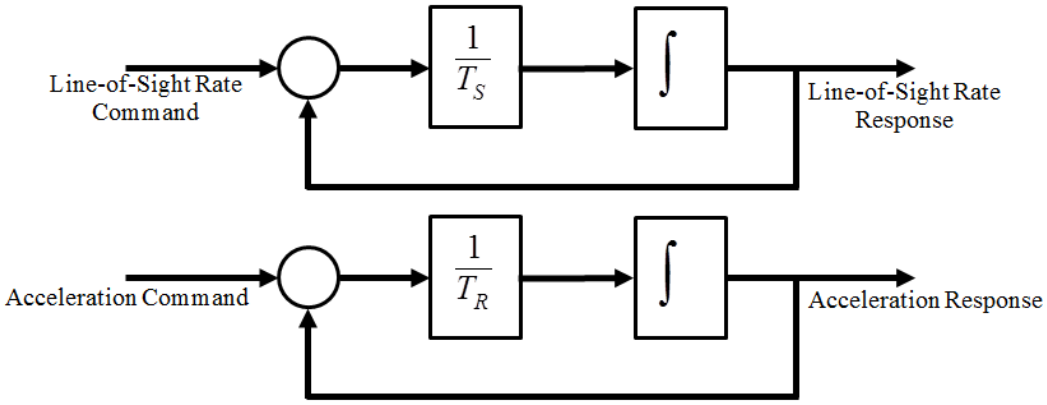


**Figure 13 First Order Seeker & Acceleration Response Representation**

Seeker gimbal dynamics are derived and shown in Eq.(49).

$$\ddot{\lambda}_S = \frac{\dot{\lambda} - \dot{\lambda}_S}{T_S} \tag{49}$$

In addition to above equation, range dependent seeker LOS rate is added then the LOS rate, which is used by the guidance, is shown in Eq.(50).

$$\dot{\lambda}_{SN} = \dot{\lambda}_S + \dot{\lambda}_N \tag{50}$$

It can be seen that the disturbed LOS rate is integrated and utilized for the missile kinematic equations. The true LOS angle is derived and shown in Eq. (51).

$$R_Y = P_{TY} - P_{MY} \text{ and } R_X = P_{TX} - P_{MX}$$

$$\lambda = \arctan\left(\frac{R_Y}{R_X}\right) = \arctan\left(\frac{P_{TY} - P_{MY}}{P_{TX} - P_{MX}}\right)$$

$$\dot{\lambda} = \frac{\dfrac{\dot{R}_Y R_X - R_Y \dot{R}_X}{R_X^2}}{1 + \left(\dfrac{R_Y}{R_X}\right)^2}$$

$$\dot{\lambda} = \frac{\dfrac{(V_{TY} - V_{MY})(P_{TX} - P_{MX}) - (P_{TY} - P_{MY})(V_{TX} - V_{MX})}{(P_{TX} - P_{MX})^2}}{1 + \dfrac{(P_{TY} - P_{MY})^2}{(P_{TX} - P_{MX})^2}}$$

$$\dot{\lambda} = \frac{(V_{TY} - V_{MY})(P_{TX} - P_{MX}) - (P_{TY} - P_{MY})(V_{TX} - V_{MX})}{(P_{TX} - P_{MX})^2 + (P_{TY} - P_{MY})^2} \tag{51}$$

In addition, acceleration response of the missile is derived and shown in Eq.(52).

$$\dot{a}_M = \frac{a_C - a_M}{T_R} \tag{52}$$

On the other hand, acceleration command is required and is presented in Eq.(53).

$$\begin{aligned}
a_C &= NV_C\dot{\lambda}_{SN} \\
V_C &= \dot{R} \text{ where } R = \sqrt{R_X^2 + R_Y^2} = \sqrt{\left(P_{TX} - P_{MX}\right)^2 + \left(P_{TY} - P_{MY}\right)^2} \\
V_C &= \frac{1}{2}\frac{2\left(V_{TX} - V_{MX}\right)\left(P_{TX} - P_{MX}\right) + 2\left(V_{TY} - V_{MY}\right)\left(P_{TY} - P_{MY}\right)}{\sqrt{\left(P_{TX} - P_{MX}\right)^2 + \left(P_{TY} - P_{MY}\right)^2}} \\
V_C &= \frac{\left(V_{TX} - V_{MX}\right)\left(P_{TX} - P_{MX}\right) + \left(V_{TY} - V_{MY}\right)\left(P_{TY} - P_{MY}\right)}{\sqrt{\left(P_{TX} - P_{MX}\right)^2 + \left(P_{TY} - P_{MY}\right)^2}} \\
\dot{\lambda}_{SN} &= \dot{\lambda}_S + \dot{\lambda}_N \\
\dot{\lambda}_N &= \frac{R(0)}{R}C \\
\dot{\lambda}_N &= \frac{\sqrt{\left(P_{TX}(0) - P_{MX}(0)\right)^2 + \left(P_{TY}(0) - P_{MY}(0)\right)^2}}{\sqrt{\left(P_{TX} - P_{MX}\right)^2 + \left(P_{TY} - P_{MY}\right)^2}}C
\end{aligned} \tag{53}$$

Finally, although the miss distance definition is used for at the end of the scenario to understand the system performance, in Eq. (54), it is considered as time varying for but its final value is used as miss distance. In addition, note that, only lateral position difference is utilized for the formulation.

$$\varepsilon_Y = P_{TY} - P_{MY} \tag{54}$$

The engagement homing loop states are defined in Table 1 and state-space structure is constructed based on them

**Table 1 Definition of the States**

| | | | | | | | |
|---|---|---|---|---|---|---|---|
| $x_1$ | = $P_{MX}$ | : | Missile X Position | $x_7$ | = $V_{TX}$ | : | Target X Velocity |
| $x_2$ | = $V_{MX}$ | : | Missile X Velocity | $x_8$ | = $P_{TY}$ | : | Target Y Position |
| $x_3$ | = $P_{MY}$ | : | Missile Y Position | $x_9$ | = $V_{TY}$ | : | Target Y Velocity |
| $x_4$ | = $V_{MY}$ | : | Missile Y Velocity | $x_{10}$ | = $\lambda_{SN}$ | : | LOS Angle (Seeker, Noise) |
| $x_5$ | = $a_M$ | : | Missile Acceleration | $x_{11}$ | = $\dot{\lambda}_S$ | : | LOS Angle Rate (Seeker) |
| $x_6$ | = $P_{TX}$ | : | Target X Position | $x_{12}$ | = $\varepsilon_Y$ | : | Miss Distance Y |

The parameters utilized in the above equations are explained in the Table 2

**Table 2 Definition of the Parameters**

| | | | | | |
|---|---|---|---|---|---|
| $T_R$ | : | Missile Acceleration Response Time Constant | $C$ | : | Seeker LOS Noise Coefficient |
| $T_S$ | : | Seeker Gimbal Time Constant | $\dot{\lambda}_N$ | : | Seeker LOS Rate Noise |
| $a_T$ | : | Target Total Lateral Acceleration | $\dot{\lambda}$ | : | True LOS Angle |

Although the engagement equations are obtained, designer should be careful while selecting the LTV model. It is important to select dominant states to represent the response of the model to disturbances properly especially since the seeker LOS rate and the acceleration response are the dominant parameters; they are used as multipliers of as many states as possible to simulate the disturbance effects on the system. In Eq.(55), state space representation of the LTV model is presented.

$$\begin{bmatrix} \dot{x}_1 \\ \dot{x}_2 \\ \dot{x}_3 \\ \dot{x}_4 \\ \dot{x}_5 \\ \dot{x}_6 \\ \dot{x}_7 \\ \dot{x}_8 \\ \dot{x}_9 \\ \dot{x}_{10} \\ \dot{x}_{11} \\ \dot{x}_{12} \end{bmatrix} = \begin{bmatrix} 0 & 1 & 0 & 0 & 0 & 0 & 0 & 0 & 0 & 0 & 0 & 0 \\ 0 & 0 & 0 & 0 & A_{2,5} & 0 & 0 & 0 & 0 & 0 & 0 & 0 \\ 0 & 0 & 0 & 1 & 0 & 0 & 0 & 0 & 0 & 0 & 0 & 0 \\ 0 & 0 & 0 & 0 & A_{4,5} & 0 & 0 & 0 & 0 & 0 & 0 & 0 \\ 0 & 0 & 0 & 0 & A_{5,5} & 0 & 0 & 0 & 0 & 0 & A_{5,11} & 0 \\ 0 & 0 & 0 & 0 & 0 & 0 & 1 & 0 & 0 & 0 & 0 & 0 \\ 0 & 0 & 0 & 0 & 0 & 0 & 0 & 0 & 0 & 0 & 0 & 0 \\ 0 & 0 & 0 & 0 & 0 & 0 & 0 & 0 & 1 & 0 & 0 & 0 \\ 0 & 0 & 0 & 0 & 0 & 0 & 0 & 0 & 0 & 0 & 0 & 0 \\ 0 & 0 & 0 & 0 & 0 & 0 & 0 & 0 & 0 & 0 & 1 & 0 \\ 0 & 0 & A_{11,3} & A_{11,4} & 0 & 0 & 0 & A_{11,8} & A_{11,9} & 0 & A_{11,11} & 0 \\ 0 & 0 & 0 & -1 & 0 & 0 & 0 & 0 & 1 & 0 & 0 & 0 \end{bmatrix} \begin{bmatrix} x_1 \\ x_2 \\ x_3 \\ x_4 \\ x_5 \\ x_6 \\ x_7 \\ x_8 \\ x_9 \\ x_{10} \\ x_{11} \\ x_{12} \end{bmatrix} + \begin{bmatrix} 0 & 0 \\ 0 & 0 \\ 0 & 0 \\ 0 & 0 \\ 0 & B_{5,2} \\ 0 & 0 \\ B_{7,1} & 0 \\ 0 & 0 \\ B_{9,1} & 0 \\ 0 & B_{10,2} \\ 0 & 0 \\ 0 & 0 \end{bmatrix} \begin{bmatrix} a_T \\ \dot{\lambda}_N \end{bmatrix} \quad (55)$$

The definitions of the elements of the system and the input matrices are explained in the following tables.

**Table 3 Definition of the System Matrix Elements**

$$A_{2,5} \quad : \quad \cos\left( x_{10} + \frac{\pi}{2} \right)$$

$$A_{4,5} \quad : \quad \sin\left( x_{10} + \frac{\pi}{2} \right)$$

$$A_{5,5} \quad : \quad -\frac{1}{T_A}$$

$$A_{5,11} \quad : \quad -N\left( \frac{(x_7 - x_2)(x_6 - x_1) + (x_9 - x_4)(x_8 - x_3)}{T_A \sqrt{(x_6 - x_1)^2 + (x_8 - x_3)^2}} \right)$$

$$A_{11,3} \quad : \quad \frac{\left( x_7 - x_2 \right)}{\left( (x_6 - x_1)^2 + (x_8 - x_3)^2 \right) T_S}$$

$$A_{11,4} \quad : \quad \frac{\left( x_1 - x_6 \right)}{\left( (x_6 - x_1)^2 + (x_8 - x_3)^2 \right) T_S}$$

$$A_{11,8} \quad : \quad \frac{\left( x_2 - x_7 \right)}{\left( (x_6 - x_1)^2 + (x_8 - x_3)^2 \right) T_S}$$

$$A_{11,9} \quad : \quad \frac{\left(x_6 - x_1\right)}{\left((\mathrm{x}_6 - x_1)^2 + (x_8 - x_3)^2\right) T_S}$$

$$A_{11,11} \quad : \quad -\frac{1}{T_S}$$

In addition to above table, $N$ is utilized for the guidance constant in order to generate acceleration command.

**Table 4 Definition of the Input Matrix Elements**

$$B_{7,1} \quad : \quad a_T \cos\left(\arctan\left[\frac{V_{TY}}{V_{TX}}\right] - \frac{\pi}{2}\right)$$

$$B_{9,1} \quad : \quad a_T \sin\left(\arctan\left[\frac{V_{TY}}{V_{TX}}\right] - \frac{\pi}{2}\right)$$

$$B_{5,2} \quad : \quad -N\left(\frac{(\mathrm{x}_7 - x_2)(\mathrm{x}_6 - x_1) + (\mathrm{x}_9 - x_4)(\mathrm{x}_8 - x_3)}{T_A\sqrt{(\mathrm{x}_6 - x_1)^2 + (x_8 - x_3)^2}}\right) \times \left(\frac{\sqrt{\left(x_6(0) - x_1(0)\right)^2 + \left(x_8(0) - x_3(0)\right)^2}}{\sqrt{\left(x_6 - x_1\right)^2 + \left(x_8 - x_3\right)^2}}\right) C$$

$$B_{10,2} \quad : \quad \left(\frac{\sqrt{\left(x_6(0) - x_1(0)\right)^2 + \left(x_8(0) - x_3(0)\right)^2}}{\sqrt{\left(x_6 - x_1\right)^2 + \left(x_8 - x_3\right)^2}}\right) C$$

# CHAPTER 3

# ANALYSES & RESULTS

## 3.1 Pseudo 5-DOF and 6-DOF Comparison Analyses

At the early phases of a missile design, deriving the system performance requirements is crucial since the detailed design process depends on these major performance criteria. Therefore, the fidelity of the utilized simulation model is important also but using the most complex model is not possible due to reasons that are mentioned in previous sections. On the other hand, parametric study capability of the simulation model allows the designer to sweep the design space more systematically.

Pseudo 5-DOF model is a good candidate to generate requirements instead of using 6-DOF for many analyses. As mentioned before, 6-DOF is assumed to generate true data and difference of the Pseudo 5-DOF results from 6-DOF is investigated.

*Horizontal Plane Analyses*

The comparison analysis of Pseudo 5-DOF and 6-DOF is done for an incoming target that has $250\,m/s$ for a single altitude of $3000m$. In addition, the target starts its flight at the down range interval of $(4000m, 16000m)$ and the cross range (side range) interval of $(-8000m, 8000m)$. The results of the models are compared in terms of the missile final Mach number, Time-of-Flight (TOF), Miss Distance (MD) and Seeker Field-of-Regard (FOR) angle. Note that, the differences of the results except from FOR are shown in Figure 14, Figure 15 and Figure 16.

The seeker FOR is the gimbal angle, which is required for the successive lock-on to the target. The FOR angle calculation is done according to Eq.(56).

$$
\begin{aligned}
R^{(B)} &= P_T^{(B)} - P_M^{(B)} \\
R^{(B)} &= \begin{bmatrix} R_X \\ R_Y \\ R_Z \end{bmatrix}^{(B)} \\
\lambda &= \arcsin\left(\frac{-R_Z^{(B)}}{\left|R^{(B)}\right|}\right) \qquad \text{FOR Elevation Angle} \\
\gamma &= \arctan\left(\frac{R_Y^{(B)}}{R_X^{(B)}}\right) \qquad \text{FOR Yaw Angle}
\end{aligned}
\tag{56}
$$

In Figure 14, differences of final Mach number between Pseudo 5-DOF and 6-DOF are depicted. It can be observed that the differences remain below 01 so the Pseudo 5-DOF model can be assumed to generate reasonable Mach number at the end of the flight. This is important for predicting acceleration capability at the terminal phase.

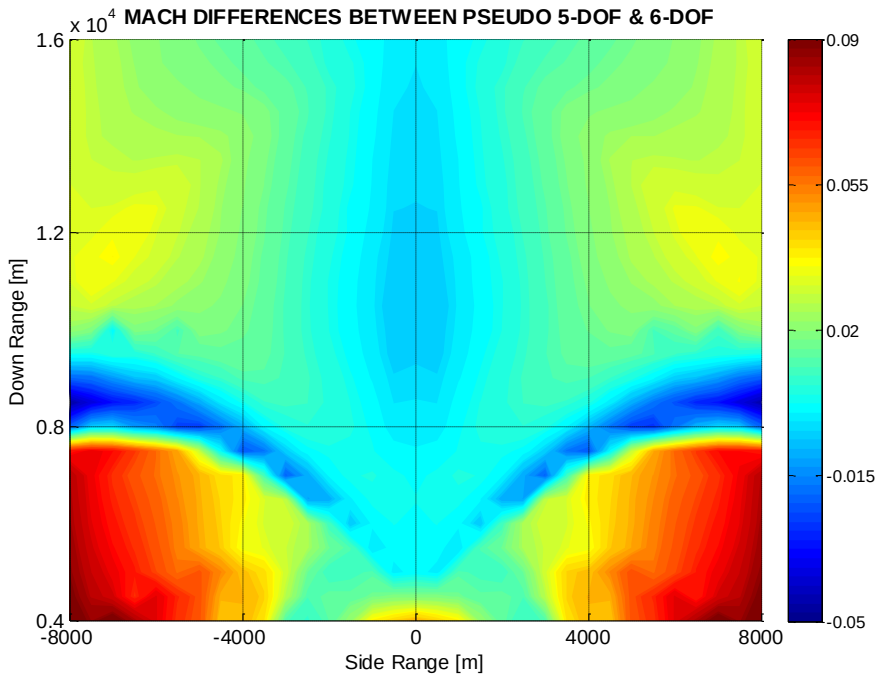


**Figure 14 Final Mach Number Differences Between Pseudo 5-DOF & 6-DOF**

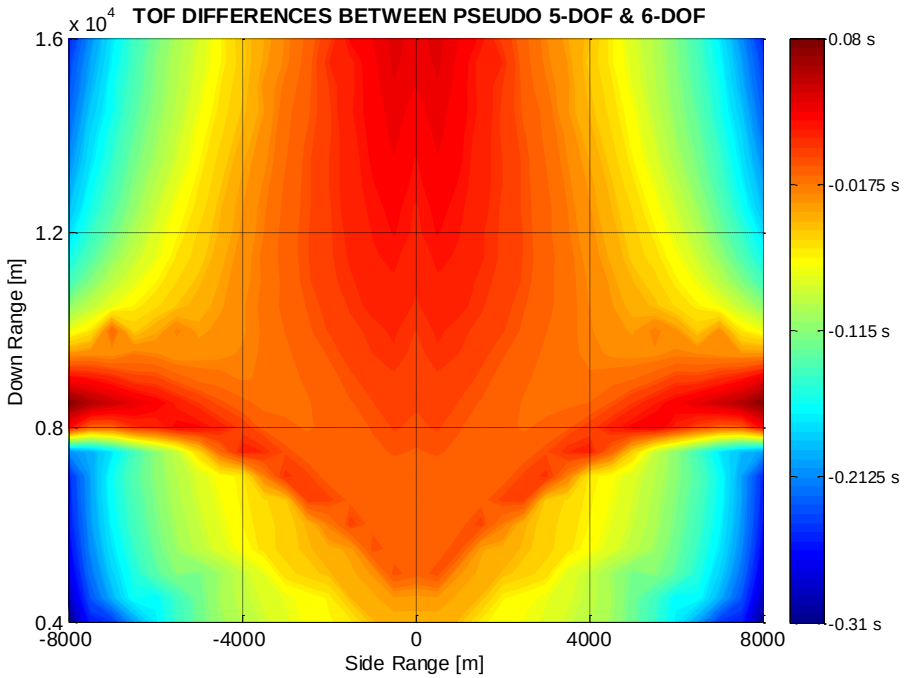


**Figure 15 TOF Differences Between Pseudo 5-DOF & 6-DOF**

In Figure 15, differences of flight time between Pseudo 5-DOF and 6-DOF are presented. It can be obtained that TOF differences are very small therefore, the Pseudo 5-DOF model can be considered to generate proper flight duration.

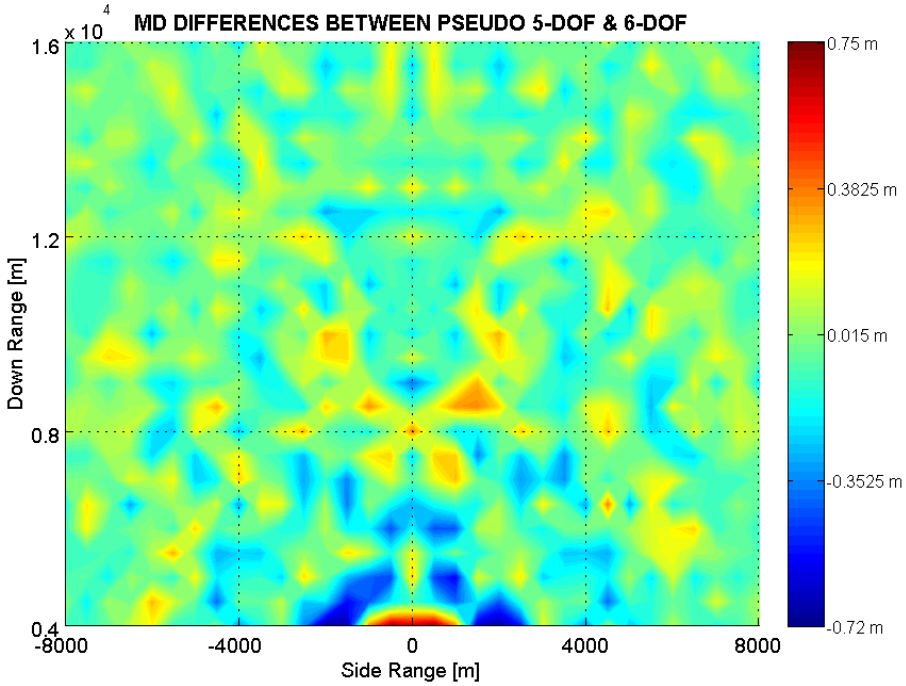


**Figure 16 MD Differences Between Pseudo 5-DOF & 6-DOF**

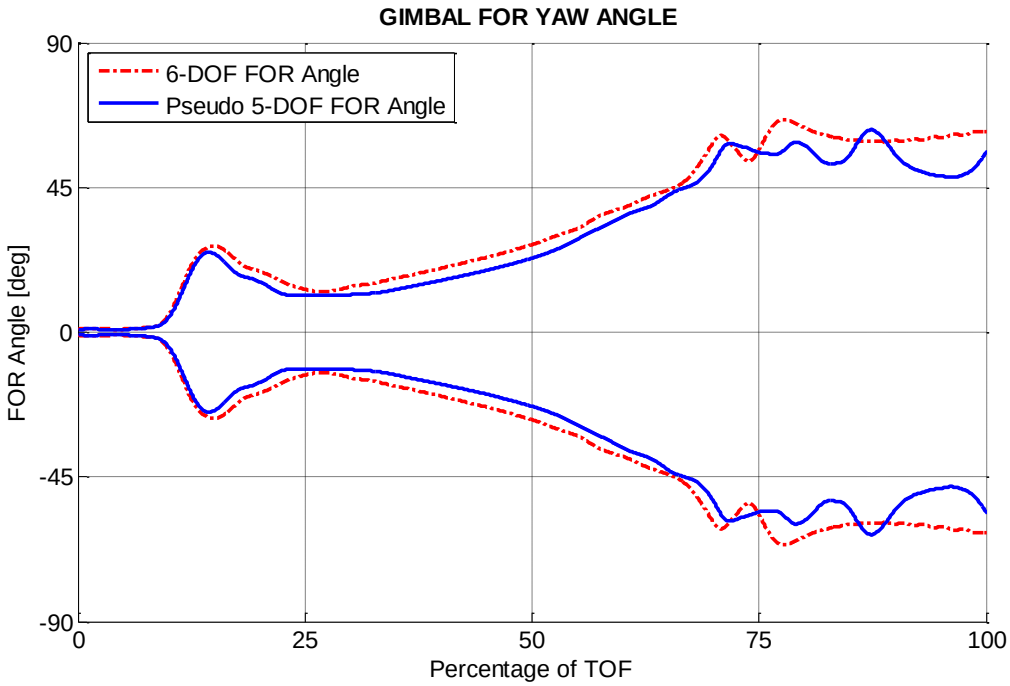


**Figure 17 Seeker FOR Yaw Angle of Pseudo 5-DOF and 6-DOF**

In Figure 16, differences of miss distance values between Pseudo 5-DOF and 6-DOF are presented. It can be shown that the differences are very small so the Pseudo 5-DOF model can be assumed to generate meaningful miss distance results.

According to the formula, which is depicted in Eq.(56), the seeker FOR yaw angle is obtained and shown in Figure 17. It is crucial for terminal phase where more precise target information is required for the guidance commands. It can be seen that the results are close to each other and note that, good position and Euler Angle estimation is necessary for accuracy of the Pseudo 5-DOF results.

Vertical Plane Analyses

The comparison analysis of Pseudo 5-DOF and 6-DOF is done for an incoming target that has $250\,m/s$ speed for a single cross range of $0m$. In addition, the target starts its flight at the down range interval of $(4000m, 16000m)$ and the altitude interval of $(500m, 5000m)$. The results of the models are compared in terms of the missile final Mach number, Time-of-Flight (TOF), Miss Distance (MD) and Seeker Field-of-Regard (FOR) angle. Note that, the differences of the results except from FOR are shown in Figure 18, Figure 19 and Figure 20.

In Figure 18, differences of final Mach number between Pseudo 5-DOF and 6-DOF are depicted. It can be observed that the differences are very small so the Pseudo 5-DOF model can be assumed to generate reasonable Mach number at the end of the flight, which is important for acceleration capability at the terminal phase.

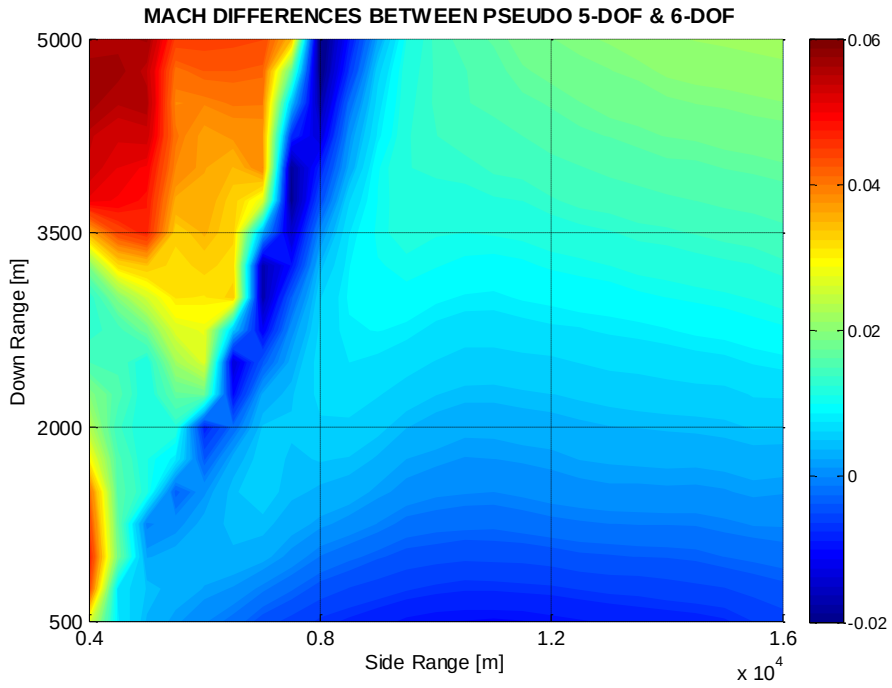


**Figure 18 Final Mach Difference (Pseudo 5-DOF and 6-DOF)**

In Figure 19, differences of flight time between Pseudo 5-DOF and 6-DOF are presented. It can be obtained that TOF differences are very small therefore, the Pseudo 5-DOF model can be considered to generate proper flight duration.

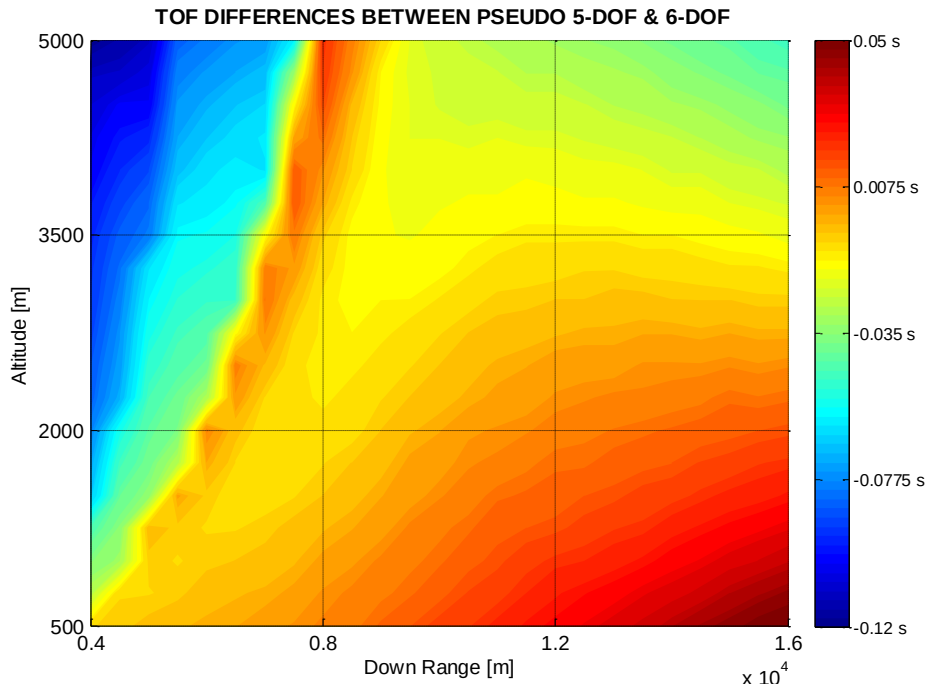


**Figure 19 TOF Difference (Pseudo 5-DOF and 6-DOF)**

In Figure 20, differences of miss distance values between Pseudo 5-DOF and 6-DOF are presented. It can be shown that the differences are very small so the Pseudo 5-DOF model can be assumed to generate meaningful miss distance results.

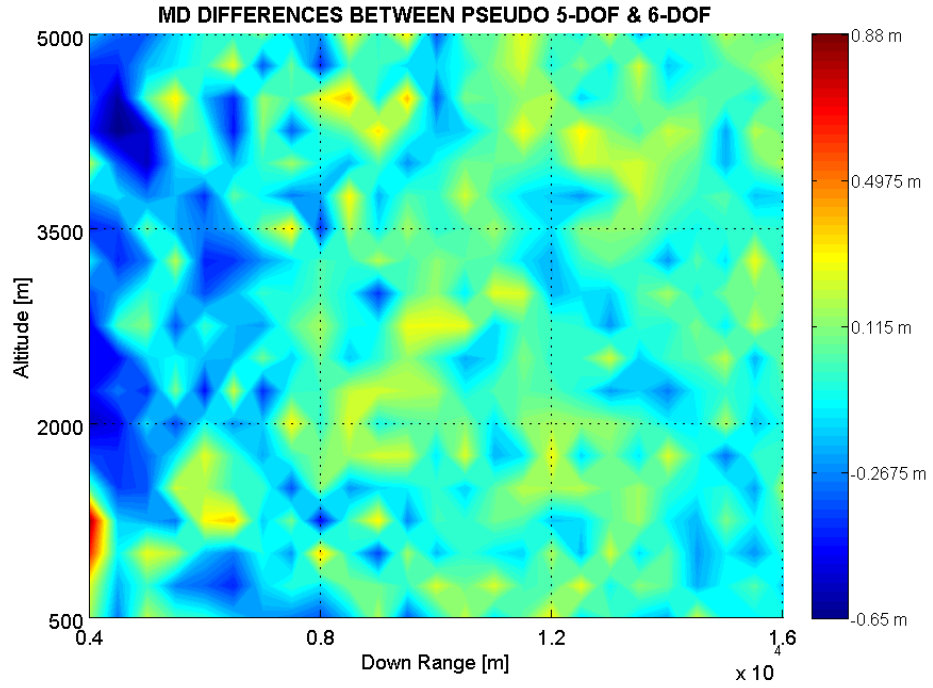


**Figure 20 MD Difference (Pseudo 5-DOF and 6-DOF)**

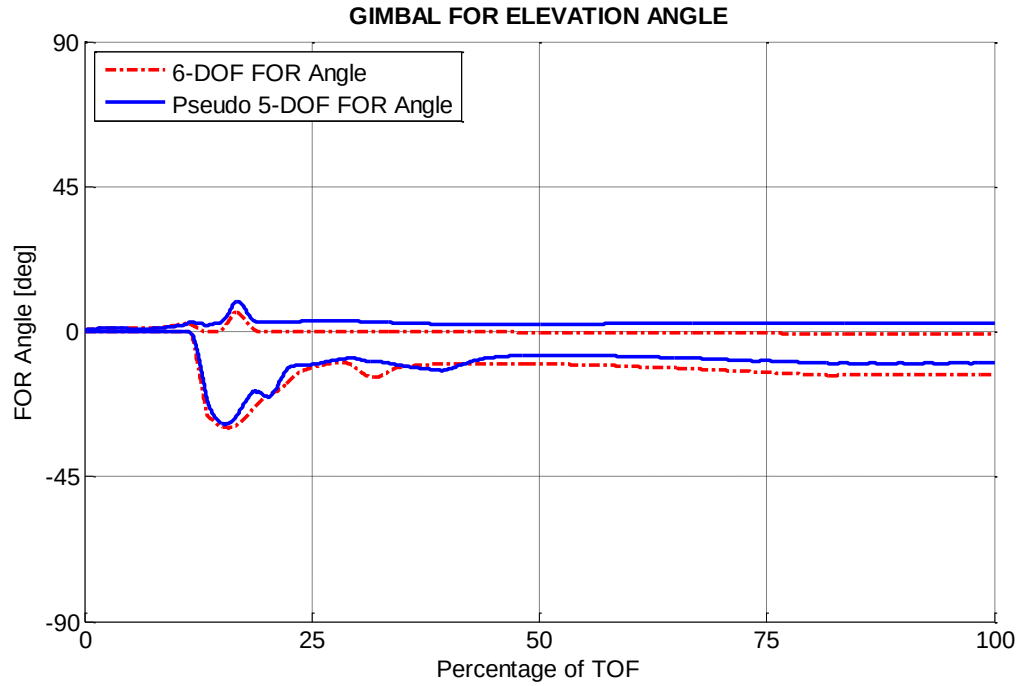


**Figure 21 Seeker FOR Elevation Angle of Pseudo 5-DOF and 6-DOF**

According to the formula, which is depicted in Eq.(56), the seeker FOR elevation angle is obtained and shown in Figure 21. It is crucial for terminal phase where more precise target information is required for the guidance commands. It can be seen that the results are close to each other and note that, good position and Euler Angle estimation is necessary for accuracy of the Pseudo 5-DOF results.

Based on the above results, Pseudo 5-DOF fidelity level is enough for deriving the missile performance requirements instead of using 6-DOF model. Therefore, same analyses can be done without the need for more information, which is crucial at the conceptual design phase.

### 3.2 Pseudo 5-DOF, 6-DOF and Adjoint Comparison Analysis

*Comparison Analysis for Target Maneuver*

In this analysis, classical Adjoint method, which is mentioned before, Pseudo 5-DOF and 6-DOF are compared in terms of the miss distance values. Note that it is not expected that the Adjoint results to be close enough to 6-DOF for all engagements but it is important to know where the technique's fidelity decreases. In order to figure out the accuracy of the models, head-on missile-target engagement scenario is considered for 3g, 5g, 7g maneuvering targets and note that the comparison analyses

are held for the terminal phase of the missile where there is not any thrust power available.

In Figure 22, miss distance values and percentage values of range-to-go between the missile and the target when the maneuver starts are depicted in x and y axes respectively. It can be seen that the miss distance values of the both Adjoint and Pseudo 5-DOF models are close to the 6-DOF and behavior of the miss distance can be captured by both of the models (Sezer et al., 2015). Since the target has 3g lateral acceleration, it does not cause dominant nonlinear effects on the linearized homing loop. In addition, missile does not require higher lateral acceleration command to intercept with the target so Mach number does not decrease so much, which cannot be implemented in the adjoint method. Only the ballistic missile speed without propulsive forces is implemented in the model therefore, extra deceleration in the missile speed cannot be modeled. Finally, since the target lateral acceleration is not high enough to cause dominant geometric nonlinearity, proper results are obtained for both models. Therefore, the adjoint technique can be considered to generates reasonable miss distance values for this engagement even when extra deceleration of the missile speed exists. On the other hand, although the Pseudo 5-DOF generates better results, adjoint method can still be used instead of the nonlinear simulation models due to drastic run time benefit.

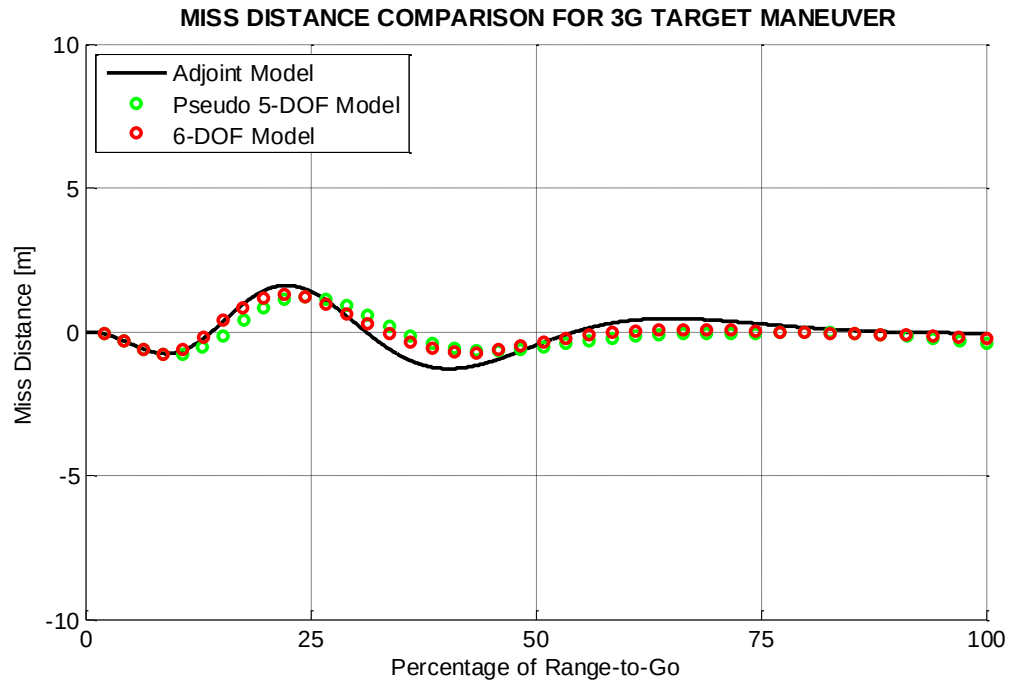


**Figure 22 Comparison of 3g Target Maneuver (Adjoint, Pseudo 5-DOF, 6-DOF)**

The analysis of Figure 22 is repeated for a target maneuvering with a constant acceleration of 5g and the results are shown in Figure 23.. It can be observed that the Adjoint model results starts to deviate from the 6-DOF especially at the higher range-to-go values. When the target maneuver increases, acceleration demand increases as well in order to intercept and the higher missile acceleration higher the deceleration in speed in the nonlinear models. On the other hand, this is not the case for the Adjoint model and the system response is obtained as if there is no deceleration and acceleration limit. For 5g target acceleration, if the maneuver starts at the higher range-to-go values; for example %50, the effect of the deceleration in speed and decrease in the acceleration capability is observed then the miss distance value increases. The Adjoint model can capture the miss distance behavior of the 6-DOF model for the lower %50 range-to-go values but the magnitude of the results can still be considered as proper for basic performance analyses but not for the whole region.

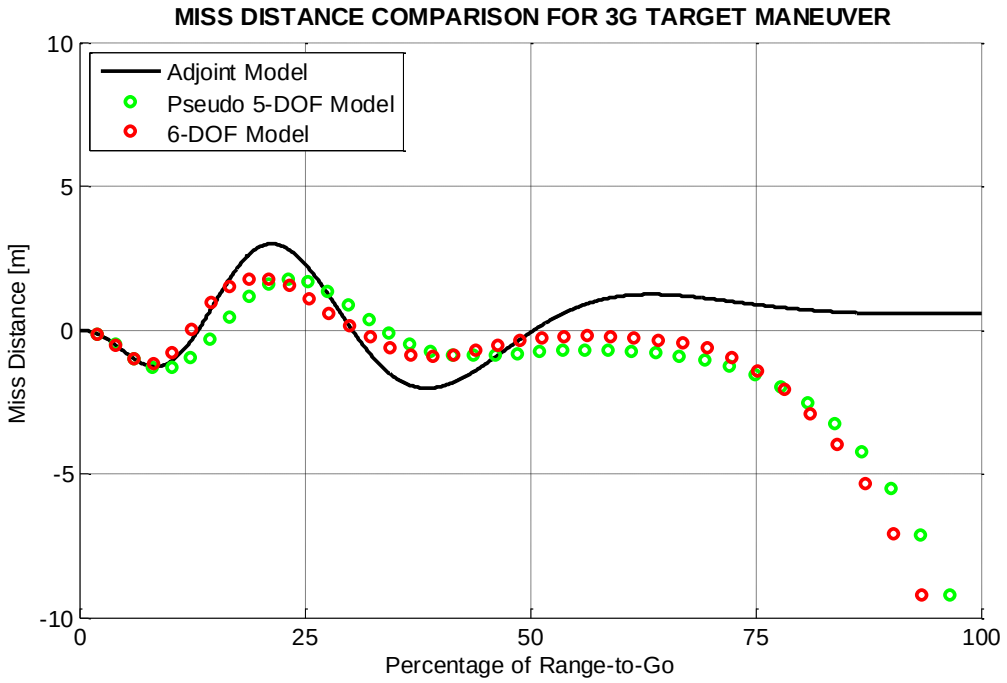


**Figure 23 Comparison of 5g Target Maneuver (Adjoint, Pseudo 5-DOF, 6-DOF)**

In Figure 24, the x and y axes are utilized to represent the same values that are mentioned in the explanation of the Figure 22. The deceleration in the speed of the missile is more dominant compared to previous analysis and adjoint results are questionable. Based on the Figure 22, Figure 23 and Figure 24, miss distance values of the 6-DOF model do not change so much with the increasing target lateral acceleration for the lower range-to-go values where the missile has enough speed to respond to the acceleration command. However, deceleration in the missile speed becomes more dominant with the higher target acceleration, which cannot be implemented in the Adjoint model.

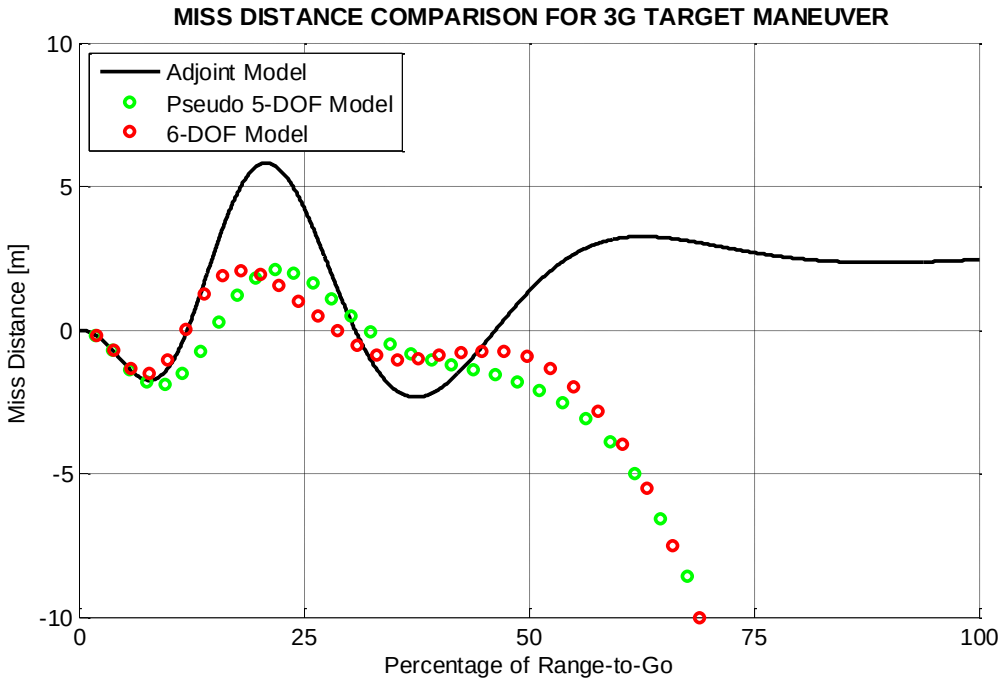


**Figure 24 Comparison of 7g Target Maneuver (Adjoint, Pseudo 5-DOF, 6-DOF)**

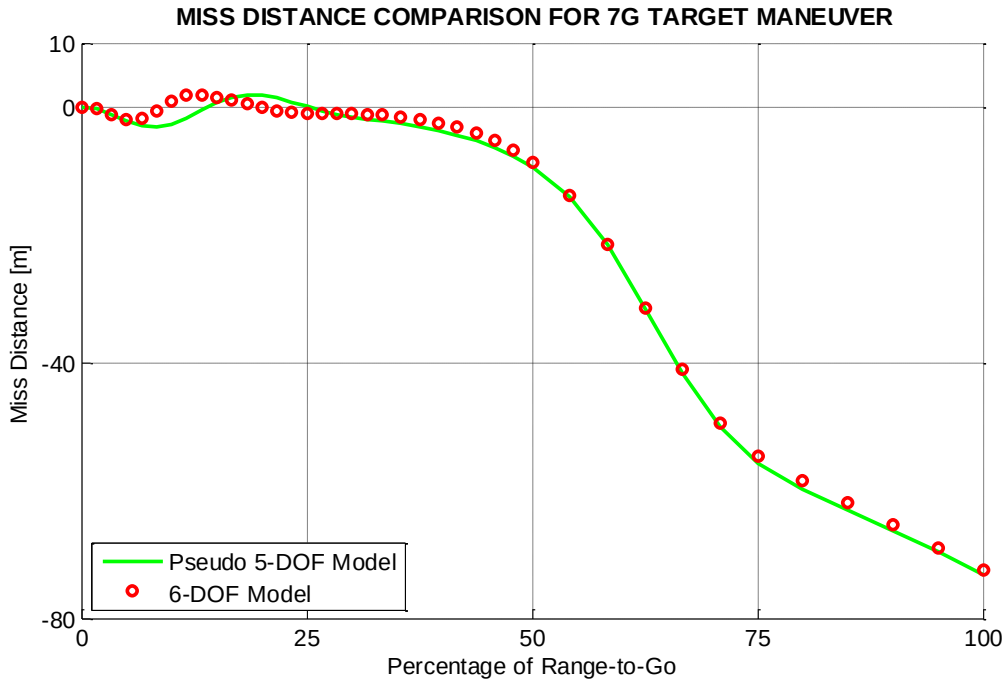


**Figure 25 Comparison of 7g Target Maneuver (Pseudo 5-DOF, 6-DOF)**

Figure 25, the miss distance values, which are not depicted due to the scale of the Pseudo 5-DOF and 6-DOF models, are presented for the 7g target acceleration completely and the same parameters are used for x and y axes. Although the Pseudo

5-DOF model has some simplifications, it still generates sufficient results in terms of magnitude and can capture the miss distance behavior even if the engagement nonlinearities become more dominant. In addition, Pseudo 5-DOF model is considered to generate proper miss distance values and it can still be observed.

*Comparison Analysis for Initial Heading Error & Target Cross Range*

In this analysis, the missile initial heading error and the target initial cross range values are considered as disturbances on the models instead of the target maneuver. Note that the initial conditions of the engagement are implemented by utilizing Eq.(37) and Eq.(38). The heading error interval of $(-10^{\circ}, 10^{\circ})$ is applied for whole range-to-go values for each initial cross range that are implemented as $(0^{\circ}, 20^{\circ})$. The purpose of the analysis is to simulate miss distance sensitivity for various range-to-go and different target cross range-to-go values at the seeker lock-on.

In Figure 26, heading errors are applied for 0° LOS angle, which is used to represent target initial cross range and all miss distance values are obtained. Then, for each range-to-go value, maximum and minimum miss distance results are calculated.

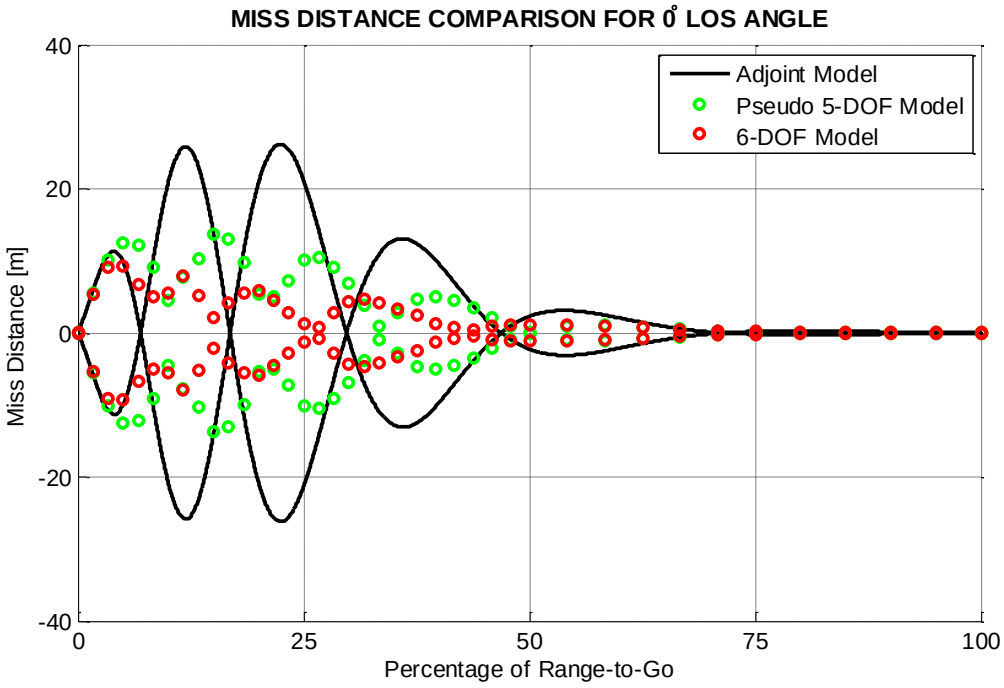


**Figure 26 MD Sensitivity for 0° LOS Angle**

It is observed that the adjoint results are not reliable compared to 6-DOF on the other hand, the Pseudo 5-DOF model results are more satisfactory as expected. Note that, although the result of the linear model is questionable, it still can capture the point where the sensitivity begins.

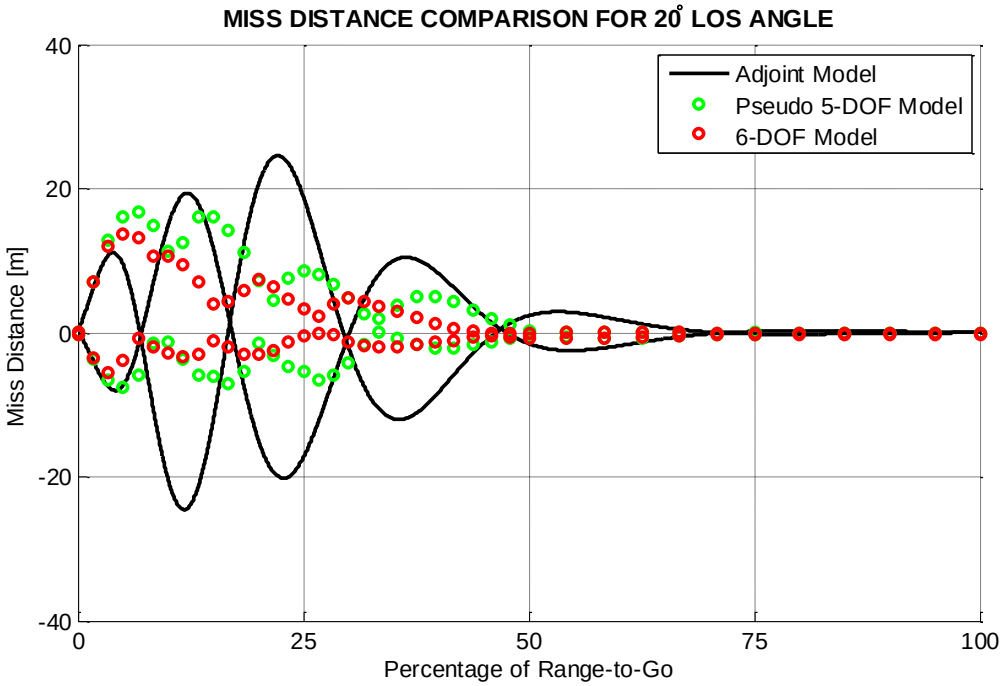


**Figure 27 MD Sensitivity for 20° LOS Angle**

In Figure 27, heading errors are applied for 20° LOS angle, which is used to represent target initial cross range and all miss distance values are obtained. Then, for each range-to-go value, maximum and minimum miss distance results are calculated for each model to understand the response of the system to initial heading errors. Similar with the Figure 26, same comments are acceptable and the Adjoint model can still generate the point where the miss distance sensitivity starts.

Although the adjoint results are not satisfactory by direct comparison with the 6-DOF, they are still useful to generate seeker lock-on range requirement.

### 3.3 Stochastic Adjoint Analysis with Describing Function

Until now, since the dominant effect of the missile deceleration on the adjoint results are observed, it is aimed to figure out the effect of the engagement nonlinearities. Therefore, a nonlinear model that includes only geometric nonlinearities, linear forward model and an Adjoint model are utilized to for the comparison analyses. The

nonlinear and linear forward simulations are the classical techniques to simulate system behavior and acceleration limit due to aerodynamic capability can be implemented on these models. On the other hand, the Adjoint model includes describing function to count in the effect of the missile acceleration capability and note that the describing function technique is valid for stochastic analyses.

Since the form of the input signal, which is acceleration command, is required to calculate the random input describing function (Gelb & Velde, 1968), covariance analysis should be done first before the adjoint analysis.

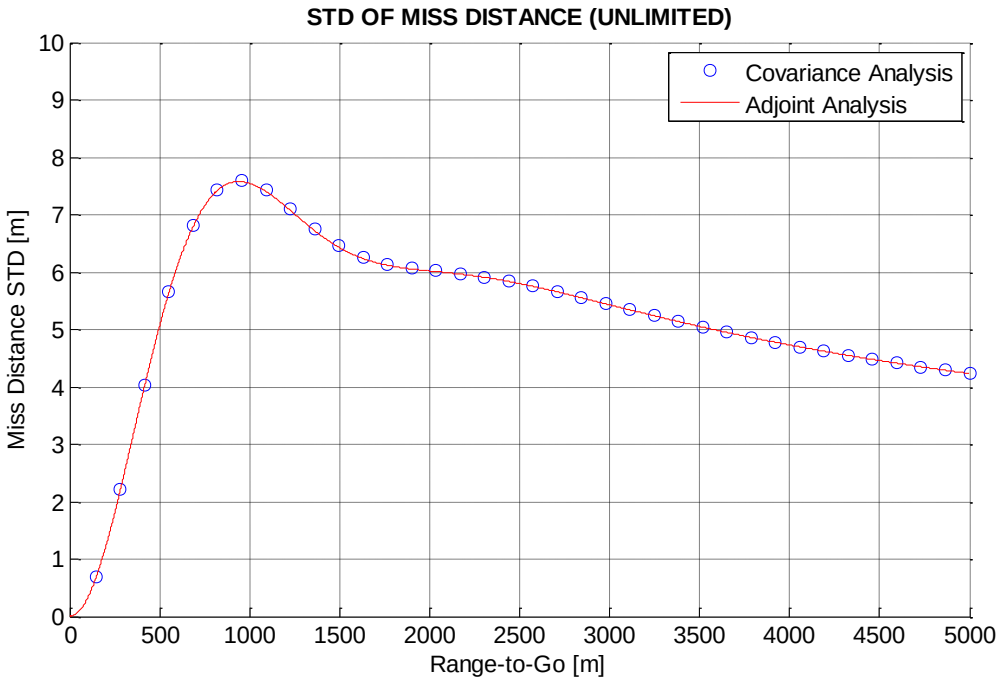


**Figure 28 Comparison of Covariance and Adjoint (Unlimited Acceleration)**

Comparison analysis of covariance and adjoint is done in order to observe the consistency of the models. Note that constant closing velocity, guidance gain value of 4 for TPNG law, first order acceleration response and seeker transfer functions with $0.4s$ and $0.2s$ time constants respectively. The head-on missile-target engagement scenario with $5000m$ initial range-to-go is considered and 3g target lateral acceleration value. In addition, the missile speed is assumed as 1.1 Mach number and the target speed is considered as $300\,m/s$. In Figure 28, the miss distance standard deviation values of the covariance and the adjoint results are depicted for various target maneuver application time and it is represented as range-

to-go values. These outcomes are obtained as is the missile has unlimited aerodynamic capability so the acceleration command is not limited. It can be seen that there is a good agreement between the results, which means that the covariance technique can be utilized to generate describing function.

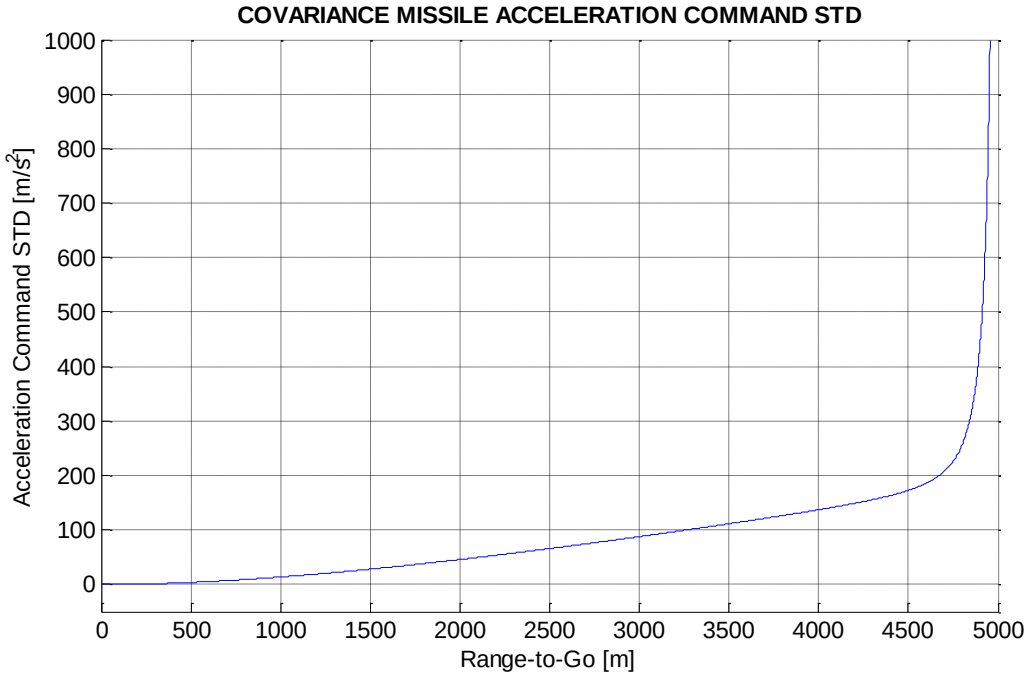


**Figure 29 Covariance Acceleration Command History (Unlimited Acceleration)**

In order to calculate the describing function, input form of the nonlinear element should be assumed and generally sinusoidal input is considered for the control applications in the literature to understand the limit cycle of the nonlinear system. However, input form of the acceleration command is necessary and a generic input form cannot be applied and the describing function can be calculated for random input signals. Since the covariance method generates stochastic results for whole time history of the engagement, standard deviation of the acceleration command form can be obtained as well. In Figure 29, the covariance acceleration command is depicted and it is used for the describing function calculation. In Figure 29, the results are shown up to maximum $1000\,m/s^2$ due to scale concern and they are utilized for the linearization calculation for the saturation element with 20g acceleration limit according to Eq.(44).

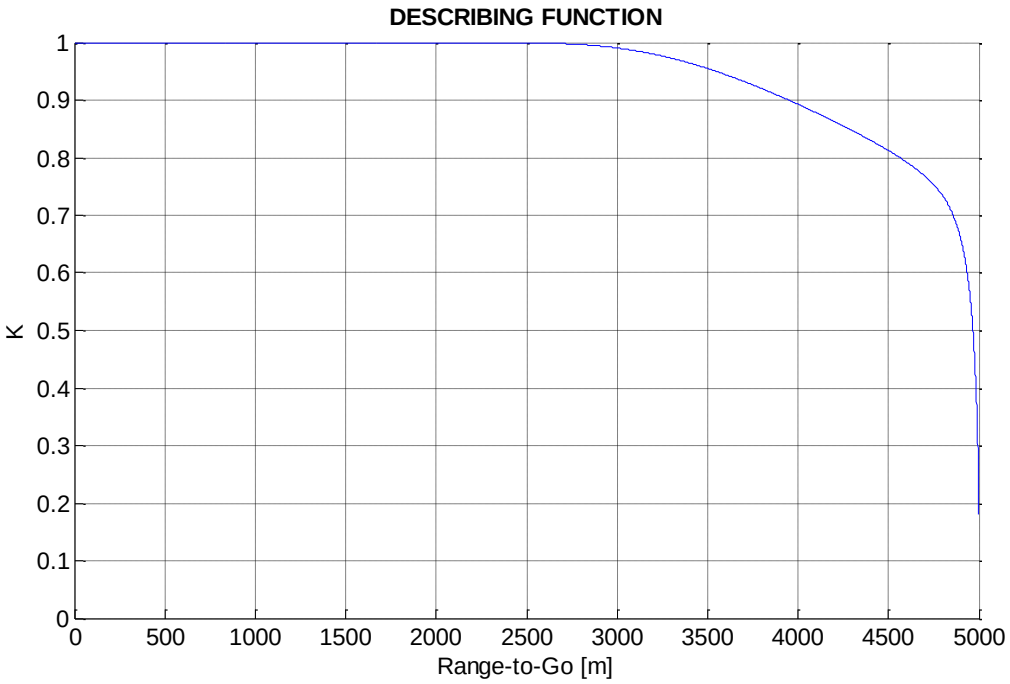


**Figure 30 Describing Function Coefficients**

In Figure 30, the describing function of the missile acceleration command is depicted also and note that the coefficients decreases with increasing command, which is shown in Figure 29.

Once the describing function is obtained, it can be used by direct multiplication on the acceleration command for both covariance and adjoint techniques. In Figure 31, the comparison analysis is held for the same engagement scenario for the 20g acceleration limit.

It can be observed that there is still a good agreement between the models, which means that the describing function is valid to represent the saturation elements of the forward simulation models.

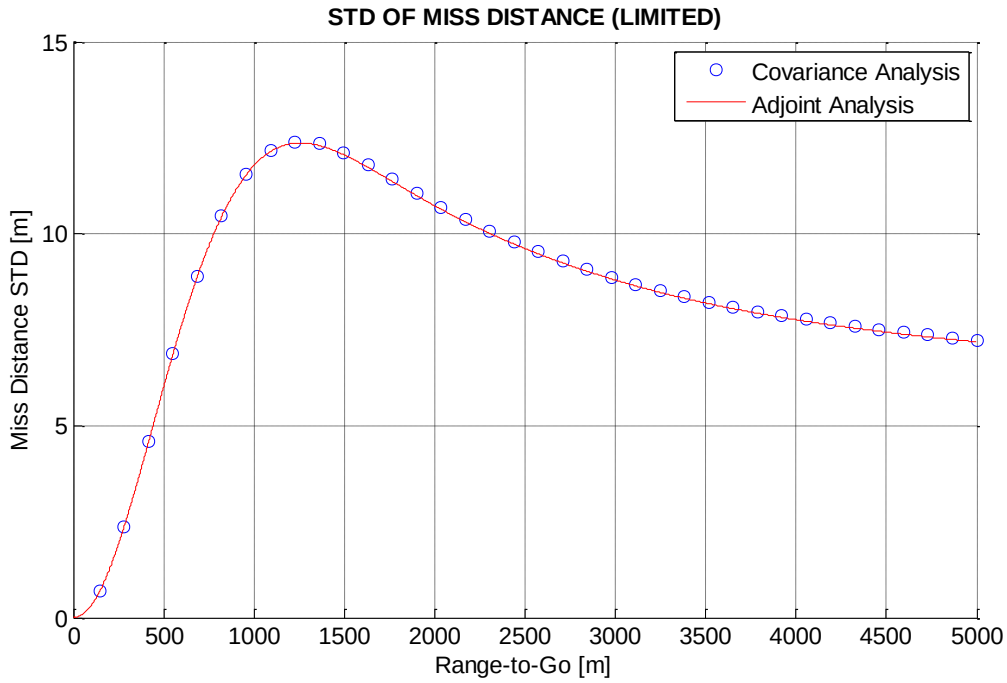


**Figure 31 Comparison of Covariance and Adjoint (Limited Acceleration)**

In order to understand the performance of the linearization technique, more comprehensive analyses are done by utilizing a nonlinear simulation, linear forward simulation and an Adjoint models. It is aimed to figure out the performance of the describing function method by comparing the adjıoint with the linear forward simulation model. In addition, the nonlinear model is used to understand the engagements geometrical nonlinear effects on the results. Therefore, it can be observed that both of the describing function performance and the effects of the geometric nonlinearities.

Comparison analyses are held for head-on missile-target engagement scenario for the same initial range-to-go, missile and target speed values mentioned for various target maneuver application range-to-go values and for two different guidance gain values of 4 and 7. On the other hand, for each possible maneuver application range-to-go value, 300 Monte Carlo runs are needed for both the nonlinear simulation and the linear forward simulation models. In addition, miss distance sensitivity analyses are done for two different target lateral acceleration values such as 3g and 7g as well.

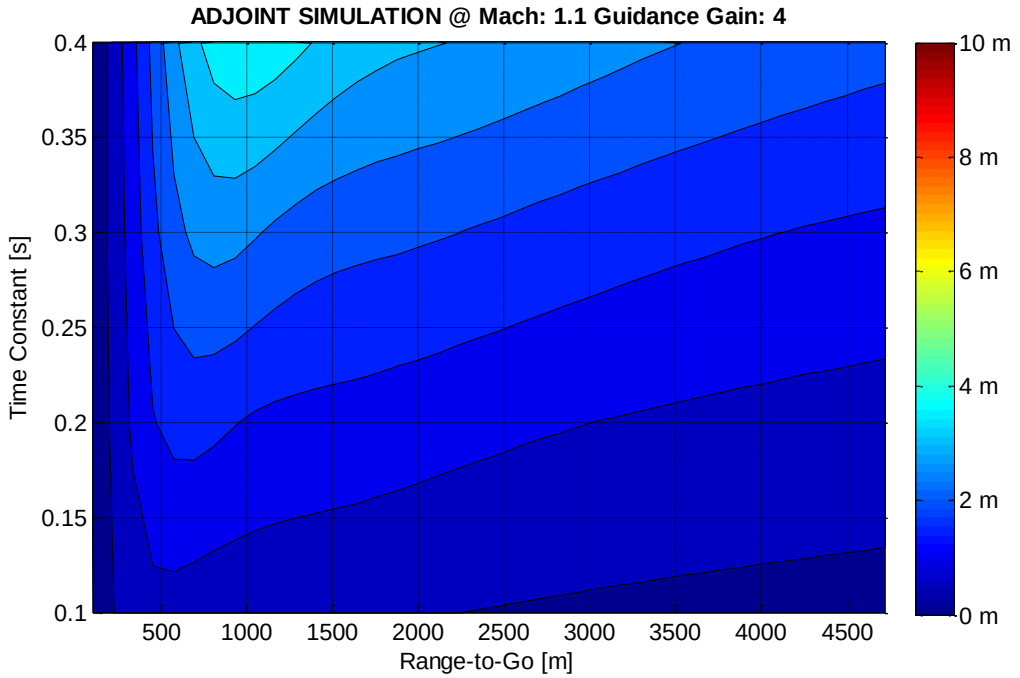


**Figure 32 MD for 3g Target Maneuver Guidance Gain of 4 (Adjoint Model)**

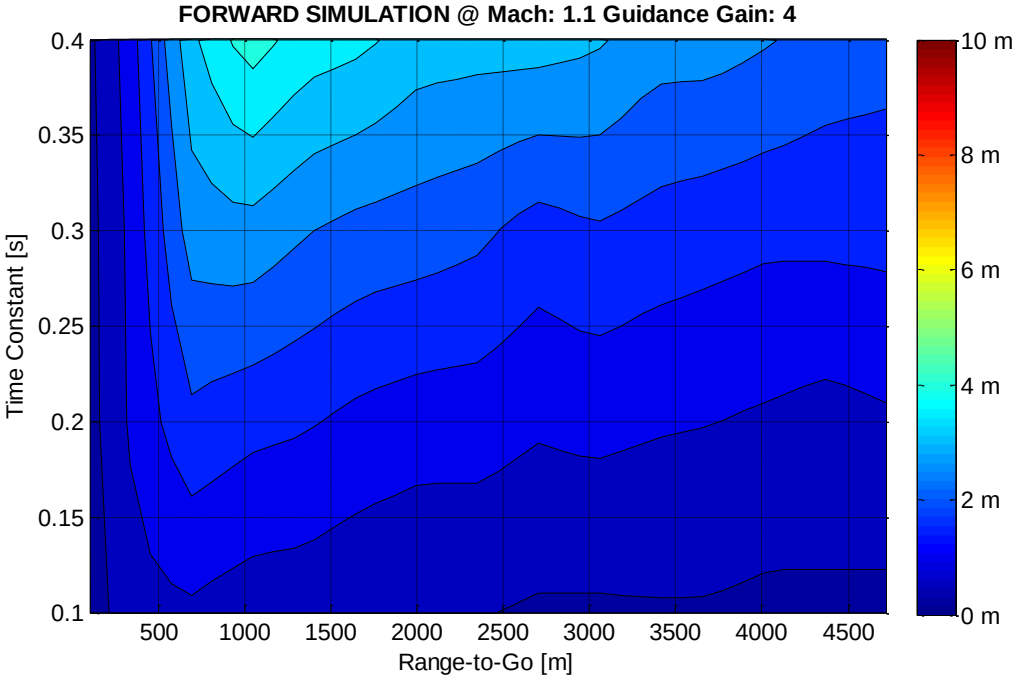


**Figure 33 MD for 3g Target Maneuver Guidance Gain of 4 (Forward Model)**

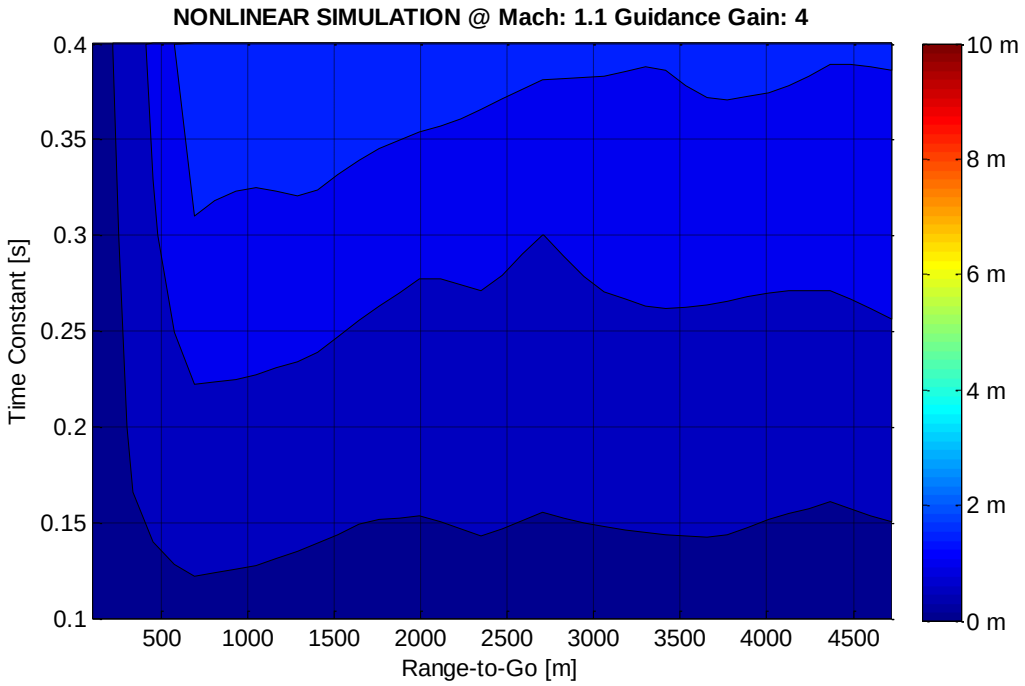


**Figure 34 MD for 3g Target Maneuver Guidance Gain of 4 (Nonlinear Model)**

In Figure 32, Figure 33 and Figure 34, miss distance standard deviations are depicted for all three models. It can be observed that there is still a good agreement between linear forward and adjoint results, which means that the performance of the describing function is satisfactory. On the other hand, nonlinear model results are different and lower miss distance values are generated due to the neglected engagement nonlinearities of the linearized homing loop.

In Figure 35, Figure 36 and Figure 37, miss distance standard deviations are depicted for all three models. It can be observed that there is still a good agreement between linear forward and adjoint results, which means that the performance of the describing function is satisfactory. On the other hand, behavior of the nonlinear model results are different but magnitudes are closer compared to comparison analysis with guidance gain value of 4 since higher constant demands higher acceleration that compensates the engagement nonlinear effects.

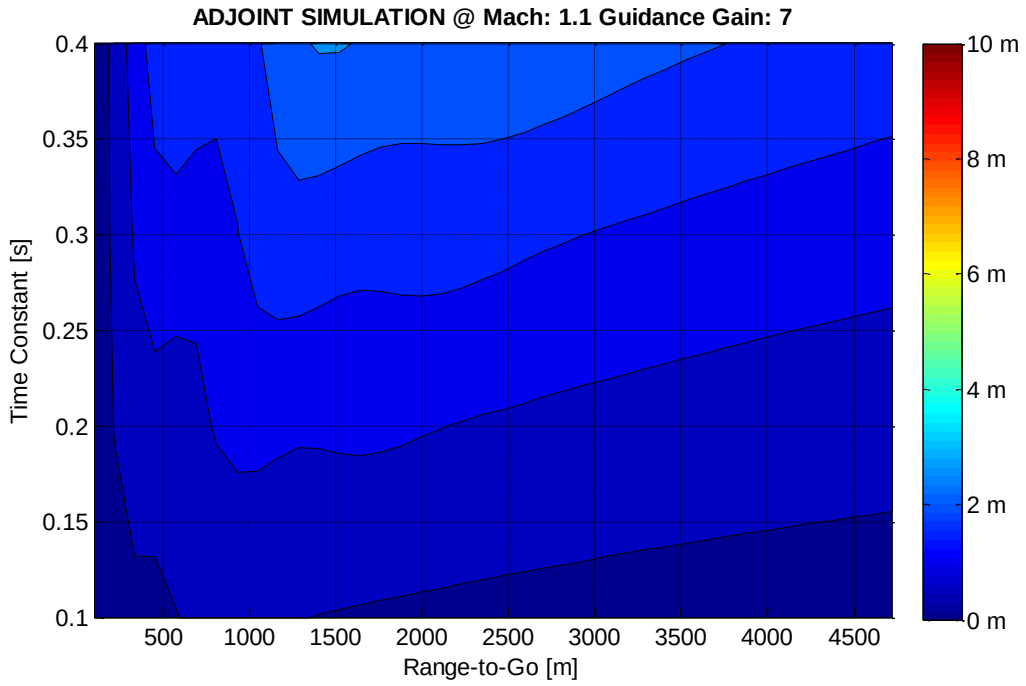


**Figure 35 MD for 3g Target Maneuver Guidance Gain of 7 (Adjoint Model)**

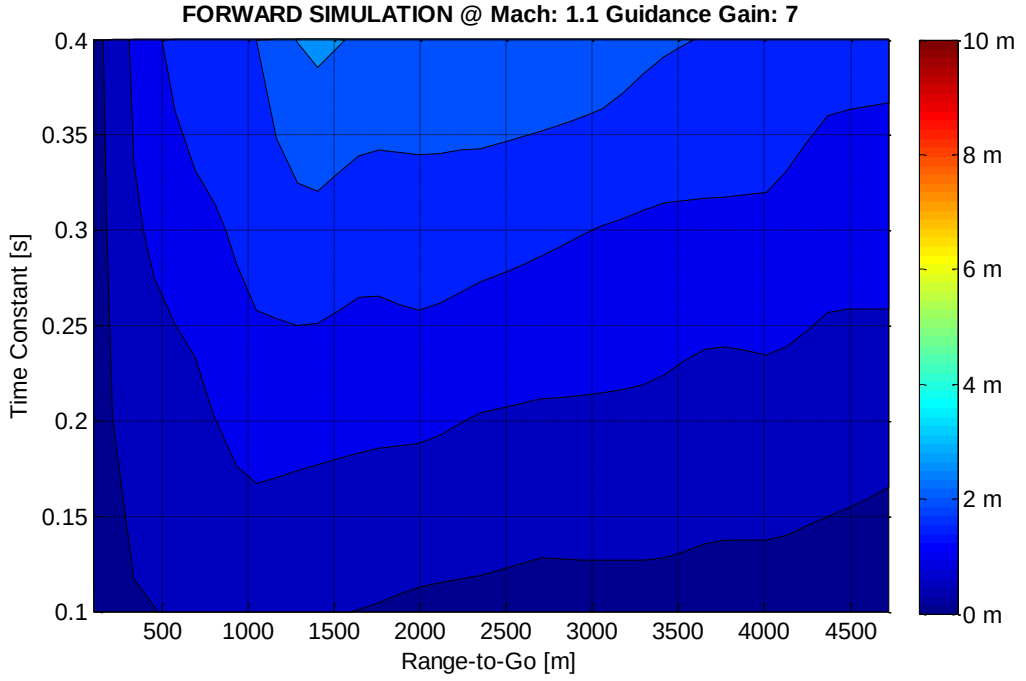


**Figure 36 MD for 3g Target Maneuver Guidance Gain of 7 (Forward Model)**

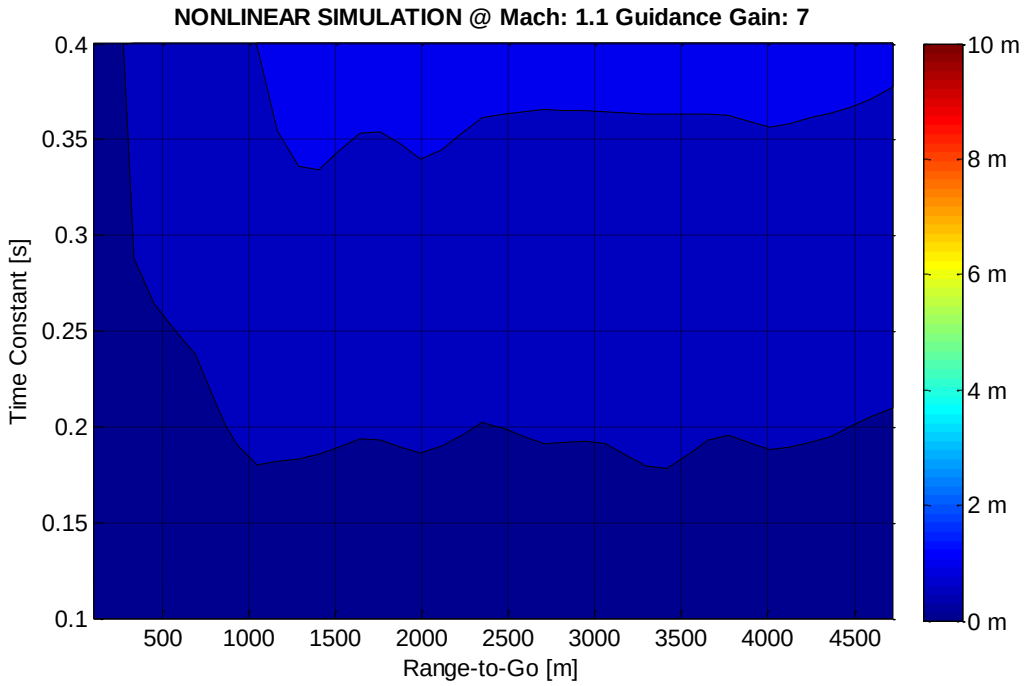


**Figure 37 MD for 3g Target Maneuver Guidance Gain of 7 (Nonlinear Model)**

In Figure 38, Figure 39 and Figure 40, miss distance standard deviations are depicted for all three models. It can be observed that there is still a good agreement between linear forward and adjoint results, which means that the performance of the describing function is satisfactory. On the other hand, since higher target maneuver is applied, engagement nonlinearities are more stressed and deviations from nonlinear model increases as well.

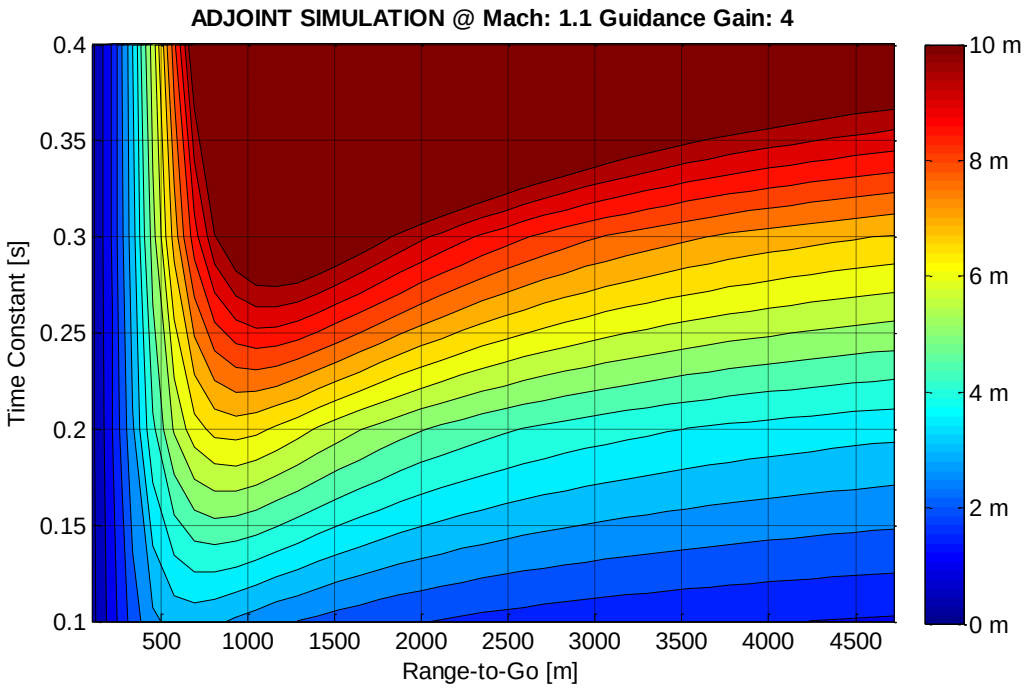


**Figure 38 MD for 7g Target Maneuver Guidance Gain of 4 (Adjoint Model)**

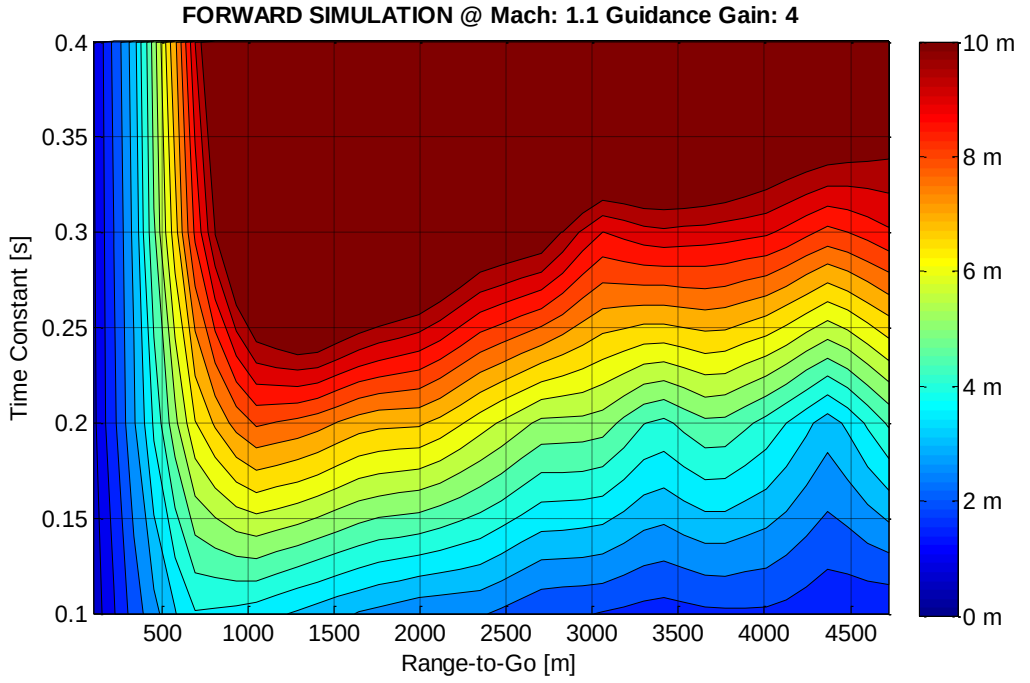


**Figure 39 MD for 7g Target Maneuver Guidance Gain of 4 (Forward Model)**

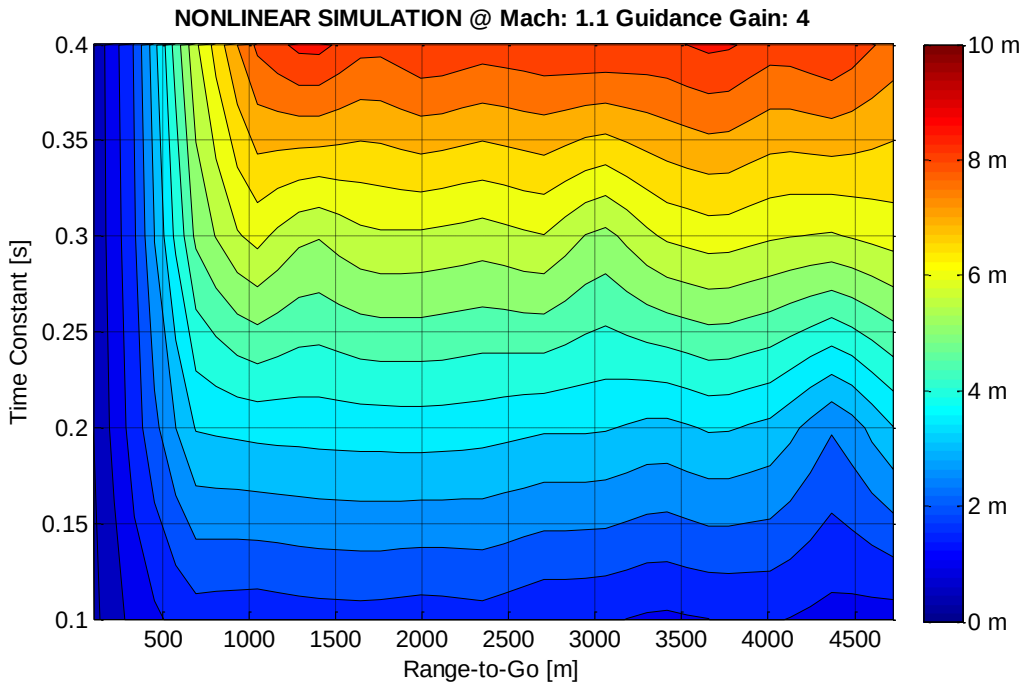


**Figure 40 MD for 7g Target Maneuver Guidance Gain of 4 (Nonlinear Model)**

In Figure 41, Figure 42 and Figure 43, miss distance standard deviations are depicted for all three models. It can be observed that there is still a good agreement between linear forward and adjoint results, which means that the performance of the describing function is satisfactory. On the other hand, since higher target maneuver is applied, engagement nonlinearities are more stressed and deviations from nonlinear model increases as well compared to 3g target maneuvers. In addition, since the higher guidance gain value compensates the engagement nonlinearities, differences in results between nonlinear and liner forward models are closer.

Finally, it can be considered that the describing function technique is convenient to represent the saturation nonlinearity. However, nonlinear effects due to engagement still exist and fidelity of the Adjoint model decreases with decreasing guidance gain value.

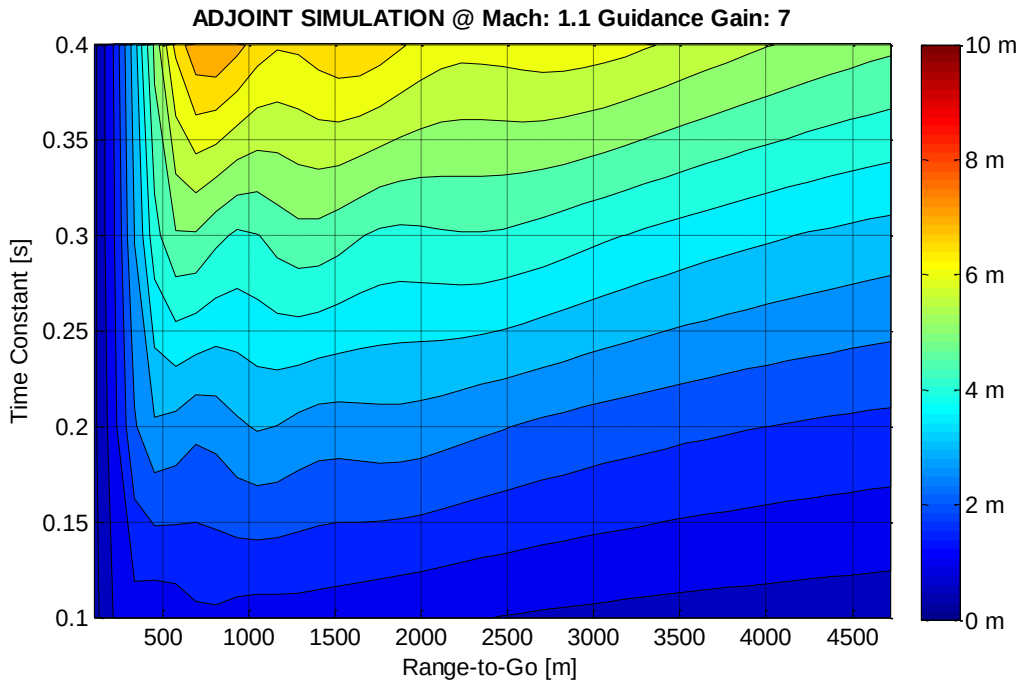


**Figure 41 MD for 7g Target Maneuver Guidance Gain of 7 (Adjoint Model)**

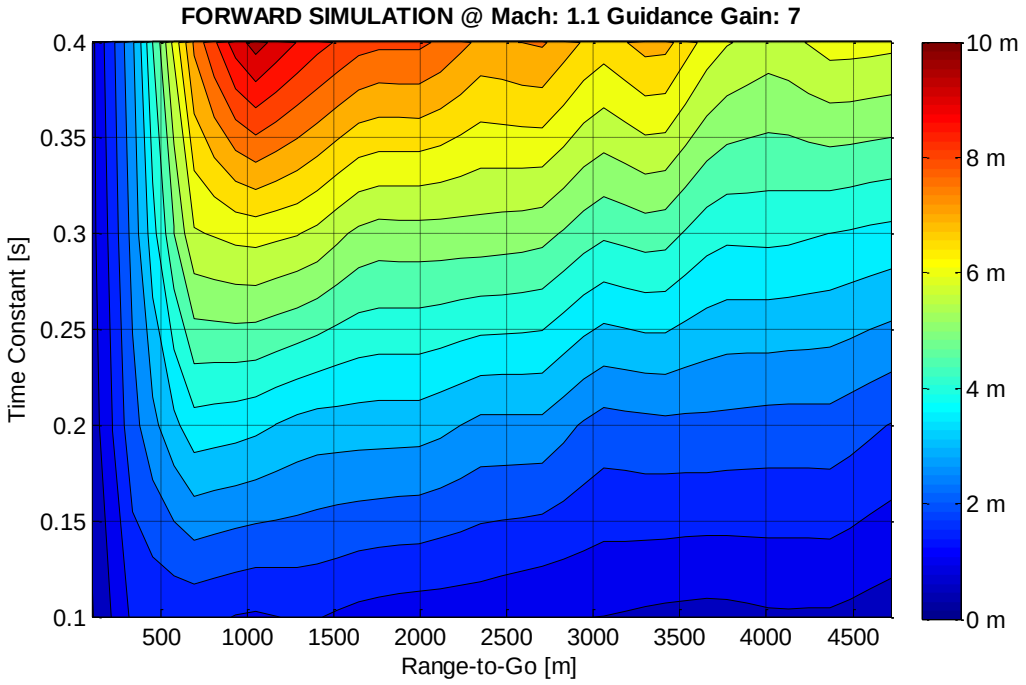


**Figure 42 MD for 7g Target Maneuver Guidance Gain of 4 (Forward Model)**

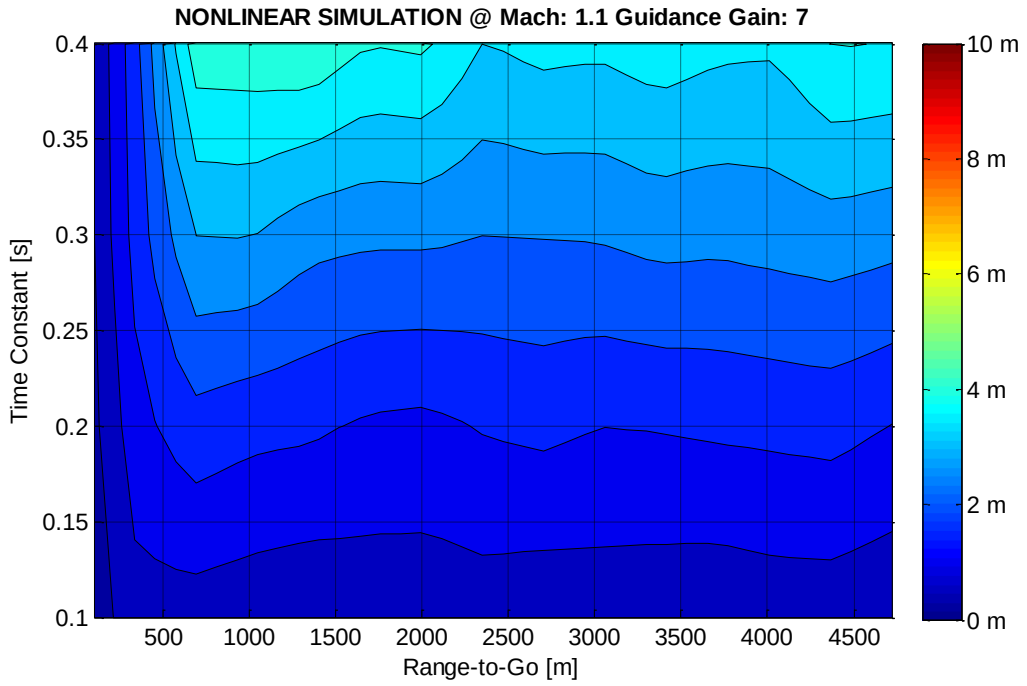


**Figure 43 MD for 7g Target Maneuver Guidance Gain of 7 (Nonlinear Model)**

### 3.4 Stochastic Adjoint Analysis for Nonlinear Engagement Scenario

In this analysis, the LTV model states are populated by utilizing nonlinear model states time history for a nominal state history so the only disturbance is the deterministic target maneuver for various range-to-go values. Then, the nominal state histories are implemented in to the state dependent coefficient form of the LTV model that is mentioned before. Note that some of the parameters of the system matrix are considered that they do not have dominant impact on the results so they are implemented as time varying parameters. On the other hand, dominant states are used in the system matrix to represent the nonlinear effects of the disturbance. In Eq.(57), the classical state space representation of the linear system is formulated.

$$\dot{x}(t) = A(x,t)x(t) + B(x,t)u(t) \tag{57}$$

$A(x,t)$ and $B(x,t)$ are used for the system and input matrices respectively and note that each matrix depends on the states and time explicitly. However, LTV equation that are expressed in Eq.(55) is nonlinear homing equations and should be linearized. An operating point is necessary for the classical linearization but in order to implement this form in the adjoint method, the classical technique is not valid. Therefore, the nominal state values are considered as operating point for each time

step and dependence on the on the system states should be discarded as well in the system matrix and the new form is depicted in Eq.(58).

$$\dot{x}(t) = A(t)x(t) + B(t)u(t) \tag{58}$$

Note that, it is not possible to represent the effects of all states on the system response completely so some of the elements in the system matrix should be assumed as unresponsive to the disturbances. In addition, disturbance magnitudes should be in a proper region in order not to violate the linearity assumption.

The linearization process is held for a set of nominal trajectories for the different target maneuver times, which is considered as down range values in this analysis, when the seeker is considered to lock-on. Then, it is required to validate the LTV model for different disturbances to figure out their magnitudes are in the proper interval for the reasonable response. Note that, if the disturbances are high enough to deviate much from the nominal trajectory, the accuracy of the LTV model becomes questionable. Therefore, the nonlinear model and the LTV model are compared in terms of one deterministic and one stochastic disturbance such as, initial heading error angle and seeker range dependent LOS rate noise respectively for a two different range-to-values.

*Linear Time Varying Model Validation*

In Figure 44, deterministic heading error angle values of 0°, -5° and 5° are considered for a scenario that starts at 3000m range-to-go but the target maneuvers when the down range is 2000m. It can be observed that there is a good agreement between the response of the LTV model and the nonlinear model for each heading error angle. Note that, $0^{\circ}$ angle represents the nominal trajectory but the LTV model still generates reasonable results compared to the nonlinear model.

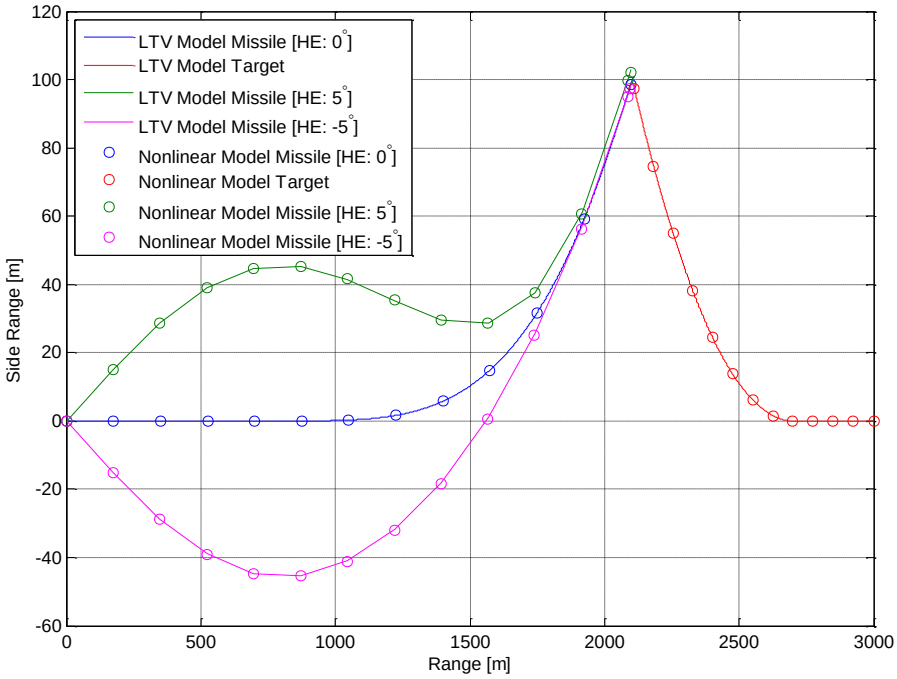


**Figure 44 Nonlinear and LTV Model for Target Maneuvers at 2000m Range**

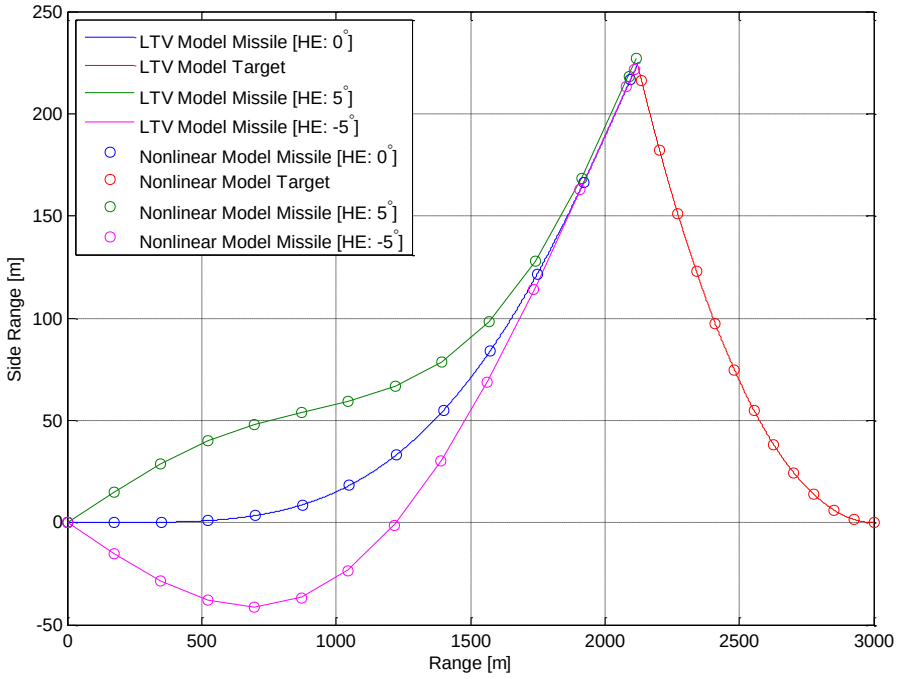


**Figure 45 Nonlinear and LTV Model for Target Maneuvers at 3000m Range**

In Figure 45, heading error angle values of 0°, -5° and 5° are considered for a scenario that starts at 3000m range-to-go but the target maneuvers when the down range is 3000m. It can be observed that there is a good agreement between the

response of the LTV model and the nonlinear model for each heading error angle. Note that, $0^{\circ}$ angle represents the nominal trajectory but the LTV model still generates reasonable results compared to the nonlinear model.

In addition, although the trajectories are close to each other, miss distance value should be compared since it is the main parameter for the performance analyses. Therefore, initial heading error disturbance is applied for various target maneuver times, which are represented by the down range values of the interval of (100m, 3000m) with 100m spacing. In Figure 46, miss distance values for the same heading error values of 0°, -5° and 5° are shown.

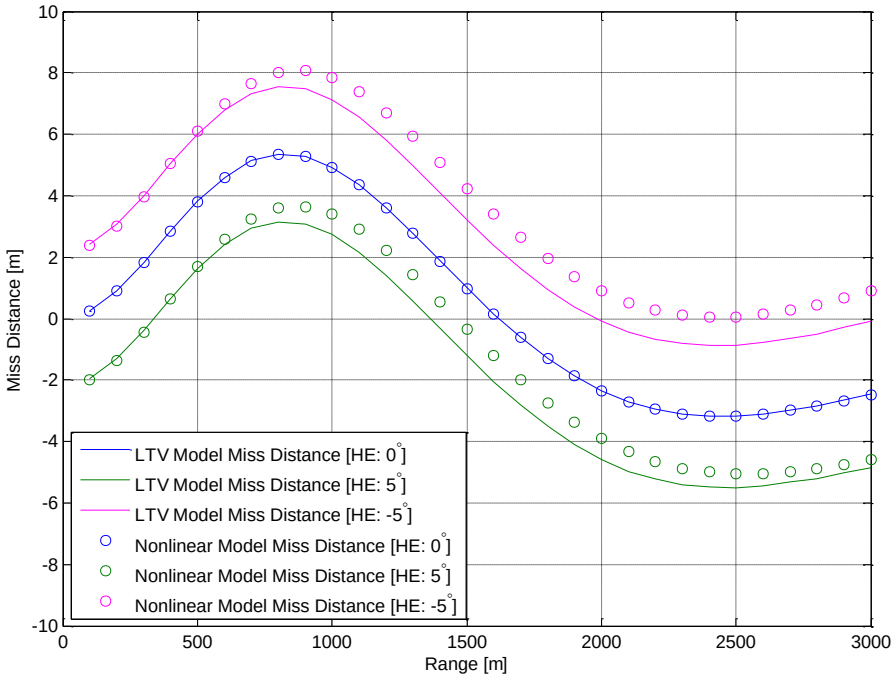


**Figure 46 MD of Nonlinear and LTV Model**

In Figure 46, it is obtained that the deviations of the LTV from the nonlinear model increases with the early maneuver time as expected since the target acceleration is the most dominant parameter that shaped the trajectory. In addition, the initial heading angle and the maneuver directions are important as well.

Finally, the LTV model can be considered to generate proper miss distance results for the initial heading error angle of the interval of (-5°, 5°).

The stochastic analyses are held for a disturbance parameter, which is mentioned as seeker range dependent LOS rate noise, for 5000m to 200m and finally for 100m range-to-go values. The noise is applied at the beginning of the simulation to represent the seeker noise from the seeker lock-on.

In Figure 47, mean miss distance values of the nonlinear and LTV models are shown for various down range values and it is observed that the disturbance mean and variance values are in the acceptable region for the LTV model.

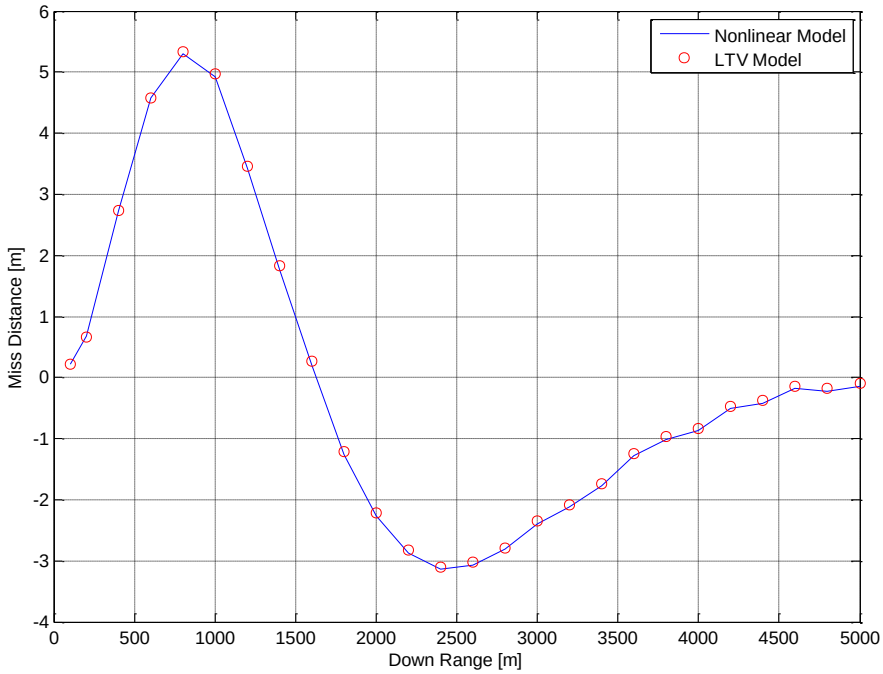


**Figure 47 Mean MD of the Nonlinear and LTV Models with Seeker Noise**

On the other hand, root mean square (RMS) values of the miss distance are presented in Figure 48 and the results are almost perfectly match to each other, which means that the LTV model is an appropriate for the disturbances that are implemented.

Note that, since white noise is applied as stochastic disturbance, the mean values of the trajectory do not change too much and the variance of the white noise is in the linear region as well so the results are very close to each other.

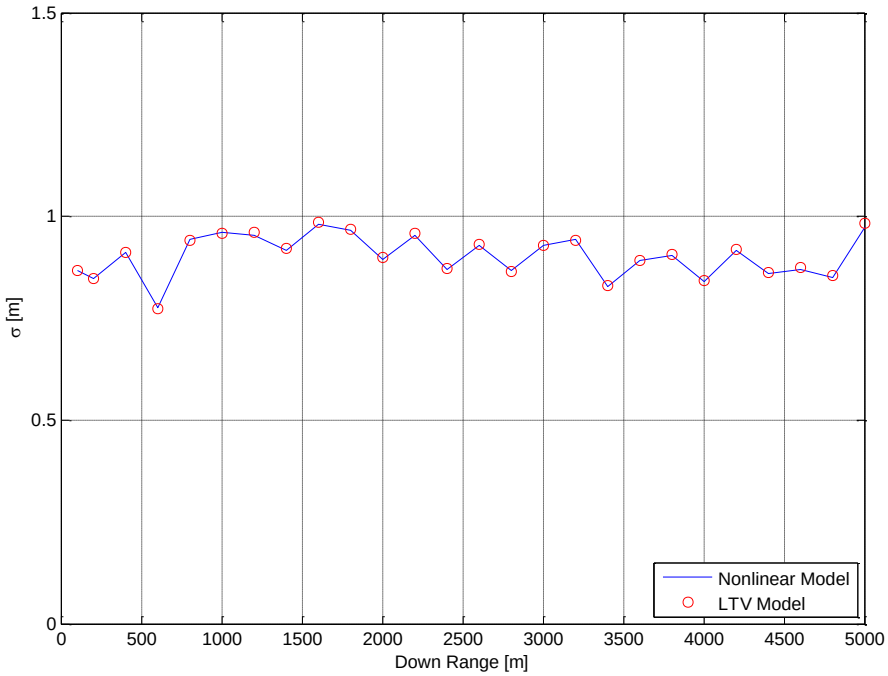


**Figure 48 RMS MD of the Nonlinear and LTV Models with Seeker Noise**

*Adjoint Analyses*

In the previous section, the LTV model is validated for various target maneuver application times against deterministic and stochastic disturbances. Once the LTV model is validated, an adjoint of this LTV can be generated also.

Since the main concern is to implement the engagement nonlinear effects in the homing loop for the Adjoint model, stochastic analysis should be needed for the power of the method.

In order to figure out the advantage of utilizing the adjoint method for the stochastic analysis, a procedure is explained in Figure 49. It is required that $N$ monte carlo runs for each $M$ number of the target maneuver application times, which results $N \times M$ run number in total. On the other hand a single adjoint run is sufficient for $M$ number of the various target maneuver times, which means $N$ times less analyses are enough as well. In addition, the adjoint method has the ability to generate disturbance effects on the system response separately otherwise, each input is required to be analyzed to get the same outcome by utilizing the LTV and the nonlinear models.

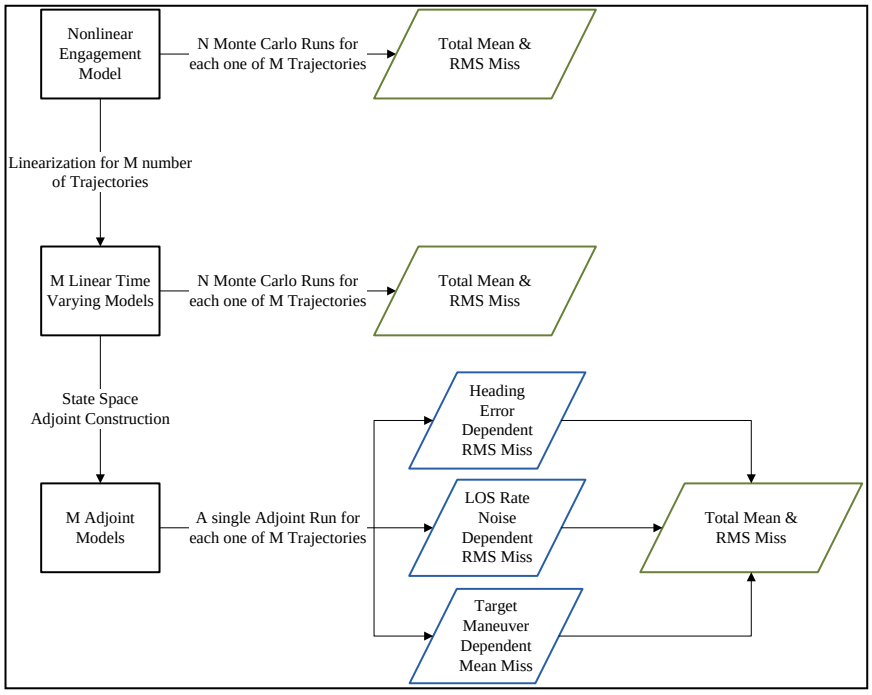


**Figure 49 Adjoint Analysis Procedure for Nonlinear Engagement Scenarios**

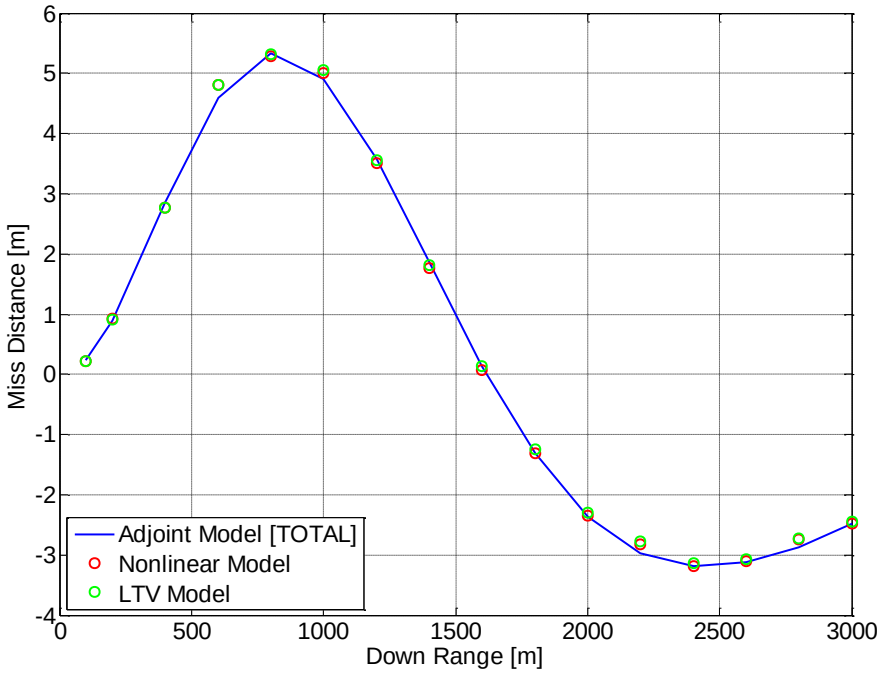


**Figure 50 Mean MD Comparison for Seeker Lock-on at 3000m**

In Figure 50, mean miss distance values seeker lock-on at 3000m range-to-go values are depicted and it can be observed that all of the three model results are almost perfectly matched.

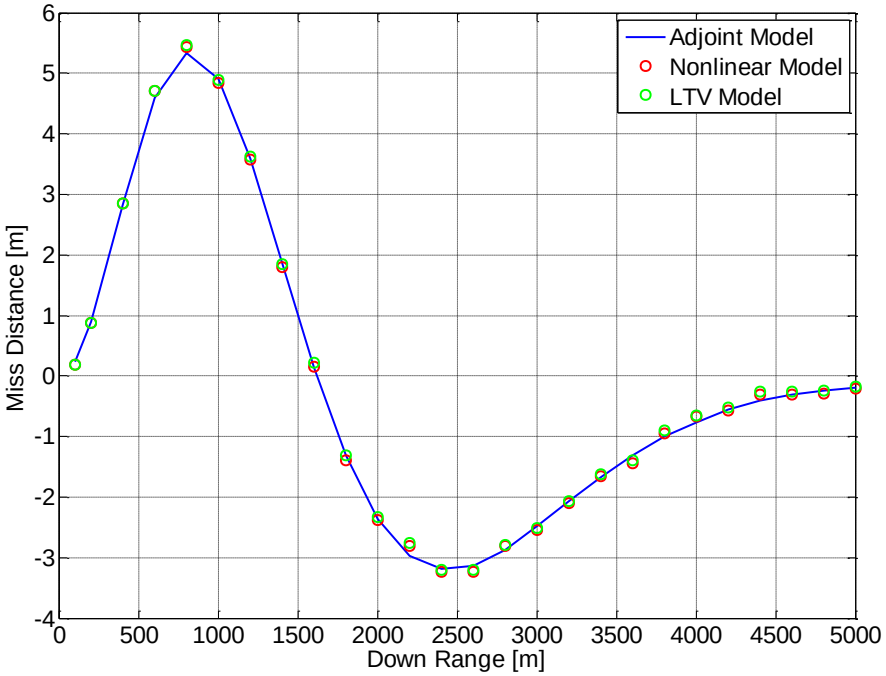


**Figure 51 Mean MD Comparison for Seeker Lock-on at 5000m**

In Figure 51, mean miss distance values seeker lock-on at 5000m range-to-go values are depicted and it can be observed that all of the three model results are almost perfectly matched.

In addition to the above mean values, miss distance RMS values are presented for 3000m and 5000m range-to-go values at seeker lock-on in Figure 52 and Figure 53. It is observed that the total RMS value of the adjoint is almost perfectly matched with LTV and nonlinear. In addition, LTV and nonlinear models require $N \times M$ total run number when only $N$ adjoint runs are enough to get the same results and weights of the disturbances on the system response can be obtained by the Adjoint model also. Note that for the 5000m scenario, heading error does not have an important effect on the results since the seeker locks-on at the higher range compared to 3000m scenario. However, heading error is more dominant for the 3000m scenario and since the seeker noise is applied less compared to 5000m scenario, its effect on the results decreases as well.

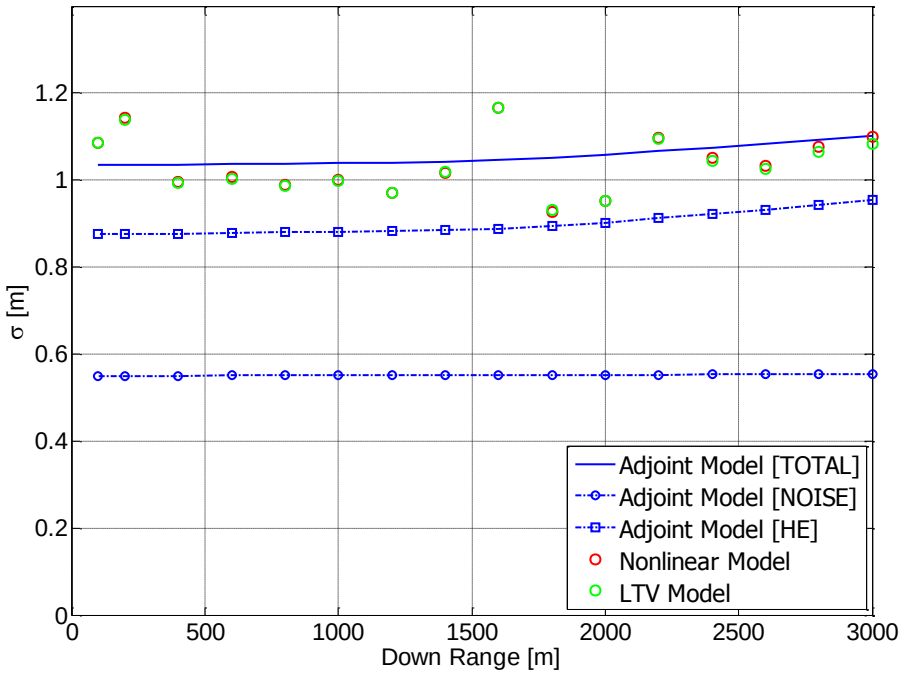


**Figure 52 RMS MD Comparison for Seeker Lock-on at 3000m**

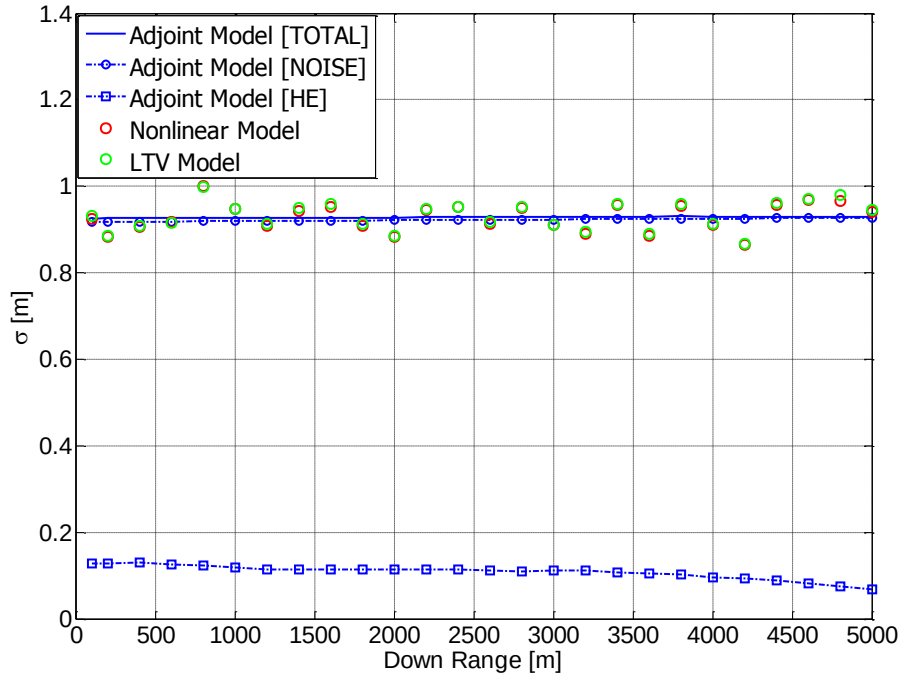


**Figure 53 RMS MD Comparison for Seeker Lock-on at 5000m**

*Additional Disturbance Parameter Analysis (Target Maneuver)*

In a classical approach of the adjoint method, which is mentioned, target maneuver cannot be applied as stochastic parameters in time as studied in the literature since it

is the major parameter that shapes the nominal trajectory. Therefore, since the Adjoint model is valid only for a defined nominal trajectory, it is not valid for stochastic analysis where the target maneuver is random in time.

If the stochastic analysis process is deeply investigated, it is observed that the RMS value of the adjoint method is the standard deviation of the mean miss distance values where the target may start maneuver in time.

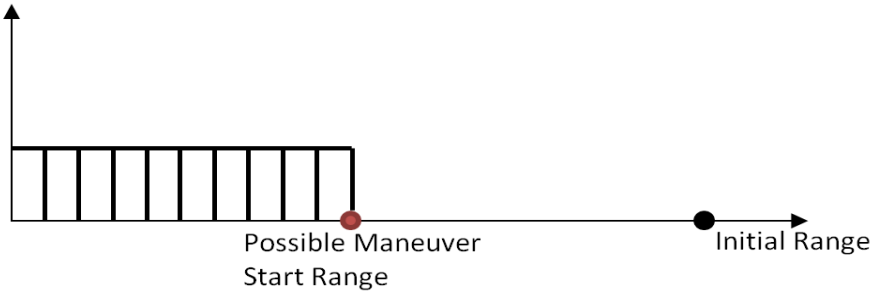


**Figure 54 Uniformly Distributed Target Maneuver**

In Figure 54, uniformly distributed target accelerations in time is shown for a single possible target maneuver start range. The adjoint method generate RMS miss distance values for each possible maneuver start ranges for uniformly distributed target maneuvers in time if the proper power spectral density is implemented. The adjoint technique results in many miss distance values for various target acceleration time for the adjoint time step resolution. If the step time of the Adjoint model is small enough, the miss distance values of the deterministic analysis can be considered the response of the uniformly distributed target maneuver in time for a possible maneuver start range. Therefore, the standard deviations of the mean miss distance values back in the adjoin time can be considered the RMS values of the stochastic target maneuver disturbance.

According to this logic, same approach can be applied for the nonlinear engagement adjoint analysis to observe the stochastic target maneuver that is uniformly distributed in time. However, note that there must be enough adjoint mean miss distance values so the outcomes are interpolated in range without violating the behavior of the results to obtain higher number of mean miss distance values.

Therefore, once the mean miss distance values are obtained and they are interpolated according to the down range values in order to increase the number of the outcome. Then, the formula that is depicted in Eq.(59) is utilized to get the stochastic response of the target maneuver.

$$\sigma^2 = \sum_{i=1}^{A}\sum_{j=1}^{i}\left(x_j - \mu\right)^2 p(x)$$
$$\mu = \sum_{i=1}^{A}\sum_{j=1}^{i} x_j p(x) \tag{59}$$

In the above equation, $A$ is used to represent the maximum number of the mean miss distance values and $i$ is utilized for the number of the miss distance with respect to the down range. In addition, the mean and the variances changes with the increasing data number and depicted as $\sigma$ and $\mu$ respectively. Finally, $p(x)$ is used to represent different probabilities of the stochastic target maneuver in time and in this analysis, it is considered as constant since uniform maneuver distribution is applied in time.

In Figure 55, RMS response of the system for stochastic target maneuver, initial heading error disturbance and seeker noise are presented for 3000m range-to-go value.

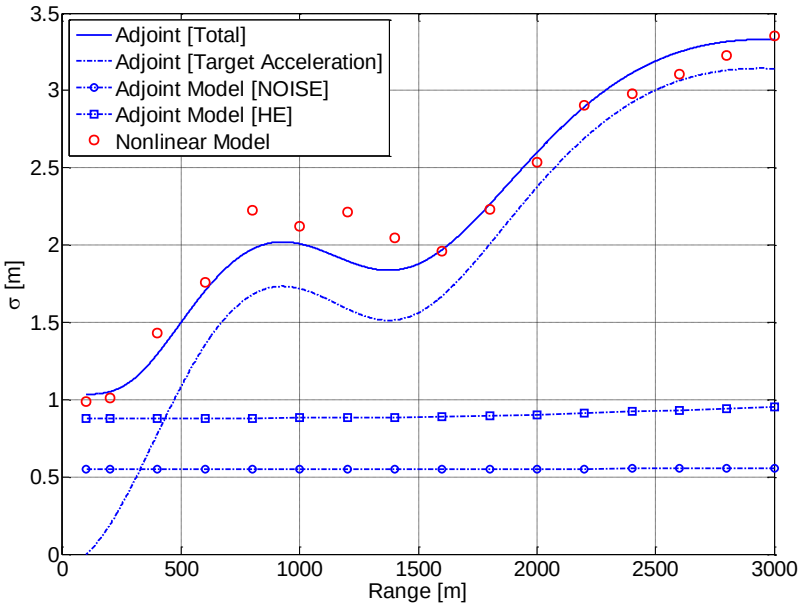


**Figure 55 RMS MD Comparison for Seeker Lock-on at 3000m**

Then, in order to calculate the total root mean square of the miss distance values for the all disturbances such as target maneuver, initial heading error and LOS rate noise, the formula expressed in Eq.(41) is utilized.

It can be observed that the target maneuver is the most dominant disturbance as mentioned and the total miss distance values of the adjoint are close to the nonlinear model results.

In Figure 56, RMS response of the system for stochastic target maneuver, initial heading error disturbance and seeker noise are presented for 5000m range-to-go value.

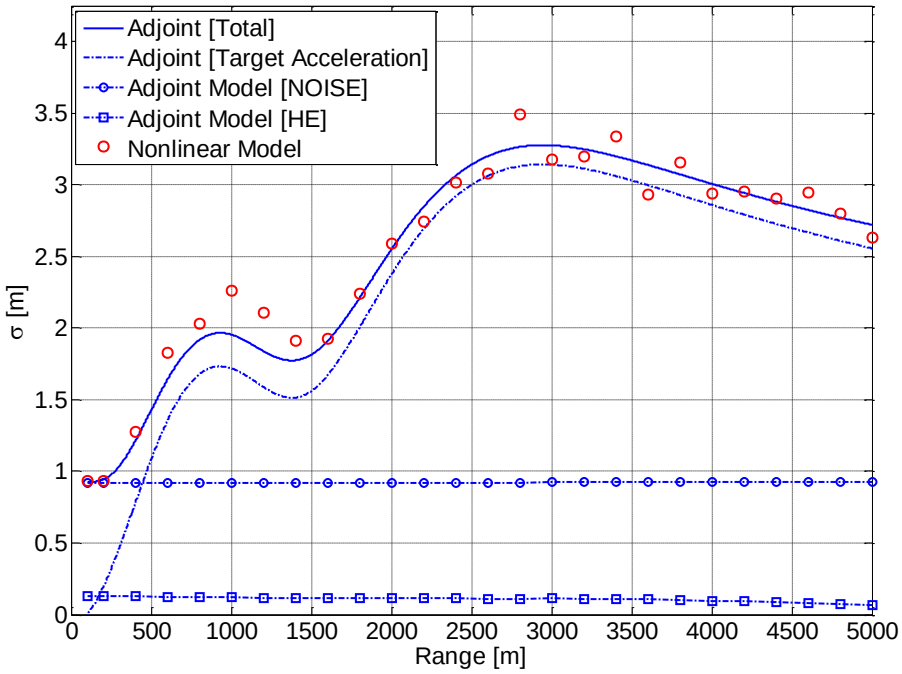


**Figure 56 RMS MD Comparison for Seeker Lock-on at 5000m**

Similar with the previous results, the target maneuver is the most dominant disturbance and outcomes of the models are almost perfectly matched with each other without utilizing the power spectral density that cannot be implemented, for the target acceleration.

# CHAPER 4

# CONCLUSION

In this thesis study, Pseudo 5-DOF model and adjoint method are investigated in to figure out their capability in terms of the fidelity and the validity of the requirement analysis.

The adjoint is a powerful technique for the early design phases of a missile in terms of the ability of parametric study and time. In addition, it allows the designer to understand the effects of the disturbances on the system response in single run. However, fidelity of the adjoint method is not enough as the design of the missile matures so more complex simulation models are required. Pseudo 5-DOF model is a good candidate to fill this gap between Adjoint and the 6-DOF models due to its level of fidelity and parametric analysis capability.

In addition, adjoint method is still valid for some requirement analyses although its fidelity level is not sufficient for example, seeker lock-on range requirement. As explained in the previous sections, adjoint miss distance values are questionable compared to 6-DOF but it is still a good candidate for deriving the seeker lock-on range requirement since the method can capture the point where the miss distance sensitivity starts from.

Finally, the adjoint method is investigated in more detail to increase the capability. For nonlinear engagement adjoint analyses, implementing target maneuver as a stochastic disturbance is not possible by using the classical approaches that are available in the literature. However, it is feasible to apply in the adjoint by utilizing the logic, which is explained, and response of the system to stochastic target maneuver can be obtained without using the power spectral density.

As a future work, the logic that is mentioned would be studied in more detail for the other randomly distributed target maneuvers instead of uniformly distributed one.

In conclusion, it is crucial for the designer to know how much fidelity is needed and which analyses can be done with the available models. At beginning of the design phases, adjoint is a powerful method to analyze integrated guidance and control parameters. Then, the Pseudo 5-DOF has enough fidelity to derive many detailed requirements.

## REFERENCES


Bucco, D. (2010). “Aerospace Applications of Adjoint Theory”. Defence Science and Technology

Bucco, D., Zarchan P. (2012). “On Some Issues Concerning the Adjoint Simulation of Guidance Systems”. AIAA Guidance, Navigation and Control Conference

Fleeman, E. U. (2001). “Technologies for Future Precision Strike Missile Systems – Missile/Aircraft Integration”. Paper presented at the RTO SCI Lecture Series on “Technologies for Future Precision Strike Missile Systems”, held in Tbilisi, Georgia, 18-19 June 2001; Bucharest, Romania, 21-22 June 2001; Madrid, Spain, 25-26 June 2001; Stockholm, Sweden, 28-29 June 2001, and published in RTO-EN-018

Gelb, A. Joseph, K. F., Nash, R. A., Price, C. F. & Sutherland, A. A. (2001). “Applied Optimal Estimation”. THE M.I.T. PRESS

Gelb, A., & Velde, W. E. Vander. (1968). “Multiple-input Describing Functions and Nonlinear System Design”. McGraw-Hill Book Company

Hildreth, B., Linse, D. J., Ph.D., & Park, L. (2008). “Pseudo Six Degree of Freedom (DOF) Models for Higher Fidelity Constructive Simulations”. AIAA Modeling and Simulation Technologies Conference and Exhibit.

Laning, J. H. J., & Battin, R. H. (1956). “Random Process in Automatic Control”. McGraw-Hill Book Company.

Moorman, M. J., Warkomski, E. J., Lam, Q. M., & Elkanick, M. E. (2005). “Extending Adjoint Simulation Design Beyond its Traditional Role”. AIAA Guidance, Navigation and Control Conference and Exhibit

Sezer, E., Nalcı, M. O., & Kutay, A. T. (2015). “A Comparative Study of a Pseudo Five Degree of Freedom and an Adjoint Model Against a Six Degree of Freedom Model for Fidelity Assessment”. AIAA Modeling and Simulation Technologies Conference.

Weiss, M. (2005). “Adjoint Method for Missile Performance Analysis on State-Space Models”. Journal of Guidance, Control and Dynamics, Vol.28, No.2.

Weiss, M., & Bucco, D. (2005). “Handover Analysis for Tactical Guided Weapons Using the Adjoint Method”. AIAA Guidance, Navigation and Control Conference and Exhibit.

Zarchan, P. (1979). “Complete Statistical Analysis of Nonlinear Missile Guidance Systems - SLAM”. Journal of Guidance, Control and Dynamics, Vol.2, No.1.

Zarchan, P. (2012). “Tactical and Strategic Missile Guidance Sixth Edition”. American Institute of Aeronautics and Astronautics, Inc., Volume 239.

Zipfel, P. H. (2007). “Modeling and Simulation of Aerospace Vehicle Dynamics Second Edition”. American Institute of Aeronautics and Astronautics, Inc.